Spectrum Monitoring in Cognitive Radio Networks using Error Vector Magnitude

Narayan Nepal

A thesis submitted for the degree of
Doctor of Philosophy
in
Electrical and Electronic Engineering
at the
University of Canterbury,
Christchurch, New Zealand.

July 2018

I dedicate this thesis to my dearest wife Dr. Jaya Tiwari, whose unconditional love, unselfish support provided me the strength to continue along the research journey

and

my lovely son Jayan Nepal who became the part of my life and added extra joy and happiness during the course of this strenuous journey.

Abstract

The proliferation of new operators, innovative services and wireless technologies has caused radio spectrum resources to become scarce. This scarcity has led to the concept of cognitive radio (CR) communication. Spectrum sensing is a critical component of CR networks for spectrum utilization. It is the process in which the CR users or the secondary users (SUs) exploit unused licensed or unlicensed frequency bands providing minimal interference to the primary users (PUs). Spectrum sensing can be categorized into two types : out-of-band sensing and in-band sensing. Out-of-band sensing searches for an idle channel by sensing multiple channels sequentially until an available channel is found. In-band sensing monitors a channel periodically while using it, in order to detect the return of PUs, so that SUs can vacate the channel immediately upon detection of returning PUs. This periodic spectrum sensing causes SUs to halt its communication frequently. This causes a tradeoff between maintaining high communications efficiency in the secondary network and avoiding disruption to the primary network.

In this thesis, we use error vector magnitude (EVM) to develop a novel in-band sensing technique that allows SUs to perform spectrum monitoring during transmission. EVM is being increasingly employed in the wireless industry and has already become part of several wireless standards. However, this metric has been overlooked in the context of CR despite having significant advantages. One advantage is that the SU transmitted signal gets canceled out during EVM calculation, therefore we do not require a sophisticated self-interference cancellation (SIC) technique as required by full duplex (FD) techniques. The other advantage is that the EVM technique utilizes fewer symbols, does not require any subcarriers to be reserved, provides results much before demodulation and decoding thus giving us real time results. This monitoring method differs from a spectrum sensing method in that the monitoring is applied during reception of packets. It involves detecting the emergence of PUs during periods in

which the SUs are communicating. This method doesn't halt the SU communication, hence a significant gain in SU throughput is obtained. This spectrum monitoring technique supplements the traditional spectrum sensing and provides enhanced communications efficiency.

In the first part of this thesis, we study the performance of the EVM based PU monitoring technique in orthogonal frequency division multiplexing (OFDM) based CR networks. We utilize the pilot tones that are inherent to many OFDM based standards to measure the EVM as the difference between the received and transmitted pilot tones. We show that a step change in the EVM curve is sufficient to detect a PU during ongoing SU transmission. The technique also allows us to locate the bits corrupted by the PU's arrival by looking at the EVM values of the pilot tones.

In the second part of this thesis we analytically characterize the performance of the proposed method. We derive the probability density function (PDF) of the EVM based statistic. We then analyze the detection performance with the complementary receiver operating characteristics (CROC) curve in terms of type I and type II error probabilities. In order to simplify the analytical expression, a Laplacian approximation method is also provided. We also present the joint PDF of the test statistic towards the detection of the reappearing PU. A throughput performance of the proposed detector is also analyzed. Simulation results illustrate that the EVM based detection performs better than the energy detection (ED) method.

In a later part of the thesis, we show the application of the sequential change detection also known as the quickest detection method to the EVM based detector. Motivated by the results from CROC analysis and considering the importance of detection delay in spectrum sensing, we develop an exact quickest detection scheme by using a traditional cumulative sum (CUSUM) test. Simulation results show that the quickest EVM detection significantly outperforms the quickest ED.

Acknowledgements

First of all, I would like to express my sincere gratitude to my supervisors, Professor Philippa A. Martin and Professor Desmond P. Taylor for their continuous support, insightful suggestions, guidance, motivation, technical advise and patience during my doctoral studies.

I would like to express my sincere thanks to Dr. Alan Coulson for your excellent technical guidance and quick feedback on my research works. You have motivated me in modeling research problem correctly and provided me a good direction.

I would like to thank Professor Philippa A. Martin and University of Canterbury for funding me to present my research at IEEE Vehicular Technology Conference 2016 in Montreal, Canada.

I would also like to thank all my family members for their constant love and support. Special thanks to my beloved wife Jaya for your endless support, love and understanding. I would not have completed this thesis without your sacrifice and infinite patience. Thanks to my son Jayan for adding joy and happiness in our life.

Lastly, my thanks to all the Nepalese friends in Christchurch with whom I have shared many precious moments that will stay in my memory for a long period of time.

Contents

List of Figures

List of Tables

Abbreviations

3G	Third Generation
4G	Fourth Generation
5G	Fifth Generation
AWGN	Additive White Gaussian Noise
CDF	Cumulative Distribution Function
CFO	Carrier Frequency Offset
CLT	Central Limit Theorem
CR	Cognitive Radio
CROC	Complementary Receiver Operating Characteristics
CSI	Channel State Information
CUSUM	Cumulative Sum
dB	Decibel
DFT	Discrete Fourier Transform
DPC	Dirty Paper Coding
DOF	Degree of Freedom
DVB-T	Digital Video Broadcasting-Terrestial
ED	Energy Detection
EVM	Error Vector Magnitude
FCC	Federal Communications Commission
FD	Full Duplex
FFT	Fast Fourier Transform

GPS	Global Positioning System
HD	Half Duplex
ICI	INter Carrier Interference
i.i.d	Independent and Identically Distributed
INR	Interference to Noise Ratio
IoT	Internet of Things
ISI	Intersymbol Interference
LO	Local Oscillator
LTE	Long-Term Evolution
MIMO	Multiple Input Multiple Output
M-PSK	M-ary Phase Shift Keying
MSE	Mean Square Error
NBI	Narrowband Interference
NP	Neyman-Pearson
OFCOM	Office of Communications
OFDM	Orthogonal Frequency Division Mutliplexing
PA	Power Amplifier
PAPR	Peak to Average Power Ratio
PDF	Probability Density Function
PHY	Physical
PSD	Power Spectral Density
PU	Primary User in a Cognitive Radio Network
QAM	Quadrature Amplitude Modulation

QoS	Quality of Service
QPSK	Quadrature Phase Shift Keying
RF	Radio Frequency
RMS	Root Mean Square
ROC	Receiver Operating Characteristics
RX	Receiver
SFO	Sampling Frequency Offset
SIC	Successive Interference Cancellation
SISO	Single Input Single Output
SNR	Signal to Noise Ratio
STO	Symbol Timing Offset
SU	Secondary User in a Cognitive Radio Network
TX	Transmitter
UWB	Ultra-Wideband
W-CDMA	Wideband Code Division Multiple Access
WiMAX	Worldwide Interoperability for Microwave Access
WLAN	Wireless Local Area Network
WRAN	Wireless Regional Area Network

Chapter 1

Introduction

1.1 Cognitive Radio Concept

Over the last decade, there has been a tremendous growth in wireless communication technologies. Starting from first generation (1G) to currently being developed fifth generation (5G) and Internet of Things (IoT) systems, we have witnessed a rapid growth in the number of devices like smart phones, ipads, tablets, TVs, computers, smart watches, global positioning system (GPS) devices etc. It is predicted that by 2021, there will be 16 billion devices connected [4]. As a result, a significant amount of wireless data traffic is expected. Fig. 1.1 shows the wireless data traffic which is expected to reach about 49 exabytes per month by the year 2021 [1]. A similar trend is shown for mobile video traffic in Fig. 1.2 [1]. These trends clearly indicate that there will be huge demand for radio spectrum in the future. Therefore, for 5G networks, researchers are exploring the possibilities to use idle spectrum in the millimeter wave range of $30 \sim 300$ GHz to improve bandwidth [5]. However, the available frequency resources are becoming scarce due in part to the current fixed spectrum allocation policy. These policies are governed by regulatory bodies, such as Federal Communications Commission (FCC) in the United States and Office of Communications (OFCOM) in the United Kingdom who allocates frequency bands to particular licensed users for a specified period of time and no interruption from unlicensed users is allowed [6–8].

This fixed spectrum allocation policy cannot fulfill the demand from users who are always expecting better broadband services and higher data rates. On the other hand, several studies and reports have indicated large portions of the allocated spec-

trum are under-utilized and are idle over a wide range of frequencies in the spatial and temporal domains [6, 9, 10]. It is found that high utilization is common in the cellular and FM radio bands. It has been reported by the FCC that many licensed frequency bands remain unused nearly ninety percent of the time [9, 11, 12]. Records show that the spectrum utilization ranges from 15% to 85%, where it is found that the utilization is more intense below 3 GHz and spectrum is under-utilized in the 3-6 GHz bands [9, 12]. The fixed spectrum allocation policy does not allow provision for using these under-utilized spectral resources allocated to licensed users by unlicensed users. This policy has led us to a situation where there would be no more frequencies to license out for new and innovative wireless applications. As a result, the development and implementation of new radio-based services would be more difficult all over the world. Therefore, dynamic spectrum allocation and management are essential for future wireless networks [13].

In this regard, CR has emerged as a technique to overcome this spectrum scarcity.

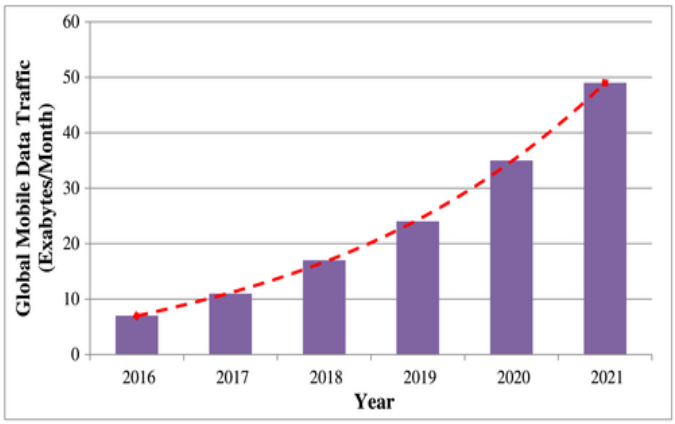

Figure 1.1: Global mobile traffic growth rate [1].

CR dynamically manages and shares unoccupied spectrum with secondary users (SUs) with minimal interference to primary users (PUs). It was first proposed by J. Mitola [14] as an intelligent radio transmitter/receiver which is aware of its surrounding radio frequency (RF) environment and can adjust its operating parameters such as

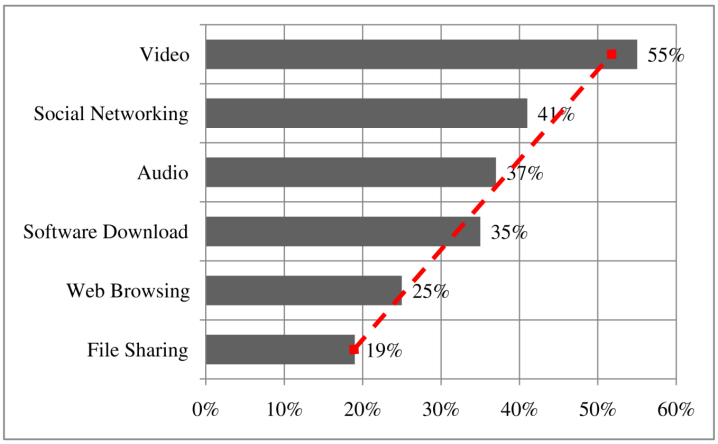

Figure 1.2: Application wise growth of mobile data traffic [1].

transmit power, modulation and coding scheme etc., dynamically. A CR cycle is presented in Fig. 1.3. It consists of the four main functions which are spectrum sensing, spectrum management, spectrum sharing and spectrum mobility [2]. Spectrum sensing is done to find the spectrum holes and spectrum management is executed to utilize these holes without causing interference to the PU. Spectrum sharing allows the SU to share the spectrum with the PU. Finally, spectrum mobility allows the SUs to move into an empty channel after vacating the current operating channel.

The CR improves the spectrum utilization by allowing SUs to access the licensed channel opportunistically when the PU is absent. The process of detecting the presence or absence of the PU is called spectrum sensing [9] and is explained in detail in chapter 2. Spectrum sensing is used for a fraction of the time and if the channel is determined to be unoccupied, then the SU is allowed to transmit for the remaining fraction of time. A CR enabled SU has to continuously sense the channel to avoid interference with the PU and if the PU is detected, the SU has to immediately stop operating within the specified channel and has to find new free channel space for continuing the current operation. This continuous sensing process, called periodic spectrum sensing, suspends SU transmission periodically to sense for reappearing PU causing frequent halts in SU transmission [15]. This leads to an inefficient usage of

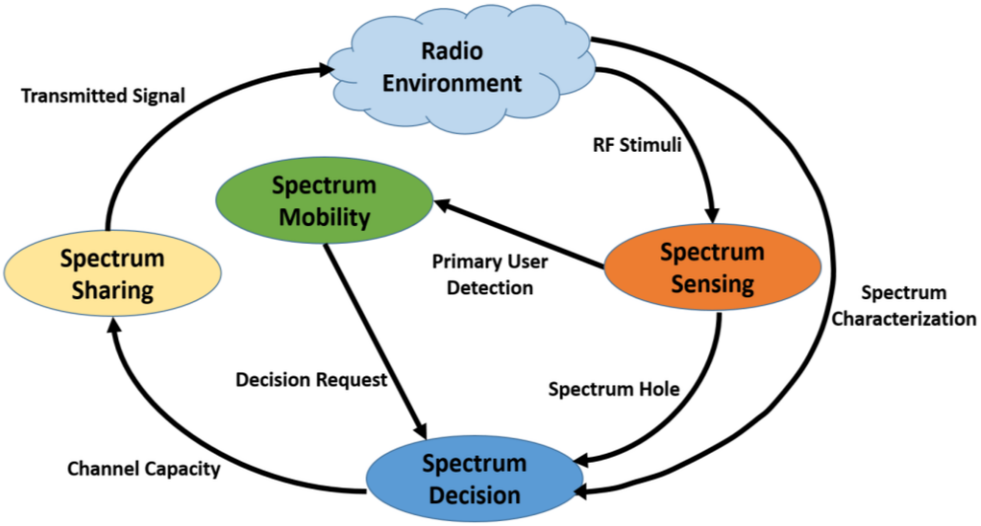

Figure 1.3: Cognitive Radio Cycle [2].

the available spectrum and consequently to a reduction in the CR network capacity. With this periodic spectrum sensing, there exists an inherent tradeoff which results in either compromising SU throughput or PU quality of service (QoS) [16–19]. This necessitates a new communication method which would monitor the frequency band without interrupting the SU communications.

This thesis contains a new frequency domain based spectrum monitoring method that detects the reappearing PU during ongoing SU transmission. An OFDM system is considered for SU transmission. This method doesn't halt the SU communication, hence a significant gain in SU throughput can be obtained. This monitoring technique supplements the traditional spectrum sensing and provides enhanced communications efficiency.

1.2 Motivation

As discussed in Section 1.1, traditional spectrum sensing techniques rely on periodic spectrum sensing, which reduces the CR network throughput as it frequently interrupts the SU transmission. In this regard, several research efforts have been made on spectrum monitoring which does not halt SU ongoing communication [15, 20–27].

A detailed schematic diagram is presented in Section 2.2 of chapter 2. The spectrum monitoring method differs from a conventional spectrum sensing method in that the monitoring is applied during reception. It involves detecting the emergence of PUs during periods in which the SUs are communicating.

The techniques mentioned in [15, 20–27] have their own merits and drawbacks. The method in [18, 24] has a complex SU decoder which strips-off the SUs transmitted signal from the received signal and carries out energy detection spectrum sensing in the remaining signal. However, this method only works under the ideal assumption of perfect signal decoding which is very difficult to achieve in practice. In [22], a spectrum monitoring method is proposed for OFDM based CR by observing a change in the number of reserved subcarriers. This method sacrifices its throughput as a certain number of subcarriers are always reserved. The method in [26] requires an SU transmitter to periodically insert zero-energy intervals in selected subcarriers and as a result this method suffers from low throughput performance. Hence, increasing the CR throughput under the constraint of reducing interference to the PU is a real challenge. Apart from these techniques, there are FD (Full duplex) techniques which are extensively used in CR to assist SUs in simultaneous sensing and transmission [28–32]. With FD radios equipped at the SUs, it can simultaneously sense and access the vacant spectrum and thus significantly improves sensing performance and data transmission efficiency. However, the performance of these techniques [28–32] solely depends on the self-interference cancellation (SIC) capability of the system. Hence, we believe that simpler and more practically implementable spectrum sensing and monitoring techniques are lacking in the literature.

Different from these techniques, in this thesis, we consider an error vector magnitude (EVM) technique suitable for OFDM based CR. EVM measures the square root of the error vector power, which is defined as the mean squared error (MSE) normalized by the mean squared signal power. EVM is being increasingly employed in the wireless industry and has already become part of several wireless standards like

W-CDMA and the IEEE 802.11 family of WLAN, LTE, 5G etc [33, 34]. These standards use EVM to measure the inband error of digitally modulated signals. EVM has been defined originally as a performance metric for transmitters, but now it is used in receiver design and for more general signal analysis [35]. However, this metric has been overlooked in the context of CR despite having significant advantages. One advantage is that the SU transmitted signal gets canceled out during EVM calculation, therefore we do not require any sophisticated SIC method as required by FD techniques. The other advantage is that the EVM technique utilizes fewer symbols, does not require any subcarriers to be reserved and provides results much before demodulation and decoding thus gives us real time results. The focus of this thesis is on developing a new spectrum monitoring method using EVM technique for OFDM based CR networks. The primary objectives are to increase the detection performance and throughput enhancement of the CR enabled SUs.

1.3 Thesis Contributions

This thesis explores and evaluates the application of EVM to detect the PU during ongoing SU communication and develops a new inband sensing scheme for OFDM based CR system. Previously spectrum monitoring techniques have been explored for CR systems that resulted in low throughput performance and high computational complexity. Moreover, the EVM metric has not been used either for spectrum sensing or monitoring purpose in OFDM based CR system. Our method is generic and can measure EVM using any embedded pilot tone pattern. Throughout the thesis, we have followed the IEEE 802.11 ac pilot structure by way of practical example although the analysis done in this thesis is general and may apply to any pilot tone pattern.

The novel contribution of this thesis can be summarized as follows.

- The thesis addresses the problem of reduced throughput due to the periodic spectrum sensing and monitoring in CR networks. The problem is approached

by proposing a novel algorithm using the EVM metric which has not been exploited for such purposes in the context of CR. The proposed method

(a) exploits the pilot tones that are inherent to many OFDM based standards which are typically used for channel estimation and synchronization purposes,

(b) utilizes fewer symbols and performs spectrum observation at the SU receiver,

(c) is direct and gives us real time results as the EVM metric can be obtained much before demodulation and decoding of the received packets.

- A new quickest spectrum sensing technique is proposed based on the EVM based change detection to analyze the detection delay performance.

- The performance of the proposed method is evaluated both analytically and via simulations. These evaluations

(a) reveal the CROC performance of the proposed detection method in AWGN channel. The results show that EVM based detector performs better than the conventional energy detector.

(b) show that the throughput performance of EVM based detection is significantly higher than energy based detection.

(c) show that CUSUM EVM performs better than CUSUM energy detection.

(d) reveal that for lower false alarm rates quickest EVM always outperforms the quickest energy detection method.

(e) shows that the asymptotic approximation provided for the Bessel function over-estimates CUSUM, particularly at lower values of interference to noise ratio (INR).

1.4 Thesis Organization

The rest of this thesis is organized as follows:

Chapter 2

This chapter presents a short summary of the different spectrum access techniques. This is followed by a review of the different types of spectrum sensing methods for CR networks that are in use today. Next, an overview of OFDM based CR is presented along with the spectrum monitoring method used in this thesis.

Chapter 3

In this chapter the EVM based PU monitoring technique is described and its analytical and simulated performance are presented. The proposed technique detects the reappearing PU during ongoing SU transmission. This technique also has the ability to find the location of the bits corrupted by the PU's arrival by looking at the EVM values of the pilot symbols.

Chapter 4

The focus of this chapter is to analytically characterize the performance of the EVM based detector proposed in chapter 3. First the PDF of the EVM test statistic is presented. Next, the detection performance is analyzed with the CROC curves in terms of type I and type II error probabilities. Then, the joint PDF of the test statistic towards the detection of the reappearing PU is presented. Two types of PU are considered in this chapter. In order to simplify the analytic results on detection performance, the exact distribution of the EVM test statistic is approximated by a Laplacian approximation. Finally, system performance is evaluated by simulation primarily for the additive white Gaussian noise (AWGN) channel.

Chapter 5

This chapter shows the application of the sequential change detection also known as the quickest detection method to the EVM based detector discussed in chapter 4. The aim of this chapter is to develop a statistical framework to analyze detection delay,

subject to certain false alarm constraints and more importantly to design a scheme that can minimize the detection delay. To analyze the quickest detection, Page's CUSUM algorithm which is optimal by Lorden's minimax formulation is described. An asymptotic analysis of the CUSUM EVM algorithm is also provided.

Chapter 6

Finally, this chapter summarizes our novel contributions of the thesis and outlines possible directions for future research

1.5 List of Publications

This section lists the publications resulting from this PhD study.

Journal:

1. **Nepal, N**.; Martin, P.; Taylor, D.; Coulson, A.,"Performance Evaluation of EVM based Primary User Monitoring in Cognitive Radio Systems", submitted to *IET Communications*, Under Review, June 2018.

2. **Nepal, N**.; Martin, P.; Taylor, D.; Coulson, A.,"On the Performance of Quickest Spectrum Sensing for EVM based Change Detection", submitted to *IET Communications*, Under Review, July 2018.

Conference:

1. **Nepal, N**.; Martin, P.; Taylor, D.,"EVM based Primary User Monitoring in Cognitive Radio Systems", in *IEEE Vehicular Technology Conference (VTC Fall)*, Montreal, Canada, pp.1-5, 18-21 Sept. 2016.

Chapter 2

Background and Literature Review

This chapter provides the relevant background information required for the subsequent chapters. Section 2.1 presents CR network paradigms with their underlying assumptions about network side information and the practicality of obtaining this information. In Section 2.2, an overview of different types of spectrum sensing methods are given. Section 2.3 discusses OFDM based CR systems. A brief overview of spectrum monitoring approach in OFDM based CR is also discussed. Finally, Section 2.4 concludes the chapter with a short summary.

2.1 Cognitive Radio Network Paradigms

Based on the spectrum access techniques, CR networks can be broadly categorized using underlay, overlay and interweave paradigms [13]. There are diverse opinions available in the literature about the use of the terms underlay, overlay and interweave [13, 36]. In this thesis, we follow the classification provided by A. Goldsmith et al in [13]. These network models basically differ depending on the knowledge that is needed to coexist with the primary network. The knowledge may include information regarding the activity, channel, encoding strategies and transmitted data sequences of the PUs with which the SUs share the spectrum. Apart from this, a hybrid paradigm which uses the combination of these three paradigms is considered as a potential spectrum access technique in CR [37], [38], [39]. Fig. 2.1 graphically illustrates these paradigms which are briefly discussed in the following paragraphs.

2.1.1 Underlay Paradigm

Under the underlay paradigm, simultaneous transmission of the primary and the secondary users are allowed as long as the interference level at the PU side remains acceptable. The maximum allowable interference level at the PU is measured by an interference threshold that guarantees the reliable operation of the PUs regardless of the SUs spectrum utilization [13, 40–43]. Beamforming techniques with the help of multiple antennas can be used to maintain the interference at the PU within tolerable limits [44]. In many cases, the SU transmitter spreads its power across wider bands so that the transmission does not exceed an acceptable level of interference to the PU receiver [36]. This technique can be used in ultra-wide-band (UWB) or spread spectrum communication [13,41–43]. Restricting transmit power leads to a significant reduction in channel capacity and radio coverage in the secondary network. Based on the worst case assumption that PU transmits all the time, this approach does not rely on detection and exploitation of spectrum white space.

Although, SUs can obtain the spectrum opportunities in the presence of PUs by underlay access, the available spectrum is not fully utilized in idle states because the transmit power is always restricted by the interference threshold regardless of the PU's state. The possibility of transmitting without interruption is an advantage that underlay access offers, but this mode can transmit with maximum rate only when the PU is silent. Transmission is also restricted to short-range communications due to the strict transmission power limitations [13, 41, 44].

2.1.2 Overlay Paradigm

Like the underlay approach, the overlay paradigm also allows concurrent primary and secondary transmissions [40]. This paradigm assumes the SU to have adequate knowledge of the PU codebooks and messages, and that channel gains mitigate the interference at the secondary receiver. The interference mitigation technique can be carried out with the help of advanced sophisticated signal processing techniques such

as dirty paper coding (DPC) or SIC [13, 41, 43, 45]. The codebook information can be obtained if the PUs follow a uniform standard for communication based on a publicized codebook or they could broadcast their codebooks periodically [46]. A PU message might be obtained by decoding the message at the secondary receiver.

The overlay model assumes that the PU message is known at the secondary transmitter when the PU begins its transmission. The SUs utilize this knowledge and assign part of their power to assist (relay) the PU transmissions. A two user interference channel where the secondary transmitter has knowledge of the PU's message can be considered as a simplistic example of an overlay CR network. By careful choice of the power split, the increase in the PUs SNR due to assistance from cognitive relaying is exactly offset by the decrease in the PUs SNR due to the interference caused by the remainder of SUs transmit power used for its own communication [13, 43, 45]. Implementing DPC is highly complex [47] and is feasible only when perfect non-causal knowledge of PU channel state information (CSI) is available [45]. Concurrent primary and secondary transmissions in the overlay technique can potentially provide higher throughputs but this improvement quickly disappears as the distance between the primary and secondary transmitters increases [36]. In practice, this approach is difficult to implement due to the high level of cognition and cooperation required between primary and secondary systems.

2.1.3 Interweave Paradigm

The interweave approach is the original approach to CR [14]. It is the first concept evolved with CR communication. It encompasses interference avoidance or opportunistic techniques which require SUs to communicate opportunistically using spectral holes in space, time and frequency which are not occupied by the PUs [13, 41]. SUs opportunistically using these spectrum holes without affecting the PUs is a technique called interweave communication [41, 43, 48]. The SU is permitted to utilize the spectrum when the PU is inactive. In this case, the SU transmission power is not restrained as the PU interference tolerance level is no longer an operational con-

dition but is limited by the range and duration of available spectral holes [49]. This intermittent nature of interweave communication may delay some application flows significantly (eg, transmitting a short file, fetching a web page etc.) if the PU happens to arrive while the SU is scanning for a new available channel.

Under this paradigm, an accurate spectrum sensing mechanism is required to find the spectrum holes so that the SU does not cause any harmful interference to the PU. It should also be noted that when the PU reappears in a certain licensed channel, the SU should immediately vacate the channel and be switched to another unoccupied channel. We have considered interweave network paradigm throughout the thesis.

2.1.4 Hybrid Paradigm

Hybrid paradigms using a combination of the aforementioned paradigms have great potential to improve the efficiency of spectrum sharing [37], [38], [39]. Fig. 2.1 illustrates the idea of hybrid access method. Under interweave spectrum access, SUs are not allowed to cause any interference to the primary network. Therefore, the SU must periodically monitor the radio spectrum to detect spectrum occupancy and only opportunistically communicate over spectrum holes. This approach may reduce effectiveness of spectrum utilization. On the other hand, interweave spectrum access may offer superior system performance, such as outage probability and error probability as compared to underlay and overlay networks given the same propagation environment [50]. In underlay spectrum access the SUs and PUs can simultaneously share the same licensed spectrum provided that the secondary transmit power is adjusted to meet the interference power constraint imposed by the PU. The spectrum utilization is improved effectively in underlay spectrum access compared to the interweave scheme as spectrum can be utilized at any time.

Different from the traditional three spectrum access modes, in a hybrid interweave-underlay CR system, the SU adaptively switches between interweave and underlay approaches according to the state of the spatial spectrum [51]. In particular, one

transmission slot of the hybrid cognitive transmission always consists of two phases, a sensing phase and a data transmission phase as in [52]. In the first phase, the SU, listens to the spectrum allocated to the PU to detect the state of the PU. In the second phase, the SU adapts its transmit power based on the sensing results. If the spectrum is sensed idle in the first phase, taking advantage of not requiring the interference constraint, the SU operates in interweave mode with maximum transmit power. In contrast, if the PU is active, the SU must switch to underlay mode under the interference power constraint imposed by the PU.

The throughput performance of an interweave system is seriously affected by the quality of spectrum sensing, while underlay CR systems manipulate their transmission strategy according to a fixed interference temperature constraint, without exploiting the traffic pattern (or activity profile) of the PU. Hence, through combining interweave and underlay spectrum schemes, the spectrum utilization can be improved. The interweave approach ignores the interference tolerance capability of the PUs and focuses only on the bursty PU traffic. The possibility of having secondary transmission with full power is neglected in the underlay based approach. In this context, the interweave-underlay hybrid spectrum can overcome the aforementioned drawbacks and achieve higher secondary throughput while protecting the PUs [53–57].

2.2 Overview of Spectrum Sensing for Cognitive Radio

Spectrum sensing refers to the process of sensing a channel for a fixed amount of time called sensing time to detect PU signals in order to determine its availability to SUs [58, 59]. Once a channel is sensed idle, it can be utilized by SUs until its PU's return to the channel [9]. Spectrum sensing can be categorized into two types [59]: out-of-band sensing and in-band sensing. Out-of-band sensing is searching for an idle channel by sensing multiple channels sequentially until an available channel is found.

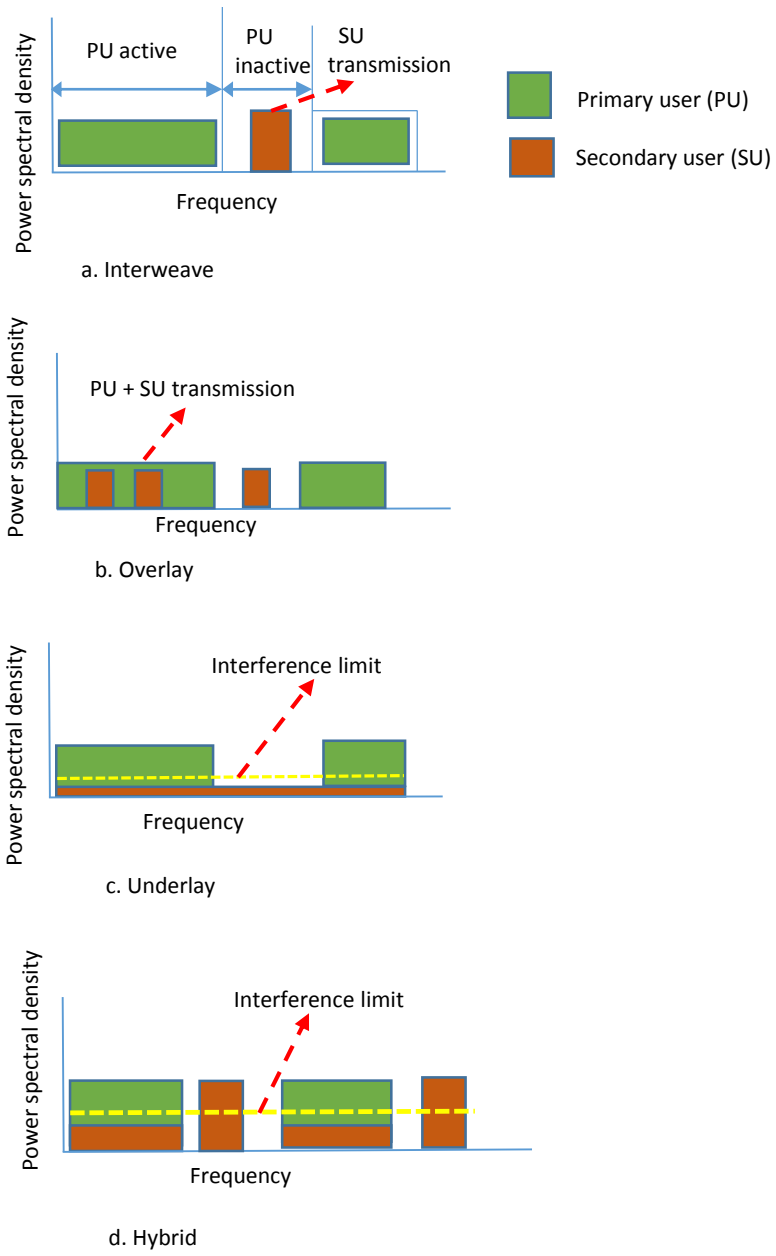

Figure 2.1: CR network paradigms.

In-band sensing monitors a channel periodically while using it, in order to prevent interference with the PU. Since the PUs are given priority in accessing their own channel, SUs must vacate the channel as soon as they detect the PUs. It is desirable to perform in-band sensing as frequently as possible for fast detection of the returning PUs. However, such in-band sensing incurs significant overhead and requires the SU to stop its transmission periodically. This periodic spectrum sensing requires tradeoff

between maintaining high communications efficiency in the secondary network and avoiding disruption to the primary network.

In this thesis, we propose a novel in-band sensing technique that permits SUs to perform spectrum monitoring during transmission. Generally, spectrum sensing techniques can be classified as primary transmitter detection, primary receiver detection and interference management [58]. Primary transmitter detection is based on detecting the primary user transmission using local observations at the SU [59]. Primary receiver detection aims at finding the PUs that are receiving data within the communication range of a SU [9,58,59]. Interference temperature is an interference assessment metric proposed by the FCC which aims to measure the interference experienced by the PU [48]. Based on the difficulties that lie in employing primary receiver detection and interference temperature management, most of the literature on spectrum sensing focuses on primary transmitter detection to identify the presence or absence of the

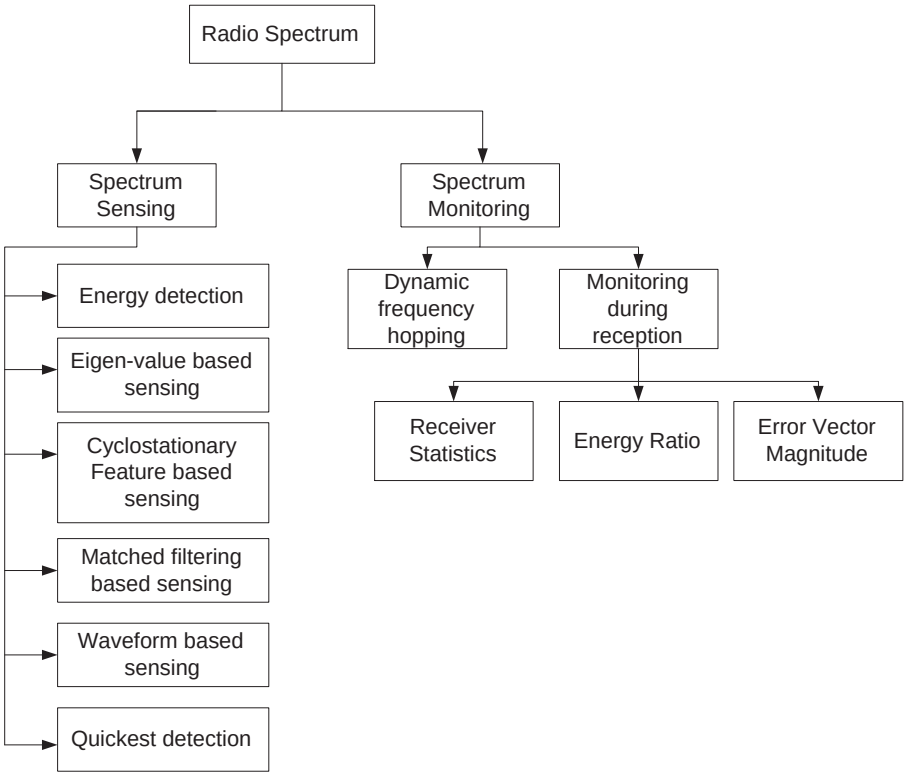

Figure 2.2: Classification for the spectrum sensing approaches.

PU signal transmission [6, 9, 59]. A detailed survey of various spectrum sensing techniques for primary transmitter detection are presented in [6, 58–66]. These different spectrum sensing techniques for primary transmitter detection are listed in Figure 2.2. They have their own operational requirements, advantages and disadvantages from the practical perspectives which are discussed below.

2.2.1 Energy Detection Based Spectrum Sensing

Energy detection is the most commonly used sensing technique because of its low computational and implementation complexities [6, 41, 60, 67–72]. It is known as a blind detection technique as it does not require any information about the PU signals [41,60,67]. In this method, the energy in the signal, received by the SU is used to determine the presence or absence of the PU. Primarily, the decision statistic of the energy detector, which is defined as the average or total energy of a certain number of observed samples, is compared with a predetermined threshold in order to ascertain the presence or absence of the PU [6, 9, 41, 58, 60, 69, 70, 73]. The performance of the energy detector is evaluated with two parameters: probability of detection (P_D) and probability of false alarm (P_F) [6, 9, 60, 69]. P_D is defined as the probability of detecting the PU correctly while P_F is deciding that the PU is present while it is actually absent. The goal of energy detection is to maximize the probability of detection subject to a predefined probability of false alarm [6, 67].

Energy detection can be formulated as a binary hypothesis testing problem [6, 41, 60, 67–70],

$$\begin{aligned} H_0 &: y(l) = w(l) \\ H_1 &: y(l) = \overbrace{x(l) * h(l)}^{s(l)} + w(l). \end{aligned} \tag{2.1}$$

Here, $y(l)$ is the received signal with $x(l)$ and $w(l)$ denoting the PU signal and the zero mean, additive white Gaussian noise (AWGN). The channel impulse response is denoted by $h(l)$ and $s(l)$ is the received PU signal with channel effects. In the absence

of the PU, hypothesis H_0 is true and $y(l)$ consists only of noise i.e., $w(l)$ whereas the PU signal $s(l)$ is present along with $w(l)$ under hypothesis H_1. The corresponding test statistic is obtained as,

$$Z(y) = \frac{1}{L}\sum_{l=0}^{L-1}|y(l)|^2, \tag{2.2}$$

where L is the length of the observation sequence. Furthermore, the test statistic Z has a central chi-square square distribution with $2L$ degrees of freedom for H_0 hypothesis, while it has a non-central chi square distribution with $2L$ degrees of freedom for H_1 hypothesis [74]. Based on the central limit theorem, when the number of samples is large ($L > 250$), Z can be accurately approximated by a Gaussian distribution [75, 76]. The corresponding approximated expressions of P_F and P_D for AWGN channel can be expressed as

$$P_F = Pr(Z(y) > \lambda|H_0) = Q\left(\frac{\lambda - \sigma_w^2}{\sigma_w^2/\sqrt{L}}\right) \tag{2.3}$$

$$P_D = Pr(Z(y) > \lambda|H_1) = Q\left(\frac{\lambda - \sigma_w^2(1+\gamma)}{\sigma_w^2(1+\gamma)/\sqrt{L}}\right), \tag{2.4}$$

where $\gamma = \frac{\sigma_s^2}{\sigma_w^2}$ is the instantaneous signal to noise ratio (SNR) and σ_s^2 and σ_w^2 denote the variance of the received PU signal with channel effects and noise, respectively. $Q(.)$ is the standard Gaussian complementary cumulative distribution function and λ is the predefined threshold. In general, the variance of the PU signal is unknown to the CR, and hence λ is calculated by the assumed noise variance and desired P_F. As it is impossible to know the exact noise variance in practice, the P_F and P_D results are highly dependent upon the accuracy of noise variance estimate. Therefore, a small variation in noise variance estimation can cause significant loss in the detection performance.

Although energy detection is easy to implement, it suffers from different drawbacks such as noise variance uncertainty, inability to differentiate interference from PUs and

the noise, and poor performance under low SNR values [77].

2.2.2 Matched Filtering Based Detection

Matched filtering based detection is the optimal detection technique in stationary Gaussian noise channels when the information about the PU signal is known to the SU as it maximizes the received signal-to-noise ratio (SNR) [9,78]. The matched filter output is compared with the threshold in order to verify the existence of the PU. This detection scheme requires less time to achieve high processing gain, but it requires a priori knowledge of the PU signal such as modulation type, frame format, pulse shape as well as accurate synchronization at the SU [69, 72, 79]. In CR, such knowledge is not readily available to an SU, thus making it a highly complex detection scheme to implement [6,59,72]. Because of these drawbacks, the match filtering based detection technique is not practical in the context of spectrum sensing [80].

2.2.3 Cyclostationary Feature Based Sensing

Cyclostationary based detectors exploit the cyclostationary features of the received signals to detect the presence of the PU in a given spectrum [48,60,72,73]. Cyclostationary features of a signal may be related to its carrier frequency, symbol structure such as cyclic prefix, chip, code or hop rates, as well as their harmonics, sums and differences [81]. As different transmission systems have different cyclostationary features; therefore with sufficient knowledge the detector can distinguish different types of PUs. Detection is based on the cyclic spectral density and is able to separate the PU signal from noise due to the fact that white noise has little correlation hence its cyclic spectral density is weak. Therefore, a cyclostationary feature detector can perform better than an energy detector in discriminating against noise due to its resilience to the uncertainty in noise power [82]. However, it is computationally complex and requires very long observation times [73,83]. Moreover, it requires the knowledge of the cyclic frequencies of the PUs, which may not be available to the SUs. Also, cyclostationarity can be destroyed by channel fading and is susceptible to sampling

clock offset [84].

2.2.4 Eigenvalue Based Sensing

Eigenvalue based sensing utilizes functions of the eigenvalues of the sample covariance matrix as test statistics. The main idea behind eigenvalue based sensing is to exploit correlation in the received signal if a PU is present. The eigenvalue distributions of the sample covariance matrices differ under the H_0 and H_1 hypotheses. By exploiting this difference, eigenvalue based techniques make decisions about the presence or the absence of the PU signal. This sensing scheme does not require knowledge of the noise variance information in the observation. Thus, it is considered as a potential solution to the challenging and problematic noise uncertainty conditions [85–87]. As noise variance has no use in eigenvalue based sensing, changes or uncertainty of noise variance have only a minor effect on sensing performance. However, this sensing method still has the drawback of high implementation complexity.

2.2.5 Waveform Based Sensing

Waveform based detectors are a simplified version of the matched filtering detection method, where the exact signal transmitted by the PU is required for optimum detection. These detectors aim to detect a prior known signal or sequence expected within the PU signal through correlation detection [69, 77, 88]. Most existing wireless communication systems introduce pre-known patterns such as pilot signal, preamble, etc. to assist synchronisation, signal detection and other purposes [72]. The detection of the PU signal is carried out by performing correlation between the received signal and a known copy of the pattern. Waveform detectors have little implementation complexity as knowledge available to the SU detector is restricted to signals known through standards and specifications. The waveform detector assumes that a pattern exists in the PU signal that is perfectly known to the SU and detectable. However if the detector is required to detect the wide range of PU, the database of known patterns may become large and complex to manage. In general, waveform

detectors have better detection performance and require shorter time over the energy detector [69, 77].

2.2.6 Quickest Detection

Quickest detection is a form of sequential change detection, that differs fundamentally from block detection and the sequential hypothesis testing method discussed above. This detection scheme does not aim to decide between the hypotheses H_0 and H_1, instead it tries to detect a change of the hypothesis with minimum delay [89,90]. The block based detection approaches aim to maximize the detection probability subject to constraints on the false alarm probability. In addition to the detection probability, the detection delay is also an important performance metric in CR. If a PU stops transmission, then a SU should detect this event quickly, in order to be able to start its own transmission quickly. A small detection delay will allow SUs to take short transmission opportunities. On the other hand, if the PU starts transmission, the SU should detect this event as quickly as possible, in order to vacate the band for the PU. A small detection delay will allow the design of the spectrum reuse scheme that has minimal impact on the licensed users.

In quickest detection problems, samples are observed sequentially. Initially, the samples are drawn from a fixed distribution. At an unknown time, the distribution will change if the PU becomes operational. The objective is to detect the occurrence of the change with minimal delay, such that the delay between the point at which the change actually occurs and the point at which the algorithm detects such a change is minimized, subject to a certain false alarm rate [41, 90, 91]. Thus, agile and robust detection can be obtained by utilizing the theory of quickest detection [6, 92].

2.2.7 Error Vector Magnitude (EVM) based Sensing

EVM based sensing, which is the focus of this thesis, utilizes the square root of the ratio of the mean error vector power to the mean reference power [93]. In a perfect

system, free of noise and non-linearities, the measured vector and the reference vector would be identical, and the EVM would be zero. Conversely, a large EVM suggests that the measured symbol is significantly displaced from the ideal reference vector which can only be the result of noise, distortions and interference effects. EVM is being increasingly employed in the wireless industry as well as in the research community [94]. It can easily identify the type and source of degradation in a wireless communication system. It is considered as a more convenient symbol level performance metric than bit error rate [95]. It differs from traditional spectrum sensing in that, it doesn't require a quiet period for spectrum sensing and allows simultaneous sensing and transmission in CR. In this technique, spectrum sensing is performed at the SU receiver.

EVM can be computed much before demodulation and decoding of the received packets, thus giving the real time result which is a strong requirement for detecting the reappearing PU in CR [93, 96]. Between consecutive sensing intervals, traditional spectrum sensing provides no information about the status of the frequency band. If the duration of sensing is too large, then the SU network throughput becomes low and if the duration of sensing is too small, then the interference to the PUs becomes excessive. EVM based sensing helps to get rid of this kind of trade-off in CR since the SU can monitor the frequency band without interrupting their communications. The method supplements traditional spectrum sensing and provides enhanced communications efficiency. Mainly, the decision statistic of the EVM detector, which is defined as the root mean square (RMS) error between the transmitted symbol and the received symbol measured over a certain number of observed samples, is compared with a predetermined threshold in order to know the presence or absence of the PU. The performance of the EVM detector is evaluated with two parameters : type I and type II error probability which are often called probability of false alarm and probability of missed detection.

2.3 OFDM Based Cognitive Radio

OFDM is a multi-carrier modulation technique which has proven to be a reliable and effective transmission method in many wireless systems including digital video broadcasting (DVB-T/T2), LTE, IEEE 802.16d/e WiMAX, IEEE 802.11a/g wireless LAN, and the first CR standard wireless regional area network, IEEE 802.22 WRAN. It splits the data into blocks and every block is modulated using closely spaced orthogonal subcarriers. This splitting decreases the inter-symbol interference (ISI) by making the symbol duration large enough so that the channel induced delay spread are insignificant ($< 10\%$) fraction of symbol duration. It has been recognized as a potential transmission technology for CR systems due to its several advantages for high bit-rate communications as well as its capability to dynamically allocate unused spectrum among CR users [97]. This OFDM technique provides spectral efficiency, which is most required for CR systems. It is very flexible and adaptive technology so that the subcarriers can be turned on and off according to the environment and can assist CR dynamically.

The need for complex equalizers at the receiver side is reduced while using OFDM. Other advantages of OFDM include robustness against narrow band interference (NBI), scalability and easy implementation using the fast Fourier transform (FFT) algorithm [98]. On the other hand, OFDM systems have their own challenges [97]. The OFDM signal has a noise like amplitude with a very large dynamic range referred as peak to average power ratio (PAPR) which may result in inter-carrier interference (ICI). Moreover, it is vulnerable to synchronization non-idealities, including the symbol timing offset (STO), carrier frequency offset (CFO), and sampling frequency offset(SFO) which needs special treatment [20, 99]. A typical block diagram of the OFDM based CR transmitter and receiver is shown in Fig. 2.3. Let $d = (d_1, d_2, ...d_n)$ be a data stream modulated to $x = (x_1, x_2, ...x_n)$ by an M-ary Phase Shift Keying (MPSK) or an M-ary quadrature amplitude modulation (M–QAM) modulator. The modulated data stream is then split into N slower data streams using a serial to

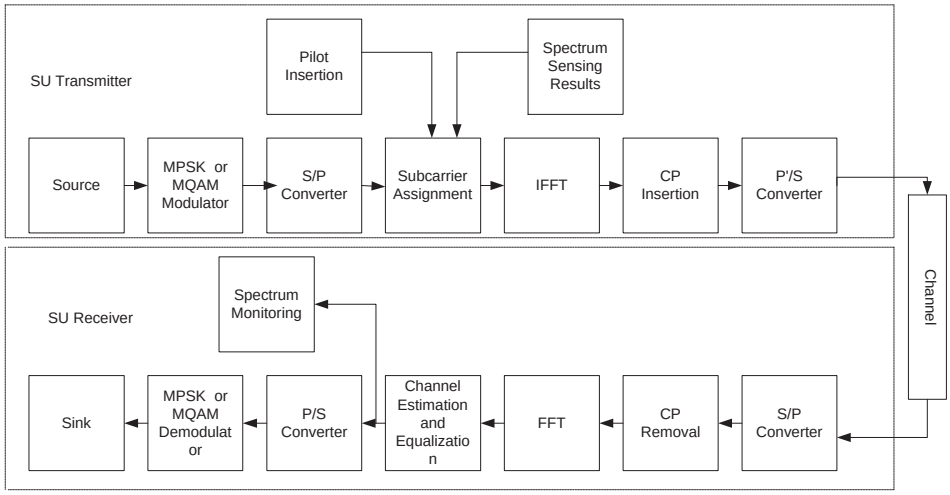

Figure 2.3: Secondary user transmitter and receiver structures.

parallel (S/P) converter. Each of these streams is transmitted on one of the N orthogonal subcarriers and then summed up to give a composite OFDM signal. We assume a contiguous block of spectrum is available for SU data transmission which allows the spectrum to be fully utilized. This decision is made by employing spectrum sensing and channel access techniques. We assume that the information from spectrum sensing about the licensed users is available at the transmitter side. We assume perfect spectrum sensing information at the start of monitoring [22, 27]. If initial spectrum sensing is not perfect, then it will degrade the spectrum monitoring performance. Based on the results of spectrum sensing we modulate data and pilot symbols on the set of available subcarriers for SU transmission. The SU transmitter that sends packets is referred to as the source and a SU receiver that receives the packets is referred to as a sink. Our system model, shown in Fig. 2.3, starts communication after a secondary radio has gained access to a frequency band. After pilot insertion, the modulated data $X(k)$ is converted into a time domain signal by taking the N-point IFFT. Thus the transmitted OFDM signal in the discrete-time domain, excluding guard interval can be expressed as

$$x(n) = IFFT\{X(k)\} = \frac{1}{N}\sum_{k=0}^{N-1} X(k)e^{j2\pi kn/N}, \quad n = 0, 1.....N-1, \tag{2.5}$$

where k is the subcarrier index $(0, 1, ...N-1)$ with N being the total number of subcarriers. To prevent possible ISI in OFDM systems, a guard interval larger than the expected delay spread is added. This guard interval includes the cyclically extended part of OFDM symbols in order to eliminate inter-carrier interference (ICI).

At the receiver, the inverse blocks are applied. After timing synchronization and frequency synchronization, the cyclic prefix is removed. Then the received OFDM symbol is transformed again into the frequency domain through a N point DFT. The channel is then estimated and the received data is equalized after which the spectrum monitoring is done. The complex data output is then mapped to bits again through the demodulator and applied later to the received block to recover the original source bits.

2.3.1 Spectrum Monitoring in OFDM Based Cognitive Radio

In interweave CR networks, the SU must sense the spectrum to detect its availability prior to communication. Moreover, the SU should be able to monitor the spectrum in order to vacate quickly as soon as PU appears in the current operating channel. During monitoring time, the SU does not access the spectrum and this period is called the quiet period [21]. The traditional spectrum monitoring techniques rely on periodic spectrum sensing during the quiet period. This periodic spectrum sensing suspends SU transmission periodically leading to a significant reduction in CR network throughput. In this periodic spectrum sensing an inherent tradeoff always exists which results in either compromising SU throughput or PU quality of service (QoS).

Therefore, it is always desirable to search for a method by which SUs can monitor the frequency band without interrupting their communications. Such methods can detect the reappearance of the PU during SU transmission. This monitoring technique supplements the traditional spectrum sensing and provides enhanced com-

munications efficiency [22]. In fact, the signal construction for the SU can assist the spectrum monitoring to happen without involving quiet periods. If OFDM is considered as a physical transmission technique for SU, then a frequency domain based approach can be employed to monitor the spectrum during SU reception. One technique is to add either an additional feature to the ordinary SU OFDM signal or to exploit the inherent features of the OFDM signal like cyclic prefix and pilot tones. We are exploiting the inherent pilot tones in our monitoring system.

There have been several research efforts [68-75] into spectrum monitoring which does not halt ongoing SU communication. These [68-75] spectrum monitoring method differs from a conventional spectrum sensing method in that the monitoring method is applied during reception without any scheduling for quiet periods. A detailed schematic classification is provided in Fig. 2.2. In [23] a two stage approach for concurrent spectrum sensing and data transmission is proposed. It requires a long sensing duration, which degrades throughput and the delay. The algorithm in [24] has a complex SU decoder which strips-off the SUs transmitted signal from the received signal using successive interference cancellation (SIC) before performing sensing. The method in [25] assumes the PU status remains unchanged during the current SU frame, but in reality a PU may have short channel holding times, and the channel status can change frequently [15]. In [26], a method is proposed that facilitates PU detection while SU transmission is in progress. The proposed method requires a SU transmitter to use OFDM to insert periodic zero-energy intervals in a selected subcarrier and to detect the energy during each interval to achieve PU detection.

In [22], a spectrum monitoring algorithm is proposed for OFDM based CR in which PU reappearance can be detected during SU transmission. This is done by sensing the change in the signal strength over a number of reserved OFDM subcarriers. The assumption made is that the PU may have spectrum holes because it also uses OFDM. However, if the reserved tones from the SU are synchronized with those spectrum holes on the PU side, this algorithm will fail. Also, it impacts SU throughput

as some subcarriers will be used as reserved tones. Another spectrum monitoring approach is proposed in [27] that counts the bit error for each received packet and compares it to a threshold value. This technique is simple and adds little complexity to the system, but the bit error counts are subject to change with different RF impairments including phase noise, CFO and SFO. Hence, the bit error count will depend not only on the presence of a PU signal, but also on the characteristics of these impairments. In addition, bit error count requires demodulation and decoding of the received signal and perfect decoding is usually hard to achieve.

EVM is an alternate performance metric that can offer insightful information concerning these impairments [100]. It is evaluated during the process of demodulation and decoding [96]. All these impairments will degrade the EVM and therefore EVM provides a comprehensive measure of the quality of the radio receiver. Its characteristics provide information about the nature of the problem or where the signal is degraded [101], [102]. Calculation of bit error would require the received signal to go through the entire receive chain, while computation of the EVM using the received symbols would be quicker [102]. This is well suited for measuring the reappearance of the PU in CR. Our work [93] is the first to use it for spectrum monitoring purposes in CR.

2.4 Chapter Summary

This chapter has provided an overview of several concepts needed for the subsequent chapters in this thesis. Firstly, several CR network paradigms were introduced. Secondly, a brief overview of different types of spectrum sensing for CR were discussed. Furthermore, an OFDM based CR was discussed. Finally, an overview of spectrum monitoring algorithms was presented.

Chapter 3

EVM Based Primary User Monitoring in OFDM based Cognitive Radio Systems

3.1 Introduction

A brief overview of the spectrum monitoring technique in OFDM based CR was provided in the previous chapter. In this chapter, we present a spectrum monitoring technique, namely the EVM based PU monitoring technique, that is suitable for OFDM-based CRs. The channel monitoring scheme consists of a series of sensing intervals which are also called quiet periods [21]. During quiet periods, the SU does not utilize the spectrum. Once the PU is detected, the SU discards the channel for a finite period of time and may select another channel to resume communication [18]. Although the quiet period is essential in the CR system, it causes performance degradation which reduces throughput and increases latency. This frequent interruption of SUs during sensing causes significant degradation in their spectral efficiency [27], [26]. In addition, even if the SU is willing to suffer a reduction in spectral efficiency by ceasing communications periodically, it has no opportunity to detect PU activity that is initiated between consecutive sensing periods. Thus, with traditional spectrum sensing, SUs are very likely to interfere with a PU that begins transmitting while the SUs are communicating. Also the interval between sensing periods can increase the latency between the start of PU transmission and the end of the SU transmission, which will be a concern for 5G systems where low latency is required [103].

Unlike spectrum sensing, spectrum monitoring involves detecting the emergence of PUs during periods in which the SUs are communicating. If spectrum monitoring determines correctly that there is no PU in the band, then the time that would have been spent performing spectrum sensing is used to deliver packets in the CR network. If spectrum monitoring detects a PU in the band during a time period in which spectrum sensing would not have been scheduled, then the disruption to the PU can be terminated more quickly. Thus the spectrum efficiency of the CR network is improved and the impact of SU communications on the PU is reduced. There are several approaches [27], [26], [104], [22] designed for spectrum monitoring, with each technique having its own merits and demerits. Different from these techniques, the EVM technique utilizes fewer symbols, provides results much before demodulation and decoding, thus giving us real-time results. Parts of this chapter have been published in [93].

The remainder of this chapter is organized as follows. In Section 3.2, a basic EVM model is described. Section 3.3 provides a system model for PU monitoring in OFDM based cognitive radio. In Section 3.4, the IEEE 802.11ac pilot structure is described. PU modelling and its detection mechanism is presented in Section 3.5. Simulation results are provided in Section 3.6. Finally, Section 3.7 ends the chapter with some concluding remarks.

3.2 Basic EVM Model

In this thesis, we use EVM as the primary figure of merit to measure the inband performance at a system level. This thesis explores and evaluates the application of EVM to detect the PU during ongoing SU communication and develops a new inband sensing scheme. EVM measures the inband error which is defined as the deviation of the estimated symbols $\hat{X}_l$ from the true data symbols X_l. The estimate $\hat{X}_l$ is obtained from the received (erroneous) symbols $\hat{Y}_l$ according to the standard, e.g., by applying equalization in WLAN. The EVM is the square root of the error vector

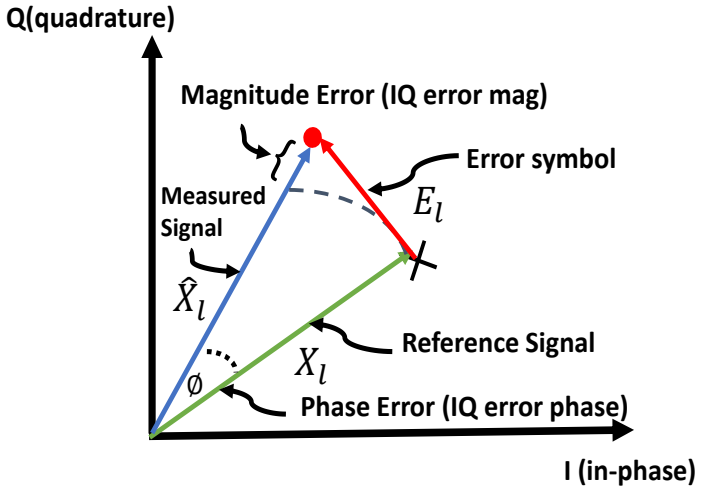

Figure 3.1: Illustration of error vector [3].

power, which is defined as the mean squared error (MSE) normalized by the mean squared signal power [105], [106]. As shown in Fig. 3.1 the resulting error (E_l) is the difference between the measured $\hat{X}_l$ and ideal symbol X_l, i.e $E_l = X_l - \hat{X}_l$. The EVM is defined as [105]

$$EVM_{rms} = \sqrt{\frac{\frac{1}{L}\sum_{l=1}^{L}|X_l - \hat{X}_l|^2}{E_s}}, \tag{3.1}$$

where L is the number of symbols over which the EVM is measured, $\hat{X}_l$ is the normalized received l^{th} symbol as corrupted by Gaussian noise, X_l is the ideal/transmitted value of the l^{th} symbol X_l, and P_0 is the average power of the chosen modulation. For large L, we can write [105], [106], [107]

$$EVM_{rms} \approx \sqrt{\frac{N_0}{E_s}} = \sqrt{\frac{1}{SNR}}, \tag{3.2}$$

where $N_0/2{=}\sigma_w^2$ is the noise power spectral density (PSD). This direct relationship to the effective inband SNR during regular operation is a major reason for the popularity of EVM. However, it only holds for data-aided EVM analysis, i.e., the true symbol locations must be known in the analysis, which is assumed throughout the thesis.

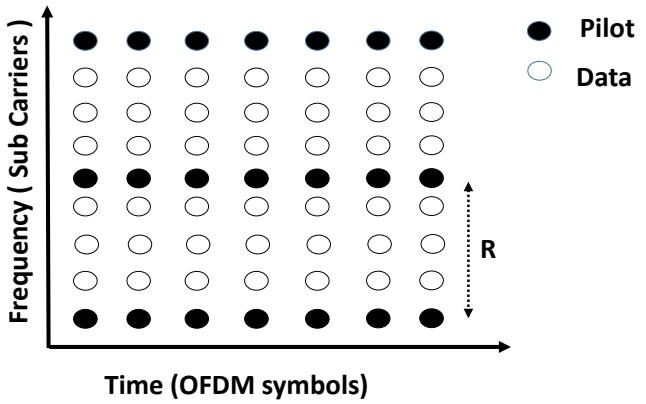

Figure 3.2: Comb type pilot arrangement.

3.3 IEEE 802.11ac Pilot Structure

In this structure, the pilot subcarriers are inserted into each OFDM symbol with equal spacing. It is assumed that the total number of pilot subcarriers is N_p and the insertion gap is R. Pilot symbols consume both power and spectrum and thus it is desirable to keep the number of pilot symbols as small as possible. Each OFDM symbol is composed of pilot and data subcarriers. Pilot subcarriers do not carry user data and instead are used to measure the channel. It is assumed that the index of the first pilot subcarriers η can be written as

$$\eta = \Big\{ k | k = mR + k_0, m = 0, 1, , ...N_p - 1 \Big\}, \tag{3.3}$$

where $k_0 \in$ [0,R). Based on the principle of OFDM transmission, it is easy to assign the pilot both in the time-domain and in the frequency-domain [108–110]. The pilot signal that is assigned to a particular OFDM block in the time domain is known as block-type pilot arrangement. This type of pilot arrangement is especially suitable for slow fading radio channels and is relatively insensitive to frequency selectivity. The pilot signals that are uniformly distributed within each OFDM block are known as a comb-type pilot arrangement [111]. This arrangement is suitable for a fast-fading channel where the channel condition changes between adjacent OFDM symbols. Here, the pilot signals are spread on selected subcarriers and repeated over multiple sym-

bols as shown in Fig. 3.2. The comb-type pilot arrangement is sensitive to frequency selectivity when compared to the block-type pilot arrangement system, i.e., the pilot spacing R must be much smaller than the coherence bandwidth of the channel. The advantage of the comb-type arrangement is its ability to track the variation of the channel caused by interference, noise and spurious signals [112]. As we are detecting PU interference in the channel, this has motivated us to use a comb-type pilot arrangement in our proposed system.

In an OFDM based CR system, the SU transmitter allocates the data transmission rate to subcarriers adaptively according to the different channel conditions. These channel conditions vary more when the assumption of constant PU occupancy state is taken away by considering a more realistic case where the PU randomly departs or arrives at the licensed channel during the secondary frame duration. Due to this, the channel condition changes significantly at the time of frame reception on the SU receiver. This makes the latter part of the frame considerably different from the one experienced by the preamble. In other words, the uncertainty of the CSI obtained at the preamble increases significantly with increase in the PU activities. These changes in the channel condition during a frame reception cause poor throughput performance of the SUs. When the channel is static throughout the frame, the channel can be estimated at the first transmitted OFDM symbol and this estimation can be used throughout the frame for equalization. However, when the channel is not static the channel must be estimated or at least tracked at every OFDM symbol. This can be achieved with the comb-type pilot arrangement [111].

3.4 System Model For PU Monitoring

We consider the CR system model shown in Fig. 3.3, where h_s and h_p denotes the channel coefficients from the secondary transmitter (SU TX) to the secondary receiver (SU RX) and from the primary transmitter (PU TX) to the SU RX respectively. The channel coefficients h_s and h_p are assumed to be static, Rayleigh distributed and

known at the SU RX. We assume initial spectrum sensing has been performed and the SU transmits an OFDM packet after detecting idle spectrum. Furthermore, we assume that SUs are capable of simultaneously transmitting and receiving on a given frequency band by using external hardware [26]. The OFDM synchronization blocks in the diagram are used to maintain frequency synchronization of the SU system. The received signal is converted to the frequency domain by the fast Fourier transform (FFT).

The pilots, spread over each OFDM symbol, are extracted and EVM is calculated as a difference between the received and transmitted pilots. If there is no PU in the band, then the calculated EVM involves only noise and receiver impairments such as estimation errors. Therefore, the EVM remains static as the impairment variance does not change significantly over time. As the PUs are oblivious to the SUs, they transmit at any time causing interference to the SU receiver. Once the PU appears, the EVM includes the PU interference and noise, which results in a step change in EVM [93]. In a realistic system a range of imperfections such as carrier leakage, IQ mismatch, non-linearity, local oscillator (LO) phase noise and frequency error are

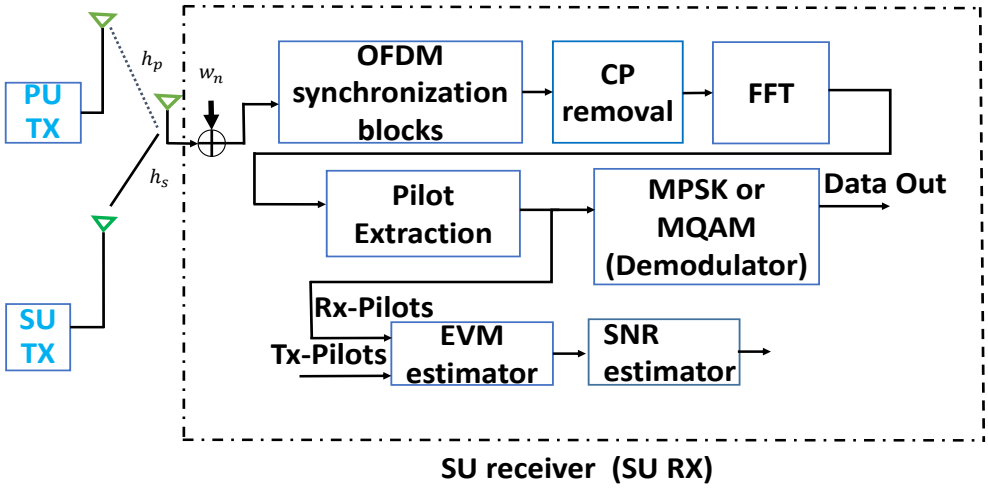

Figure 3.3: EVM-SNR estimator structure.

imposed which are considered harmful and need special treatment [113]. EVM can play a significant role in identifying and treating these impairments. We assume that EVM includes all these receiver impairments equally with and without the presence of the PU. In this case, the residual impairments, after best-effort correction, can be treated as Gaussian and contributing to the signal to noise ratio (SNR). Hence the step change in EVM from no PU to PU can equally well be detected with typical receiver impairments as with the ideal, no impairments, case. We denote the n^{th} sample of the l^{th} OFDM symbol in the time domain as $x(n,l)$. It can be obtained by taking the inverse FFT of the transmitted symbols $X(k,l)$ as

$$x(n,l) = \frac{1}{N}\sum_{k=0}^{N} X(k,l)e^{-\frac{j2\pi kn}{N}}, \tag{3.4}$$

where k is the subcarrier index and N is the FFT size of the OFDM system. The received time domain signal in the absence of the PU is given by

$$y(n,l) = h_s(n,l) * x(n,l) + w(n,l), \tag{3.5}$$

where $w(n,l)$ is a sample of complex AWGN with zero mean and variance of σ_w^2, i.e $w(n,l) \sim \mathcal{CN}(0,\sigma_w^2)$. The received signal in the frequency domain after the FFT can be written as

$$Y(k,l) = H_s(k,l)X(k,l) + W(k,l), \tag{3.6}$$

where $H_s(k,l)$ is the equivalent channel frequency response at the k^{th} subcarrier of the l^{th} OFDM symbol. $X(k,l)$ is the transmitted symbol for the k^{th} subcarrier of the l^{th} symbol and $W(k,l) \sim \mathcal{CN}(0,\sigma_w^2)$ is complex Gaussian noise. The frequency domain received signal in the presence of the PU is given by

$$Y(k,l) = H_s(k,l)X(k,l) + H_p(k,l)I_p(k,l) + W(k,l), \tag{3.7}$$

where $I(k,l)$ is the PU interfering signal at the k^{th} subcarrier of the l^{th} symbol and $H_p(k,l)$ is the equivalent baseband channel frequency response at the k^{th} subcarrier

of the l^{th} symbol. The EVM is defined as the root mean squared error between the transmitted symbol and received symbol after equalization and is given by [114]

$$EVM_{RMS}(k) = \sqrt{\frac{1}{E_s L}\sum_{l=0}^{L}\left|\frac{Y(k,l)}{H_s(k,l)} - X(k,l)\right|^2}, \tag{3.8}$$

where L is the number of symbols over which the EVM is measured and E_s is the average power for the chosen modulation. Since we are measuring the EVM using pilot tones embedded in OFDM, we follow the 802.11ac pilot structure as described in the previous section. Let $Y_p(k,l)$ be the received pilot symbols extracted from $Y(k,l)$, $X_p(k,l)$ be the known pilot symbols and $H_{ps}(k,l)$ be the channel transfer function at the η^{th} pilot subcarrier. Hence, (3.8) can be written as

$$EVM_{RMS}(k) = \sqrt{\frac{1}{E_s L}\sum_{l=0}^{L}\left|\frac{Y_p(k,l)}{H_{ps}(k,l)} - X_p(k,l)\right|^2}. \tag{3.9}$$

3.5 Hypothesis testing and test statistic

The conventional approach to spectrum sensing [21, 23–26] is to perform energy detection through the evaluation of a test statistic for a single long sensing period. The corresponding hypothesis test in AWGN can be written as

$$\begin{aligned} Y_p(k,l) &= W_p(k,l) && : H_0 \\ Y_p(k,l) &= H_p(k,l)I_p(k,l) + W_p(k,l) && : H_1, \end{aligned} \tag{3.10}$$

where $Y_p(k,l)$, $I_p(k,l)$, $H_p(k,l)$ and $W_p(k,l)$ are the received signal, transmitted PU signal, channel coefficient and the noise contribution at the pilot subcarrier, respectively. It performs periodic spectrum sensing and can't detect the PU during ongoing SU communication. The test statistic is given by

$$Z(k) = \frac{1}{L}\sum_{l=1}^{L}|Y_p(k,l)|^2 \tag{3.11}$$

and is compared with the preset decision threshold λ in order to decide whether a signal is present or not in that frequency band as

$$Z \underset{H_0}{\overset{H_1}{\gtrless}} \lambda. \tag{3.12}$$

In the proposed EVM scheme the SU can simultaneously sense and transmit [93]. Equivalently, the corresponding hypothesis expressions are given by

$$\hat{Y}_p(k,l) = H_{ps}(k,l)X_p(k,l) + W_p(k,l) \qquad : H_0$$

$$\hat{Y}_p(k,l) = H_{ps}(k,l)X_p(k,l) + H_p(k,l)I_p(k,l) + W_p(k,l) : H_1, \tag{3.13}$$

where $\hat{Y}_p(k,l)$ is the received signal in the frequency domain when the SU is simultaneously sensing and transmitting.

3.5.1 EVM Test Statistic

Let $E_p(k,l)$ denote the frequency domain error vector i.e.,

$$E_p(k,l) = \hat{Y}_p(k,l) - H_{ps}(k,l)X_p(k,l). \tag{3.14}$$

Substituting (3.13) into (3.14), the hypothesis test for the AWGN channel can be written as

$$E_p(k,l) = \begin{cases} W_p(k,l), & H_0 \\ \\ H_p(k,l)I_p(k,l) + W_p(k,l), & H_1. \end{cases} \tag{3.15}$$

The EVM test statistic can therefore be expressed as

$$Z_p(k) = \sqrt{\frac{1}{LE_s|H_{ps}(k,l)|^2} \sum_{l=0}^{L} \left| E_p(k,l) \right|^2}. \tag{3.16}$$

The novelty is the inclusion of the square root in (3.16) which affects the threshold λ_1. The test statistic in (3.16) is compared with the threshold λ_1 in order to decide

the presence of the PU in a given frequency band as

$$Z_p \underset{H_0}{\overset{H_1}{\gtrless}} \lambda_1. \tag{3.17}$$

3.6 PU Detection

The traditional frame structure model for the SU [16], consists of sensing slots and data transmission slots. The spectrum sensing is used for a fraction of the time and if the channel is determined to be unoccupied, then the SU is permitted to transmit during the remaining time. This suggests that the SUs must refrain from transmitting data when sensing the PU signal. The SU transmits only when it detects an idle spectrum. It is assumed that PU activity remains constant during a frame period. In practice, either synchronization is required between primary and secondary transmissions or the SU frame must be much shorter than the PU frame for the above assumption to be true. However, PUs can access the spectrum at any time, even during SU transmission. In this case the PUs may suffer from severe interference until the end of the SU transmission. The most stringent requirement for the SU is to sense the channel periodically in order to detect the emergence of PUs. One of the open spectrum sensing research challenges involves the adverse effect on spectrum efficiency caused by the need for secondary radios to stop communicating while performing spectrum sensing. Thus, with traditional spectrum sensing, the secondary radios are very likely to interfere with a primary radio that begins transmitting while the secondary users are communicating. More frequent spectrum sensing by secondary radios reduces the probability of interfering with the primary radios, but it also reduces the throughput and increases the delay for traffic in the secondary network.

Hence, we are interested in developing an algorithm that can detect the reappearance of the PU during SU transmission for OFDM based CR networks. We assume that the SUs use OFDM. We consider that the spectrum will be observed by the SU receiver

while it is receiving a packet and therefore the SUs need not cease transmissions while the frequency band is being examined. With this method the secondary radios can continue their communications while simultaneously monitoring the band to detect any transmissions that are initiated by the primary radios. The objective is to avoid the SUs losing transmission time due to sensing periods. We propose a PU detection technique in which the SU receiver performs spectrum observation while receiving packets. Our PU detection mechanism is more direct and is based on a metric that can be obtained immediately from the received packet, thus giving us results in real time. Unlike spectrum sensing, our system involves the detection of the emergence of PU signals during periods in which the SUs are communicating. Our proposed technique for PU detection can be used for a rate adaptation mechanism to maximize the spectral efficiency in the secondary system as well as to improve the throughput performance of SUs. The idea is to measure the EVM of the pilot symbols. Our EVM analysis is assumed for the data-aided receiver mentioned in Section 3.2, which can be used to estimate the SNR. By utilizing the mathematical relationship between EVM and SNR, the EVM estimator can reliably estimate the SNR of MPSK or MQAM signals in complex AWGN or multipath channel. A sharp decrease in the estimated SNR from one OFDM symbol to another will suggest that the channel has degraded significantly, possibly as a result of PU signal emergence. We will measure the EVM without considering the PU presence initially. However, due to PU arrival, the EVM value will be increased. Based on this, observation, we suggest that the PU detection can be determined by testing the SNR curve. If the estimated SNR decreases with the increase of symbol index, we will conclude that the PU has appeared in the channel.

3.6.1 PU modelled as Two-state Markov Chain

The performance of the CR network is highly dependent upon the PU activities. Hence, it is very important to model PU activity in CR networks. By keeping this in mind, several models in the literature have been proposed for modeling PU activity. Their purpose is to provide a realistic model of the PU activity pattern which is considered in the network by CR users in making spectrum decisions. In this regard, a

two-state Markov chain has been widely used in the literature for modeling PU activity. In the PU activity modeling by a Markov process, there are two states, i.e. 0 and 1 [115]. The IDLE state is represented by 0, i.e. spectrum is not occupied by PU, thus CR users can utilize it, while 1 shows BUSY state. Among many Markov models, the two-state Markov chain model is widely used in order to model PU activity [116–119]. The two states in this model are the BUSY and IDLE states. BUSY state indicates that a channel is currently occupied by the PU and is unavailable for CR, while the IDLE state indicates that a channel is free and there is no PU activity on the channel.

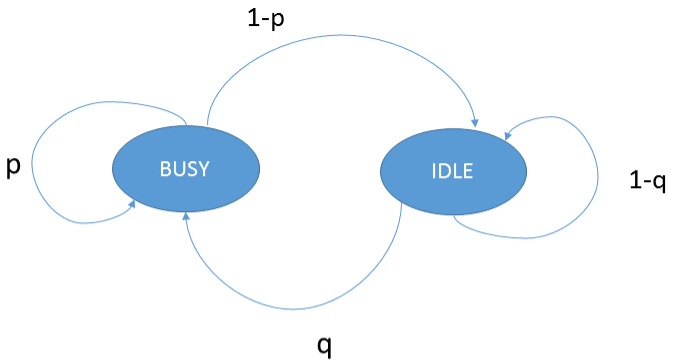

Figure 3.4: Two-state Markov chain model.

Fig. 3.4 illustrates the two-state Markov chain model. In this figure, if the channel is currently in the BUSY state then the probability that the next state of the channel will also be BUSY is p, while the probability of the next state being IDLE is 1-p. Similarly, if the channel's current state is IDLE, then its probability of remaining IDLE is 1-q, while the probability that the next state, will be the BUSY state and occupied by PU is q. For channel holding time distributions, the exponential distribution is a widely adopted model [120], [121]. In our work, we assume that both the busy and idle channel holding time are exponentially distributed with parameters λ_b and λ_e respectively. Therefore, at any time, the channel is busy with probability

given by

$$P_b = \frac{\lambda_e}{\lambda_b + \lambda_e}$$

and the idle probability is given by $P_e = 1 - P_b$. The transition probability matrix describing when the channel is in state 'z'$\in$ (0, 1) given that T_s (duration of each sample) seconds ago it was in state 'x'$\in$ (0, 1) is given by [74, pp. 20-36]

$$P_{xz}(T_s; \lambda_b, \lambda_e) = \begin{pmatrix} P_{00}(T_s) & P_{01}(T_s) \\ P_{10}(T_s) & P_{11}(T_s) \end{pmatrix},$$

$$= \frac{1}{\lambda_b + \lambda_e} \begin{pmatrix} \lambda_b + \lambda_e e^{-(\lambda_b+\lambda_e)T_s} & \lambda_e - \lambda_e e^{-(\lambda_b+\lambda_e)T_s} \\ \lambda_b - \lambda_b e^{-(\lambda_b+\lambda_e)T_s} & \lambda_e + \lambda_b e^{-(\lambda_b+\lambda_e)T_s} \end{pmatrix}. \tag{3.18}$$

We have assumed that the PU occupancy status transition occurs only once within each frame. It is further assumed that the PU status transition can be completed within one sample. The above probabilities depend on the parameters of the PU traffic model. In some applications, such as the TV licensed spectrum, the state of the licensed channel changes slowly, corresponding to small values of λ_b and λ_e. In this case, the conventional model without considering the reappearing PU may give a good approximation to the SU performance. However, in other applications, such as public safety spectrum, cellular systems, WiMAX, WLAN, the state of the licensed channel changes more frequently corresponding to large values of λ_b and λ_e.

3.7 Simulation Results

We have calculated the EVM for a M-QAM OFDM system as shown in Fig. 3.5. The EVM values are plotted against SNR. It can be seen that there is little variation in EVM for different modulation types [100]. The EVM values slightly decrease with an increase of SNR. Note that, the lower the EVM, the better the system performance. From (3.15) and (3.16) it is clear that the EVM value after PU arrival will be higher than the value when SU transmits alone. This is the idea behind using EVM as a metric for PU detection. Fig. 3.6 shows a comparison of the cumulative distribution

function (CDF) of EVM for packets corrupted by PU arrival and PU absence. From Fig. 3.6, we can see that the EVM values of packets affected by the PU are higher. Similarly Fig. 3.7 shows that the EVM values are higher when the PU arrives during SU transmission. The EVM is calculated over pilot groups of 3 OFDM symbols where each OFDM symbol contains 4 pilots. The M blocks on the x-axis represent the time series of such pilot groups. On detecting idle spectrum, the SU starts transmitting in the idle band. It is assumed that the PU appears after some time during the monitoring phase.

Simulations found that the EVM of the SU remains the same as we increase the number of OFDM symbols in the absence of the PU. For simulation, we have considered a 3-tap Rayleigh fading multipath channel, 600 OFDM symbols, 52 subcarriers, 4 pilots and CP length of 16 which corresponds to the standard parameters for WLAN 802.11ac. The simulation results shown in Fig. 3.6 and Fig. 3.7 consider the EVM when the PU is present or absent for the entire duration of the SU frame transmission. However, in practice PUs can arrive at any time, so we now model PU arrival activity.

We adopt the two-state discrete time Markov chain model which has been exten-

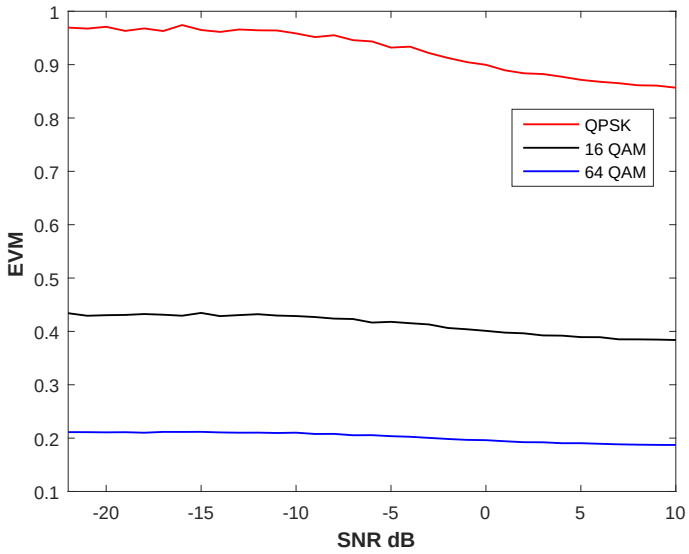

Figure 3.5: EVM vs SNR for M-QAM OFDM.

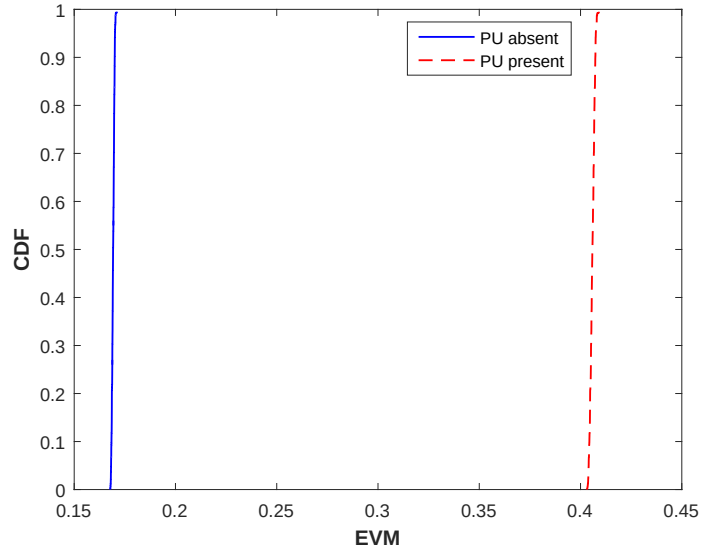

Figure 3.6: CDF of error vector magnitude.

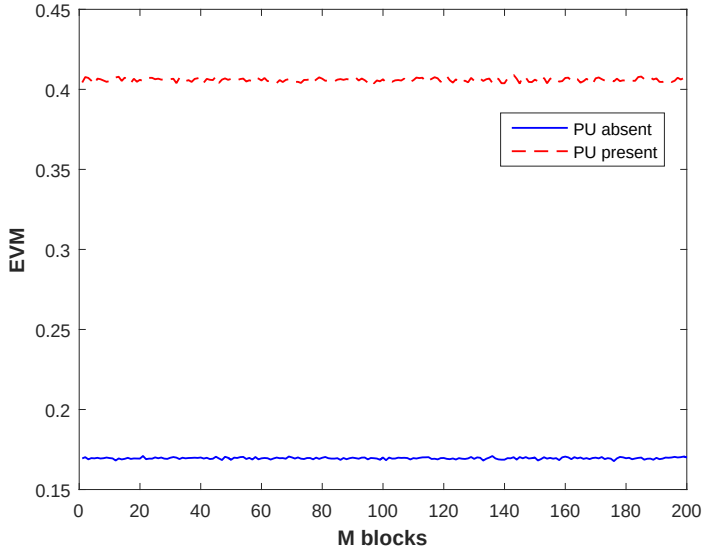

Figure 3.7: EVM vs M blocks of OFDM symbols and INR= -10 dB.

sively used for modeling PU BUSY/IDLE activity [116]. In order to model a Markov chain, we need to know the transition probability matrix **P**. In [116], a Markov-chain based method was introduced to simulate PU and SU activity in a CR system. The authors there performed an analysis of network traffic over an IEEE 802.11ac wireless access-point to determine the transition probabilities for the model. For simulation, we have chosen the same transition probability matrix from [116]. Thus we have

$$\mathbf{P} = \begin{bmatrix} P_{00} & P_{01} \\ P_{10} & P_{11} \end{bmatrix} = \begin{bmatrix} 0.8866 & 0.1134 \\ 0.5309 & 0.4691 \end{bmatrix}. \tag{3.19}$$

Fig. 3.8 shows PU detection by the EVM when its BUSY/IDLE activity is modelled as a two state discrete time Markov chain and INR of -10 dB. The traditional constraint of the CR not being able to detect PU activity while the CR user is in operation has been relaxed by the EVM based PU detection. The adopted method requires a SU transmitter to use OFDM. Each OFDM symbol contains 4 pilots. At the SU receiver, the pilots are extracted and divided into multiple groups. The EVM is calculated for each block of pilot groups. We have simulated 600 OFDM symbols which are grouped into 200 pilot groups. Therefore, each block contains only 3 OFDM symbols. The blue curve indicates the EVM of the SU alone, i.e in the absence of PU and the red curve indicates the EVM in the presence of PU. When PU appears at the time instant 50, a step change is observed after the 50th block. We have assumed PU occupancy status changes only once during the SU frame transmission, so the EVM remains high over remaining pilot groups.

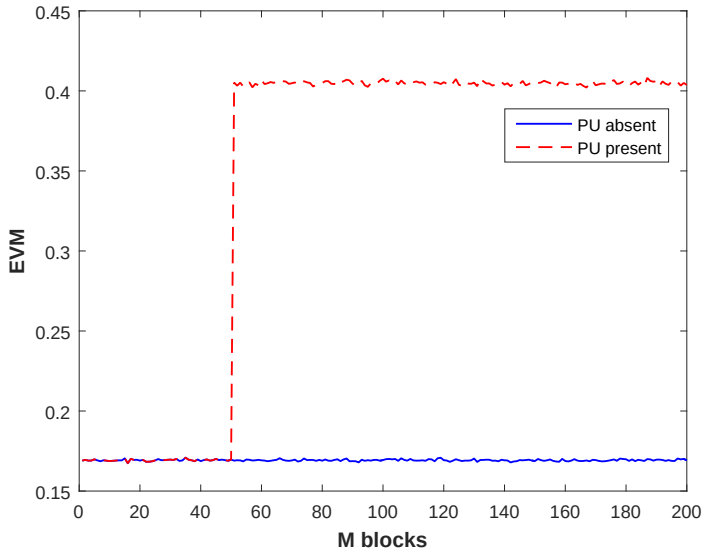

Figure 3.8: EVM in the presence of PU modelled as an BUSY/IDLE Markov chain for N_s=3 OFDM symbols and INR=-10 dB.

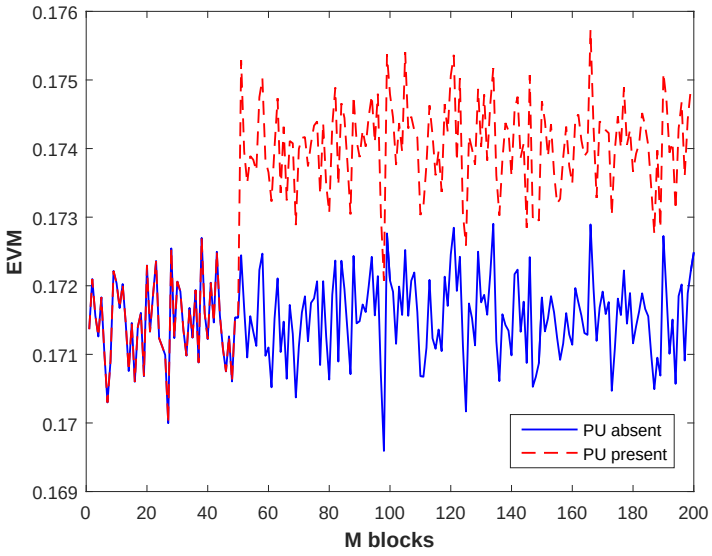

Figure 3.9: EVM in the presence of PU modelled as an BUSY/IDLE Markov chain for N_s=3 OFDM symbols and INR=-22dB.

In order to protect the primary incumbent users from interference, CR enabled SUs are required to detect incumbent signals at very low SNR. In this regard, our proposed EVM based detector can reliably detect the PU signals at a INR as low as -22 dB which is shown in Fig. 3.9.

3.8 Chapter Summary

From the preceding discussion we can deduce that there is a clear distinction in the distribution of EVM under the two hypotheses H_0 and H_1 which is the basis for the SU receiver to determine the PU arrival. The advantage of this proposed scheme is its ability to find the location of the bits corrupted by the PU's arrival by looking at the EVM values of groups of pilot symbols. Based on this the SU receiver can ask its transmitter to lower transmission rate and power, but continue to transmit data for the remainder of the frame.

Our method does not require any subcarrier to be reserved nor do we need to insert a periodic zero energy level as in [27], [26], [104] and [22]. Therefore, our proposed spec-

trum monitoring algorithm can enhance the performance of OFDM-based cognitive networks by improving PU detection performance. The conventional requirement of quiet periods to detect the emergence of PUs has been relaxed by our EVM based PU detection which gives us more time for data transmission. As a result, a significant gain in throughput can be expected.

Detection theory provides some standard tools for presenting performance which are probabilities of missed and false detection in the form of a receiver operating characteristic (ROC) or its complement (CROC). So, in the next chapter, we will study the performance evaluation of our proposed EVM detector.

Chapter 4

On the Performance of EVM based Primary User Monitoring in Cognitive Radio Systems

4.1 Introduction

In Chapter 3, we described how the EVM can detect the reappearing PU during SU transmission by observing a step change of the EVM curve for the H_0 and H_1 hypotheses. This chapter analyses the performance of the EVM based detector and then proposes an effective method for detecting a reappearing PU. We derive the joint PDF of the exact distribution of the proposed test statistic. We investigate how to simultaneously perform spectrum sensing and data transmission at the SU. We study the performance of EVM based PU monitoring for OFDM based CR networks. Our method exploits the pilot tones that are inherent in many OFDM based standards and are typically used for channel estimation and synchronization purposes. Similar to [24], our system performs spectrum observation at the SU receiver which we have shown in [93]. Our mechanism is direct and is based on the EVM metric which can be obtained immediately before demodulation and decoding of the received packets, thus giving us real-time results. Our scheme does not require periodic zero-energy intervals within a selected subcarrier as proposed in [26], nor do we require reserved subcarriers as proposed in [22].

The rest of the chapter is organized as follows. Section 4.2 describes hypothesis testing, test statistic and EVM operation mode. In Section, 4.3 we analyze the type

I and type II error probabilities. Reappearing PU is described in Section 4.4. In Section 4.5, we present simulation results and Section 4.7 concludes the chapter.

From the previous chapter we know that the frequency domain received signal in the presence of the PU is given by

$$Y(k,l) = H_s(k,l)X(k,l) + H_p(k,l)I_p(k,l) + W(k,l), \tag{4.1}$$

where $I_p(k,l)$ is the PU interfering signal at the k^{th} subcarrier of the l^{th} symbol and $H_p(k,l)$ is the equivalent baseband channel frequency response at the k^{th} subcarrier of the l^{th} symbol. We make the following two assumptions to model the PU signal.

- AS1 (Unknown deterministic signal): We assume that the PU signal is an unknown deterministic signal whose symbol duration is longer than the sensing interval. In this case, $I_p(k,l)$ is treated as independent and non-identically distributed Gaussian random signal with non-zero mean μ_I.

- AS2 (Gaussian random signal): We assume that the PU symbol period is shorter than the SU symbol period, so $I_p(k,l)$ is an independent Gaussian random signal with zero mean and variance σ_I^2.

4.2 Hypothesis Testing and Test Statistic

We now summarize the key results from chapter 3 needed to define the EVM test statistic for both hypotheses H_0 and H_1. The conventional approach to spectrum sensing [21]- [26] is to perform energy detection through the evaluation of test statistic for one long sensing period. The corresponding hypothesis test in AWGN can be written as

$$\begin{aligned} Y_p(k,l) &= W_p(k,l) && : H_0 \\ Y_p(k,l) &= H_p(k,l)I_p(k,l) + W_p(k,l) && : H_1, \end{aligned} \tag{4.2}$$

where $Y_p(k,l)$, $I_p(k,l)$, $H_p(k,l)$ and $W_p(k,l)$ are the received signal, transmitted PU signal, channel coefficient and the noise contribution at the pilot subcarrier, respectively. This type of spectrum sensing is called half duplex (HD). It performs periodic spectrum sensing and can't detect the PU during ongoing SU communication. The test statistic is given by

$$Z(k) = \frac{1}{L}\sum_{l=1}^{L} |Y_p(k,l)|^2 \tag{4.3}$$

and is compared with threshold λ in order to decide whether a signal is present or not in that frequency band as

$$Z \underset{H_0}{\overset{H_1}{\gtrless}} \lambda. \tag{4.4}$$

In FD CR, the SUs are allowed to sense and transmit at the same time. Equivalently, the corresponding hypothesis expressions are given by

$$Y_p(k,l) = H_{ps}(k,l)X_p(k,l) + W_p(k,l) \qquad : H_0$$

$$Y_p(k,l) = H_{ps}(k,l)X_p(k,l) + H_p(k,l)I_p(k,l) + W_p(k,l) : H_1, \tag{4.5}$$

where $X_p(k,l)$ represents the SU self interference signal. In such a scheme the idea is to assume perfect SIC, then the SU applies a spectrum sensing technique to examine the PU status. By applying SIC, CR can eliminate the transmitted SU signal from the received mixed signal. Thus under perfect SIC, (4.5) converges to that of HD case in (4.2).

4.2.1 EVM Test Statistic

We are interested in finding the EVM per subcarrier. We next introduce a random variable Z defined as

$$Z_p(k) = \sqrt{\frac{1}{LE_s|H_{ps}(k,l)|^2}\sum_{l=0}^{L}\left|E_p(k,l)\right|^2}, \tag{4.6}$$

where $E_p(k,l) = Y_p(k,l) - H_{ps}(k,l)X_p(k,l)$. The EVM test statistic for the two hypotheses H_0 and H_1 can be obtained as

$$Z(k) = \begin{cases} \sqrt{\frac{1}{LE_s|H_{ps}(k,l)|^2} \sum_{l=0}^{L} \left| W_p(k,l) \right|^2} & : H_0 \\ \sqrt{\frac{1}{LE_s|H_{ps}(k,l)|^2} \sum_{l=0}^{L} \left| H_p(k,l)I_p(k,l) + W_p(k,l) \right|^2} & : H_1. \end{cases} \tag{4.7}$$

This converges to the HD result in (4.3). The novelty is the inclusion of the square root in (4.6) which affects the threshold λ_1. The test statistic in (4.6) is compared with the threshold λ_1 in order to decide the availability of the PU in a given frequency band as

$$Z \underset{H_0}{\overset{H_1}{\gtrless}} \lambda_1. \tag{4.8}$$

The threshold λ_1 is parameterized according to the Neyman-Pearson (NP) criterion whose objective is to maximize probability of detection subject to a constraint on the false alarm probability. In fact, conventional energy detection can also be employed to allow SU for simultaneous transmission and sensing as noted in [29–32, 122, 123] in the form of FD spectrum sensing. The idea is to apply SIC to cancel the self interfering signal, $H_{ps}(k,l)X_p(k,l)$ in (4.5) and perform energy detection spectrum sensing on the remaining signal. In [29–32,122,123], the SU signal is typically treated as unknown at the receiver, and the effectiveness of SIC is represented using a linear "self-interference mitigation coefficient" which is applied to degrade the effectiveness of spectrum sensing. However, these SIC analyses do not account for error propagation from incorrect SU decisions feeding into the SIC process. In this thesis, we assume that the received SU pilot symbols are perfectly removed for calculating the EVM statistic, with remaining synchronization and channel estimation errors treated as AWGN having identical variances for H_0 and H_1.

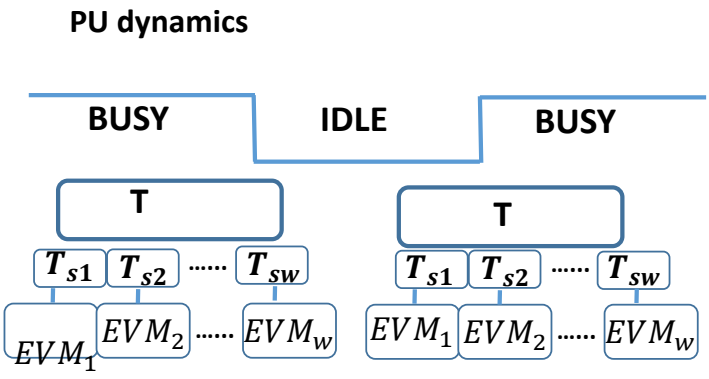

Figure 4.1: EVM operation mode.

4.2.2 EVM Operation Mode

In Fig. 4.1, the EVM operation mode is illustrated. The first line shows the PU's state transition. We adopt the two-state discrete time Markov chain model which has been extensively used for modeling the PU BUSY/IDLE activity [116]. The second line indicates the SU TX frame period T and the EVM measurement is done on the receiver side SU RX which is indicated in the third line.

Although, the SUs are sensing and transmitting simultaneously, some time after which the SU determines to transmit its data or not needs to be determined. Hence, the EVM based detection method is done over multiple (consecutive) short periods instead of one long sensing period. The motivation for this approach is to account for the tradeoff between the sensing efficiency and timeliness in detecting the PU activity. Increasing sensing duration improves sensing efficiency, however, such an increase implies delaying the time to make a decision regarding the change in PU activity. In order to sense all possible reappearances of the PU, we divide the SU's frame into g sensing durations for which we calculate g EVM values as shown in the fourth line of Fig. 4.1. For simplicity, we assume that the intervals between each periods are equal.

4.3 Type I and type II Errors

We assume that the channel fading coefficient $H_p(k)$ is constant over the sensing interval L and both the signal and noise are real valued Gaussian signals with variances σ_I^2 and σ_w^2, respectively, and both are independent signals [124–127]. We also assume $E_s = 1$ and establish Gaussian channel performance by assuming $|H_{ps}(k)|^2 = 1$. Since the samples of the pilot tone follow $\mathcal{N}(0, \sigma_w^2)$, $Z^2(k)$ will follow a chi-square distribution with $2L$ degrees of freedom (DOF) under H_0 hypothesis, i.e., $Z^2(k) \sim \chi^2(2L)$ with PDF [70]

$$f_{Z^2}(z) = \frac{L^L}{2^L \sigma_w^{2L} \Gamma(L)} z^{L-1} e^{\frac{-Lz}{2\sigma_w^2}}. \tag{4.9}$$

We are interested in finding the PDF of our decision statistic Z which is the square root of the chi-square (2L) random variable. The transformation $Y = g(Z) = \sqrt{Z}$ is a 1-1 transformation from $\chi = \{z|z > 0\}$ to $\mathcal{Y} = \{y|y > 0\}$ with inverse $Z = g^{-1}(Y) = Y^2$ and Jacobian $\frac{dZ}{dY} = 2Y$.

Therefore, according to the transformation technique, the PDF of Y is

$$f_Y(y) = f_Z(g^{-1}(y)) \left| \frac{dz}{dy} \right|$$

$$= \frac{L^L}{2^L \sigma_w^{2L} \Gamma(L)} (y^2)^{L-1} e^{\frac{-Ly^2}{2\sigma_w^2}} |2y|$$

$$= \frac{L^L}{2^{L-1} \sigma_w^{2L} \Gamma(L)} y^{2L-1} e^{\frac{-Ly^2}{2\sigma_w^2}},$$

$$f_{Z|H_0}(y) = \frac{L^L y^{2L-1} e^{\frac{-Ly^2}{2\sigma_w^2}}}{2^{L-1} \sigma_w^{2L} \Gamma(L)}, \quad y > 0. \tag{4.10}$$

The performance of the detector is characterized in terms of the CROC curve, which represents the type II (false negative) error as a function of type I (false positive) error.

Firstly, the type I error probability is given by

$$Prob[Z > \lambda_1 | H_0] = \int_{y_1=\lambda_1}^{+\infty} f_{Z|H_0}(y) dy$$

$$= \frac{L^L}{2^{L-1}\sigma_w^{2L}\Gamma(L)} \int_{\lambda_1}^{\infty} y^{2L-1} e^{\frac{-Ly^2}{2\sigma_w^2}} dy$$

To solve this equation, we apply some variable conversion for $t = \frac{Ly^2}{2\sigma_w^2}$.

$$dy = \frac{1}{2}\sqrt{\frac{2\sigma_w^2}{Lt}} dt$$

$$Prob[Z > \lambda_1 | H_0] = \frac{L^L}{2^{L-1}\sigma_w^{2L}\Gamma(L)} \int_{\frac{L\lambda_1^2}{2\sigma_w^2}}^{\infty} \left(\sqrt{\frac{2\sigma_w^2 t}{L}}\right)^{2L-1} \frac{1}{2} e^{-t} \sqrt{\frac{2\sigma_w^2}{Lt}} dt$$

$$= \frac{L^L}{2^{L-1}\sigma_w^{2L}\Gamma(L)} \frac{1}{2}\sqrt{\frac{2\sigma_w^2}{Lt}} \int_{\frac{L\lambda_1^2}{2\sigma_w^2}}^{\infty} \left(\frac{2\sigma_w^2 t}{L}\right)^{\frac{1}{2}(2L-1)} e^{-t} dt$$

$$= \frac{1}{\Gamma(L)} \int_{\frac{L\lambda_1^2}{2\sigma_w^2}}^{\infty} t^{L-1} e^{-t} dt \tag{4.11}$$

In [128], the incomplete gamma function is written as

$$\Gamma(a, s) = \int_s^{\infty} t^{a-1} e^{-t} dt, \tag{4.12}$$

Using (4.12), the type I error probability i.e., (4.11) can be written as

$$= \frac{\Gamma\left(L, \frac{L\lambda_1^2}{2\sigma_w^2}\right)}{\Gamma(L)}, \tag{4.13}$$

The same approach is applied when the PU signal $I(k)$ is present, i.e., under hypothesis H_1. However, the PDF of the decision statistic will differ according to the assumptions made for the PU signal in Section 4.1.

4.3.1 Case A

According to the assumption AS1, Z follows a non-central chi distribution with non-central parameter $\beta = \sqrt{2L\gamma}$, where $\gamma = \frac{\mu_I^2}{\sigma_w^2}$ is the interference to noise ratio (INR). The PDF under H_1 can thus be expressed as

$$f_{Z|H_1}(y) = \frac{e^{-\left(\frac{\frac{y^2}{\sigma_w^2}+\beta^2}{2}\right)} y^{2L} \beta I_{L-1}\left(\frac{\beta y}{\sigma_w}\right)}{\sigma_w^L (\beta y)^L}, \tag{4.14}$$

where $I_{L-1}(.)$ is the $(L-1)$th order modified Bessel function of the first kind. Similarly, the probability of detection is

$$P_D = Prob[Z > \lambda_1 | H_1] = \int_{\lambda_1}^{+\infty} f_{Z|H_1}(y) dy$$

$$= \int_{\lambda_1}^{+\infty} \frac{e^{-\left(\frac{\frac{y^2}{\sigma_w^2}+\beta^2}{2}\right)} y^{2L} \beta I_{L-1}\left(\frac{\beta y}{\sigma_w}\right)}{\sigma_w^L (\beta y)^L} dy \tag{4.15}$$

Assume $y = \sigma_w t$

$$\frac{dy}{dt} = \sigma_w \implies dy = \sigma_w dt$$

$$= \int_{\frac{\lambda_1}{\sigma_w}}^{+\infty} \frac{e^{-\left(\frac{t^2+\beta^2}{2}\right)} (\sigma_w t)^{2L} \beta I_{L-1}\left(\frac{\beta \sigma_w t}{\sigma_w}\right)}{\sigma_w^L \Big(\beta \sigma_w t\Big)^L} \sigma_w dt$$

$$= \int_{\frac{\lambda_1}{\sigma_w}}^{+\infty} t\left(\frac{t}{\beta}\right)^{L-1} e^{-\frac{\left(t^2+\beta^2\right)}{2}} I_{L-1}\Big(\beta t\Big) dt. \tag{4.16}$$

P_D can be expressed in terms of the generalized Marcum Q-function, which is defined as [129]

$$Q_m(a,b) = \int_b^{\infty} x(\frac{x}{a})^{m-1} e^{-\frac{x^2+a^2}{2}} I_{m-1}(ax) dx, \tag{4.17}$$

where m is a non-negative integer, and a and b are non-negative real numbers. Com-

paring (4.16) with (4.17), we have $m = L$,$a = \beta$, $b = \frac{\lambda_1}{\sigma_w}$. Thus, P_D becomes

$$P_D = Q_L\left(\beta, \frac{\lambda_1}{\sigma_w}\right) \tag{4.18}$$

and the type II error probability is given by

$$Prob[Z < \lambda_1 | H_1] = 1 - P_D = 1 - Q_L\left(\beta, \frac{\lambda_1}{\sigma_w}\right). \tag{4.19}$$

4.3.2 Case B

According to the assumption AS2, Z follows a central chi distribution whose PDF can be written as

$$f_{Z|H_1}(y) = \frac{L^L}{2^{L-1}(\sigma_I^2 + \sigma_w^2)^L \Gamma(L)} y^{2L-1} e^{\frac{-Ly^2}{2(\sigma_I^2+\sigma_w^2)}}. \tag{4.20}$$

After applying a similar procedure as above, P_D can be expressed as

$$P_D = \frac{\Gamma\left(L, \frac{L\lambda_1^2}{2(\sigma_I^2+\sigma_w^2)}\right)}{\Gamma(L)}$$

and the type II error probability is given by

$$Prob[Z < \lambda | H_1] = 1 - P_D = 1 - \frac{\Gamma\left(L, \frac{L\lambda_1^2}{2(\sigma_I^2+\sigma_w^2)}\right)}{\Gamma(L)}. \tag{4.21}$$

4.4 Laplacian approximation

P_D expressed in terms of the generalized Marcum Q-function in (4.18) is quite difficult to compute precisely. Therefore, in spectrum sensing the central limit theorem (CLT) has been extensively used to approximate P_D which yields P_D in terms of the well-known Gaussian function [18,67,130]. The CLT based approximation is accurate only for large sample size (L > 250), but is not accurate for small sample sizes [75].

In CR simple and accurate P_D approximations valid for arbitrary sample size are necessary. As our EVM based detector is designed to operate with a least number of samples, it is important to apply such an approximation method that can simplify (4.18). In [75] the authors have used a Laplacian approximation of a chi distribution to achieve the Gaussian distribution. As our EVM test statistic also has a chi distribution, we apply this Laplacian approximation to obtain P_D in terms of a Gaussian function.

We can rewrite (4.6) as

$$Z = \frac{\sigma_y}{\sqrt{2L}} \sqrt{\sum_{n=1}^{L} \left(\frac{e_{real}^2(n)}{\frac{\sigma_y^2}{2}} + \frac{e_{imag}^2(n)}{\frac{\sigma_y^2}{2}} \right)} = \frac{\sigma_y}{\sqrt{2L}} u. \tag{4.22}$$

Here, $\sigma_y^2 = \sigma_I^2 + \sigma_w^2$ is the total variance of the received signal. We define u as the second square-root summation term in (4.22). The variable u has a chi distribution $p_U(u)$ with $2L$ DOF [75]. Then, Z has the distribution

$$Z \sim p_0(Z) = \frac{\sqrt{2L}}{\sigma_y} p_U \left(\frac{\sqrt{2L}}{\sigma_y} Z \right). \tag{4.23}$$

In general, we can use (4.23) to determine the PU arrival. However, $p_0(Z)$ is somewhat complex for numerical inference. Thus, we make normal approximations to $p_0(Z)$ using a Laplacian approximation. A normal approximation of $p_0(Z)$ can be determined by approximating $p_U(u)$ with a Gaussian density $q_U(u) = \mathcal{N}(\mu_u, \sigma_u^2)$. The Laplacian approximation achieves this by using the mode and the Hessian of the log likelihood at the mode. It is highly accurate even at moderate sample sizes [75]. Therefore, Laplacian approximation consists of the following steps.

i. finding a local maximum u_{max} of the given PDF $p_U(u)$.

ii. calculating the variance $\sigma_u^2 = -\frac{1}{p''(u_{max})}$.

iii. approximating the PDF with $q_U(u) \approx \mathcal{N}(\mu_u, \sigma_u^2)$.

From (4.10)

$$p_U(u) = \frac{L^L 2^{1-L} u^{2L-1} e^{\frac{-Lu^2}{2\sigma_w^2}}}{\sigma_w^{2L}\Gamma(L)}, \quad u > 0$$

$$= \frac{L^L u^{2L-1} e^{\frac{-Lu^2}{2\sigma_w^2}}}{2^{L-1}\sigma_w^{2L}\Gamma(L)} = \frac{u^{2L-1} e^{\frac{-Lu^2}{2\sigma_w^2}}}{\frac{t}{L^L}}, t = 2^{L-1}\sigma_w^{2L}\Gamma(L). \tag{4.24}$$

Here, $\frac{t}{L^L}$ is a normalization constant that doesn't depend on u. We will ignore t for the sake of convenience. As we are working with the log-likelihood, so $p_U(u)$=log $\big(p_U(u)\big)$

$$= logu^{2L-1} + loge^{\frac{-Lu^2}{2\sigma_w^2}}$$

$$\frac{d}{du} log(p_U(u)) = \frac{d}{du}\left[logu^{2L-1} - \frac{Lu^2}{2\sigma_w^2}\right]$$

$$= \frac{1}{u^{2L-1}}(2L-1)u^{2L-2} - \frac{Lu}{\sigma_w^2} = \frac{2L-1}{u} - \frac{Lu}{\sigma_w^2} \tag{4.25}$$

To find out the local maxima u_{max}, we set (4.25) to zero, which gives

$$\frac{2L-1}{u} - \frac{Lu}{\sigma_w^2} = 0 \implies u_{max} = \sqrt{\frac{\sigma_w^2(2L-1)}{L}}. \tag{4.26}$$

Using the local maximum u_{max}, we compute the variance $\sigma_u^2 = -\frac{1}{p''(u_{max})}$, where

$$p''(u_{max}) = \frac{d^2 p_U(u)}{du^2}\bigg|_{u=u_{max}}$$

$$= -\frac{2L-1}{u^2} - \frac{L}{\sigma_w^2}\bigg|_{u=u_{max}} = -\frac{2L}{\sigma_w^2} \implies \sigma_u^2 = \frac{\sigma_w^2}{2L}. \tag{4.27}$$

Thus, $q_U(u) \sim \mathcal{N}\left(\sqrt{\frac{\sigma_w^2(2L-1)}{L}}, \frac{\sigma_w^2}{2L}\right)$. In turn, Z has the following Gaussian distribution

$$Z \sim \mathcal{N}\left(\sqrt{\frac{\sigma_w^2(2L-1)}{2}}\frac{\sigma_y}{L}, \frac{\sigma_w^2\sigma_y^2}{8L}\right)$$

When $L \gg 1$, we can write $\sqrt{\frac{2L-1}{2}} \approx 1$ and $e^x \approx 1+x$ for $x \ll 1$. Using the approximate density $p_0(Z)$ we have

$$Z \approx \sigma_w \frac{\sigma_y}{L} + \sigma_w^2 \frac{\sigma_y}{\sqrt{8L}} \mathcal{N}(0,1) \approx \sigma_w \frac{\sigma_y}{L} e^{\frac{\sigma_w \mathcal{N}(0,1)}{\sqrt{8L}}}.$$

Now, denoting $H_1 = log(Z)$, we can write

$$H_1 = log(\sigma_w \frac{\sigma_y}{L} e^{\frac{\sigma_w \mathcal{N}(0,1)}{\sqrt{8L}}}).$$

Therefore, with the Laplacian approximation, the chi distribution of our decision statistic can be approximated by the Gaussian distribution as follows

$$H_1 \approx p_0(Z) \sim \mathcal{N}\bigg(log(\sigma_w \frac{\sigma_y}{L}), \frac{\sigma_w^2}{8L}\bigg) \tag{4.28}$$

$$H_0 \approx p_0(Z) \sim \mathcal{N}\bigg(log\sigma_w, \frac{1}{8L}\bigg). \tag{4.29}$$

Following the above development, the type I and type II error probabilities may be written directly as follows. The type I error probability for the Laplacian method is approximated as

$$Prob[Z > \lambda | H_0] = \frac{1}{2} erfc\bigg(\sqrt{2L}(\lambda - log\sigma_w)\bigg) \tag{4.30}$$

and

$$P_D = \frac{1}{2} erfc\bigg(\frac{\sqrt{2L}\big(\lambda - log(\sigma_w \frac{\sigma_y}{L})\big)}{\sigma_w}\bigg)$$

$$= \frac{1}{2} erfc\bigg(\frac{\sqrt{2L}\big(\frac{1}{\sqrt{2L}}(erfc)^{-1}(2P_F) + log\sigma_w - log(\sigma_w \frac{\sigma_y}{L})\big)}{\sigma_w}\bigg)$$

$$= \frac{1}{2} erfc\bigg(\frac{(erfc)^{-1}(2P_F) - log(\frac{L}{\sigma_y})}{\sigma_w}\bigg) \tag{4.31}$$

where

$$\lambda = \frac{1}{\sqrt{2L}}(erfc)^{-1}(2P_F) + log\sigma_w \tag{4.32}$$

where P_F denotes the probability of false alarm. The type II error probability for Laplacian method is given by

$$Prob[Z < \lambda | H_1] = 1 - P_D. \tag{4.33}$$

4.5 Reappearing PU

It is commonly assumed that the PU is either absent or active during the entire sensing interval. However, in realistic cases, the PUs can change their states at any time. Thus, when the PUs become active during the SU's transmission period, the SUs cause interference to the PUs. In addition, if the PUs cease being active during the SU's transmission period, it wastes idle spectrum.

Fig. 4.2 shows the EVM response when the PU is present throughout the SU transmission and Fig. 4.3 shows the use of the EVM detecting the reappearing PU during SU transmission when the PU arrives at the 100^{th} time sample. Gains can be achieved by allowing the SUs to transmit and sense simultaneously so that they can sense the spectrum during the entire frame period. Our proposed EVM detector facilitates this kind of spectrum sensing. We are interested in deriving the type I and type II error probabilities for the proposed classifier. The type I error probability remains the same as in (4.39). In order to calculate type II error probability we utilize the following theorem 1.

Theorem 1. *Given P samples of independent identically distributed Gaussian random variables $X \sim \mathcal{N}(0, \sigma^2)$ with central chi-square distribution and R samples of independent and non-identically distributed variable $Y \sim \mathcal{N}(\mu, \sigma^2)$ with non-central chi-square distribution, where x and y have identical variance σ^2, then the sum $Z = \sum_{n=1}^{P} x_n^2 + \sum_{n=1}^{R} y_n^2$ is non-central chi-square distributed with probability density*

$$p(z) = \frac{1}{2}\left(\frac{z}{\beta\sigma^2}\right)^{\frac{P+R}{4}-\frac{1}{2}} e^{-\left(\frac{\frac{z}{\sigma^2}+\beta}{2}\right)} I_{\frac{(P+R)}{2}-1}\left(\sqrt{\frac{\beta z}{\sigma^2}}\right), \tag{4.34}$$

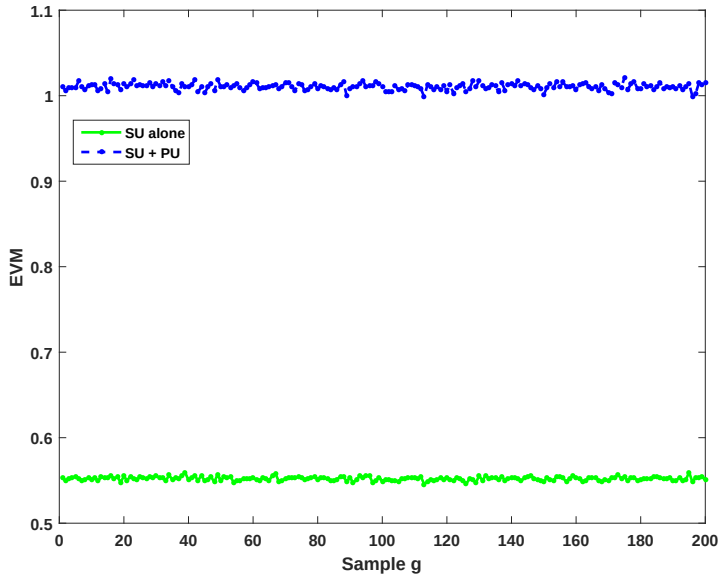

Figure 4.2: EVM response when PU is present throughout the SU transmission (INR=-10 dB).

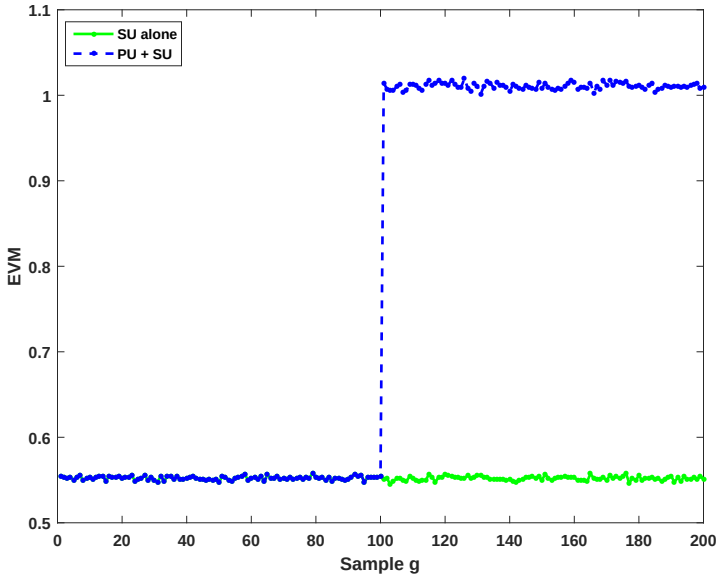

Figure 4.3: EVM response when PU arrives at the 100^{th} time sample (INR=-10 dB).

for non-centrality parameter $\beta = R\mu^2/\sigma^2$ and $I_r(.)$ the rth order Bessel function of the first kind.

Proof. From $P+R$ samples of independent identically distributed Gaussian random variable $u \sim \mathcal{N}(\mu, \sigma^2)$, without loss of generality transform to a standard variable $v = u/\sigma^2$. Then the joint distribution $p(v_1, ..., v_{P+R})$ is spherically symmetric except for a shift in centre. The spherical symmetry implies that the distribution of $w = \sum_{n=1}^{P+R} v_n^2$ depends on the means only through the squared length $\alpha = \sum_{n=1}^{P+R} \mu_n^2 = (P+R)\mu^2$. Without loss of generality set $\mu_1 = \sqrt{\alpha}$ and set $\mu_2 = \mu_3 = ... = \mu_{P+R} = 0$. Applying the standard derivation [131] for the non-central chi-square density of w produces

$$p(w) = \frac{1}{2}\left(\frac{w}{\alpha}\right)^{\frac{P+R}{4}-\frac{1}{2}} e^{-\left(\frac{w+\alpha}{2\sigma^2}\right)} I_{\frac{(P+R)}{2}-1}\left(\sqrt{\alpha w}\right). \tag{4.35}$$

For z as above, $\mu_{P+1} = ...\mu_{P+R} = \mu$ and $\mu_1 = ...\mu_P = 0$. Adjusting the non-centrality parameter to the amended sum and reversing the variance transformation for $\sigma^2 \neq 1$ results in the modified non-centrality parameter $\beta = \frac{2R|\mu|^2}{\sigma_w^2}$ and the desired density (4.34) follows for variance σ^2. □

Now, using (4.34) the joint PDF of Z for $(2P+2R)$ degrees of freedom can be written as

$$f_Z(z) = \frac{1}{2}\left(\frac{2z}{\beta\sigma_w^2}\right)^{\frac{P+R-1}{2}} e^{-\left(\frac{\frac{2z}{\sigma_w^2}+\beta}{2}\right)} I_{P+R-1}\left(\sqrt{\frac{2\beta z}{\sigma_w^2}}\right). \tag{4.36}$$

As in (4.10), the PDF of the reappearing PU proposed by our test statistic is obtained by taking the square root of (4.36) which can be written as

$$f_Z(z) = \frac{e^{-\left(\frac{\frac{z^2}{\sigma_w^2}+\beta^2}{2}\right)} z^{2L}\beta I_{L-1}\left(\frac{\beta z}{\sigma_w}\right)}{\sigma_w^L(\beta z)^L}, \tag{4.37}$$

where $L = P+R$ and $\beta = \sqrt{\frac{2R|\mu|^2}{\sigma_w^2}}$ is the non-centrality parameter. Now, the

probability of detection can be expressed as

$$P_D = \int_{\lambda_1}^{+\infty} f_Z(z)dz$$

$$= \int_{z=\lambda_1}^{+\infty} \frac{e^{-\left(\frac{\frac{z^2}{\sigma_w^2}+\beta^2}{2}\right)} z^{2L}\beta I_{L-1}\left(\frac{\beta z}{\sigma_w}\right)}{\sigma_w^L(\beta z)^L}dz$$

$$= \int_{\frac{\lambda_1}{\sigma_w}}^{+\infty} t\left(\frac{t}{\beta}\right)^{L-1} e^{-\frac{\left(t^2+\beta^2\right)}{2}} I_{L-1}\Big(\beta t\Big)dt. \tag{4.38}$$

Comparing (4.38) with (4.17), we have $m = L$, $a = \beta$, $b = \frac{\lambda_1}{\sigma_w}$. Thus, P_D can be expressed as

$$P_D = Q_L\left(\beta, \frac{\lambda_1}{\sigma_w}\right), \tag{4.39}$$

and the type II error probability is given by

$$Prob[Z < \lambda_1|H_1] = 1 - P_D = 1 - Q_L\left(\beta, \frac{\lambda_1}{\sigma_w}\right). \tag{4.40}$$

4.6 Throughput of CR networks

In this section we analyze the throughput performance of the CR networks by using the proposed EVM based detection. The conventional frame structure of the CR systems consists of a sensing slot followed by a data transmission slot as shown in Fig. 4.4 [16,24]. A SU uses τ units of time for sensing and $T-\tau$ for data transmission. An increase in the sensing time results in the higher detection probability however, the increased sensing time results in a decrease of the data transmission time and hence the throughput of the CR network. Therefore, a sensing-throughput tradeoff always exists with this type of method.

As discussed in chapter 3, our proposed scheme allows simultaneous sensing and

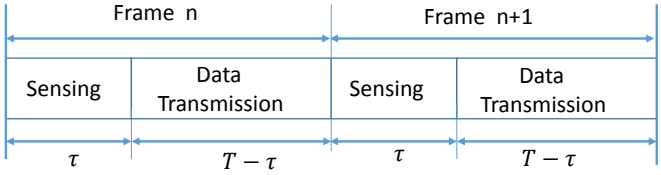

Figure 4.4: Conventional frame structure.

transmission for the SU, so it can overcome the sensing-throughput tradeoff. Under the proposed method, both the sensing and the data transmission time are maximized and their duration is equal to the frame duration T. Thus, EVM based CR system exhibits the following advantages.

- The data transmission duration is equal to the frame duration, which results in an increased throughput.
- The increased sensing time also leads to higher detection probability and therefore better protection of the PUs.
- It allows continuous spectrum sensing which ensures detection of the reappearing PUs during ongoing SU communication.

The frame structure of the EVM based detection method is presented in Fig. 4.5 [18, 24]. It consists of the single slot in which sensing and data transmission are performed at the same time using the receiver structure as presented in Fig. 3.3 in chapter 3. In this frame structure, the sensing time slot τ in the conventional frame structure is used for data transmission, which leads to an increase in the capacity of the CR network as well as facilitates the continuity of data transmission.

The average achievable throughput of a CR network that operates using the frame structure in Fig. 4.4 is given by [16, 18, 19, 24]

$$R(\tau) = R_0(\tau) + R_1(\tau) \tag{4.41}$$

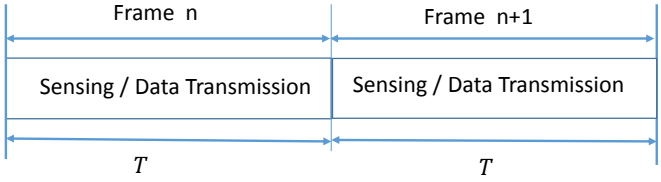

Figure 4.5: New frame structure.

where $R_0(\tau)$ and $R_1(\tau)$ are given by

$$R_0(\tau) = \frac{T-\tau}{T} P(H_0)\big(1 - P_F(\tau)\big) C_0$$

$$R_1(\tau) = \frac{T-\tau}{T} P(H_1)\big(1 - P_D(\tau)\big) C_1 \tag{4.42}$$

In the above equations, τ is the sensing duration and T is the frame duration. C_0 is the throughput of the SU when it operates in the absence of the PU and C_1 is the throughput when it operates in the presence of the PU. $P(H_0)$ and $P(H_1)$ denote the probability that the frequency band is idle and active respectively in such way that $P(H_0) + P(H_1) = 1$. From [16], C_0 and C_1 can be written as

$$C_0 = log_2\big(1 + SNR_s\big)$$

$$C_1 = log_2\left(1 + \frac{SNR_s}{1 + SNR_p}\right) \tag{4.43}$$

where SNR_s is the SU SNR and SNR_p is the PU SNR measured at the SU receiver.

EVM based sensing operates using the frame structure in Fig. 4.5, since it allows simultaneous sensing and transmission. In this case, the sensing duration becomes T instead of τ. Therefore, the throughput of the EVM based approach can be written as

$$R(T) = R_0(T) + R_1(T) \tag{4.44}$$

where the values of $R_0(T)$ and $R_1(T)$ can be calculated as

$$R_0(T) = P(H_0)\big(1 - P_F(T)\big)C_0$$

$$R_1(T) = P(H_1)\big(1 - P_D(T)\big)C_1 \tag{4.45}$$

4.7 Simulation Results

In this section we describe the simulation model used to evaluate the proposed PU monitoring mechanism. The transmitter and receiver models were designed according to IEEE 802.11ac specifications. The channel we considered in the simulation is an AWGN channel. OFDM is used at the physical layer. The simulation parameters are given in Table 4.1. The distributions of the EVM for QPSK PU and OFDM SU signal is analysed under both hypothesis H_0 and H_1 as shown in Fig. 4.6 and Fig. 4.7. The PDFs of the decision variable Z under H_0, i.e., when there is no PU in the band, are shown in both Fig. 4.6 and Fig. 4.7. Under H_1 the PDF depends on the value of INR. The additional curves are also shown under H_1 with different INR values (-15, -13, -11, -9, -5) dB. The presence of the PU is strongly indicated by the shift in the distributions even when the power of the PU's signal is much weaker than the power of the desired signal at the SU's receiver. Fig. 4.8 shows the EVM response for different values of INR. It is shown that the PU has arrived at the 100^{th} time sample. The PU presence is clearly indicated by a step change in the EVM curve for different values of INR. As the INR values decreases, the step size becomes smaller and the detection performance decreases.

The CROC of the EVM based detector for different values of INR is shown in Fig. 4.9 when 8 samples are used for EVM calculation. As expected, the detection probability increases for higher values of INR. Furthermore, it is clear from Fig. 4.9 that our Laplacian approximation agrees with the exact result. In Fig. 4.10 the CROC curve is plotted for different number of samples L under fixed INR of -5 dB. Performance

improves as the number of samples L collected increases. The CROC of the EVM based detector for different values of INR is shown in Fig. 4.11 when the number of samples in the sensing interval is L=12. As expected, the detection probability increases with increasing values of INR. Furthermore, it is clear from Fig. 4.11 that our analytical result well matches the simulated result. In Fig. 4.12 the CROC curve is plotted for different numbers of samples L under fixed INR of -15 dB. It shows the expected result that detection performance improves as the number of samples L collected increases.

In Fig. 4.13 the CROC curve is plotted for a fixed INR of -15 dB as a function of the number of active PU samples M in the sensing interval (L+M). As seen from Fig. 4.13, the detection performance improves with an increasing number of active PU samples M in the sensing interval. At M=12 and L=0, the detection performance is equivalent to that of the case when PU is present for the whole sensing interval as shown in Fig. 4.11 and Fig. 4.12. However, a PU can arrive at different time

Table 4.1: Simulation parameters

Parameter	**Value**
No. of OFDM symbols	600
FFT length	64
Bandwidth	20 MHz
No. of data subcarriers	48
No. of pilot subcarriers	4
Total no. of subcarriers	48+4=52
Modulation	64-QAM
Symbol interval	4μs
PU modulation	QPSK
SU SNR	6 dB

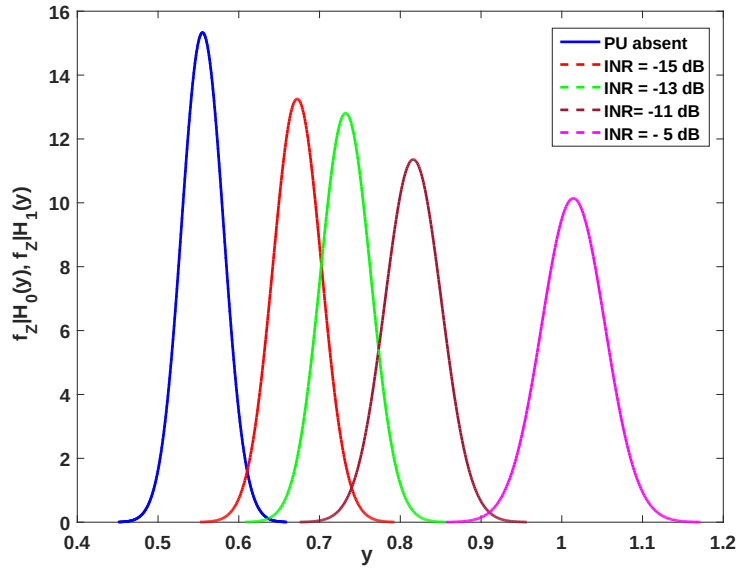

Figure 4.6: Plot of $f_{Z|H_0}(y)$ (SU only) and $f_{Z|H_1}(y)$ for different values of INR when the PU is present throughout the SU transmission.

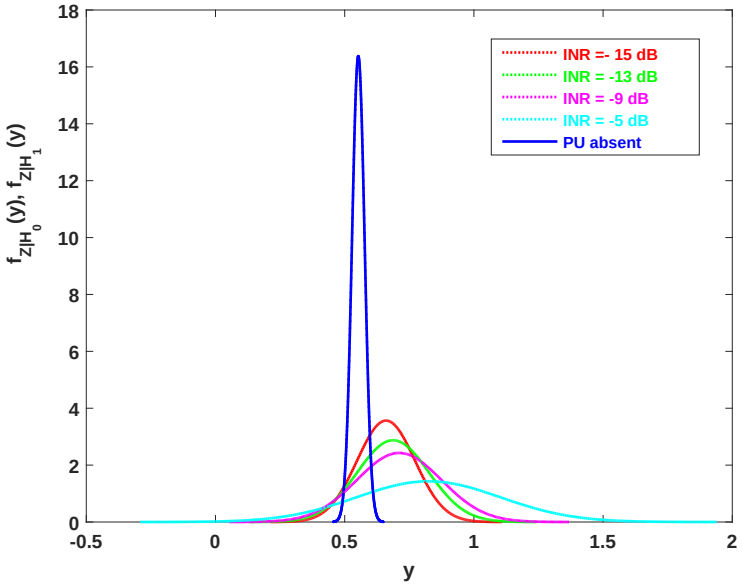

Figure 4.7: Plot of $f_{Z|H_0}(y)$ (SU only) and $f_{Z|H_1}(y)$ for different values of INR when the PU arrives at the 100^{th} time sample.

samples, which degrades detection performance. The reappearing PU scenario is the subject of ongoing research.

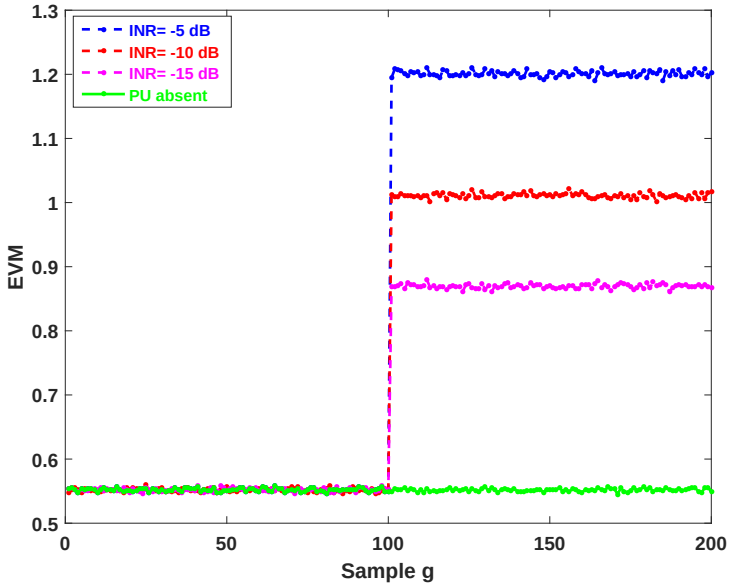

Figure 4.8: EVM response when PU arrives at the 100^{th} time sample.

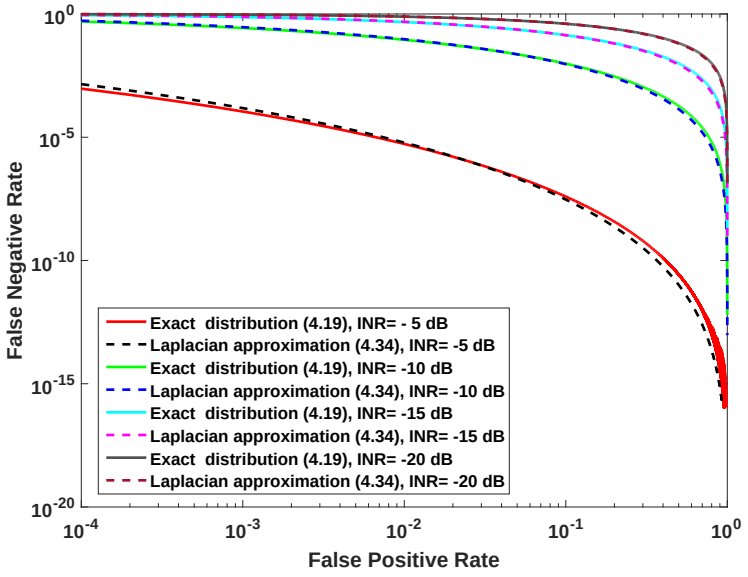

Figure 4.9: CROC curves for different INR values when L=8.

In Fig. 4.14 we have compared the proposed PU monitoring algorithm with the conventional energy detection technique. The simulated CROC curves are shown as

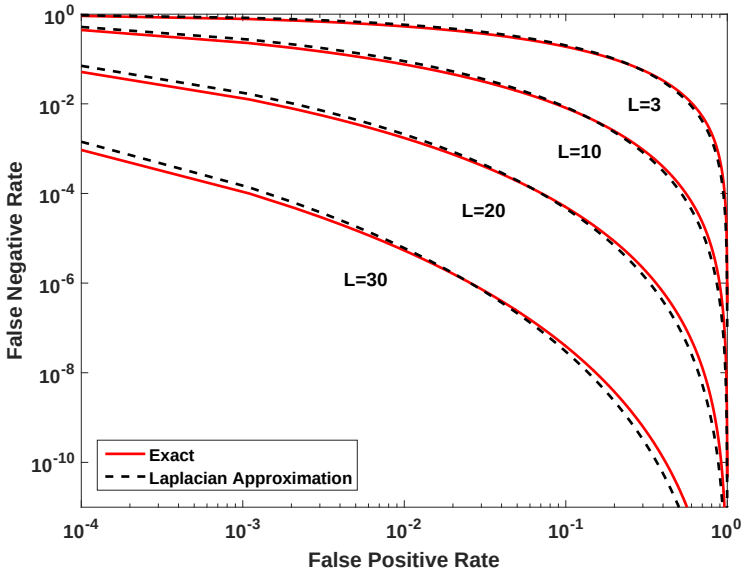

Figure 4.10: CROC curves for different number of samples with INR value of -5 dB.

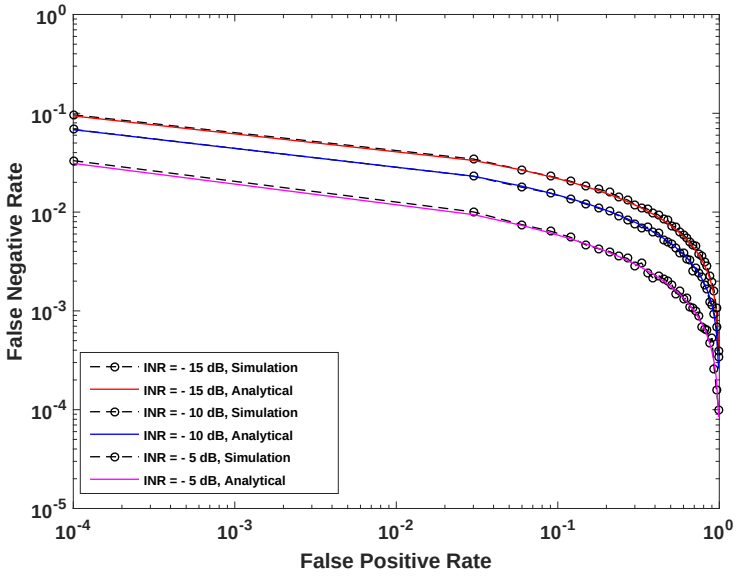

Figure 4.11: CROC curves for different INR values and L=12, when PU does not change its behavior during the sensing time.

dashed lines whereas the analytical CROC curves are shown as solid lines. For all three instances of INRs, the EVM detector shows better performance in addition to

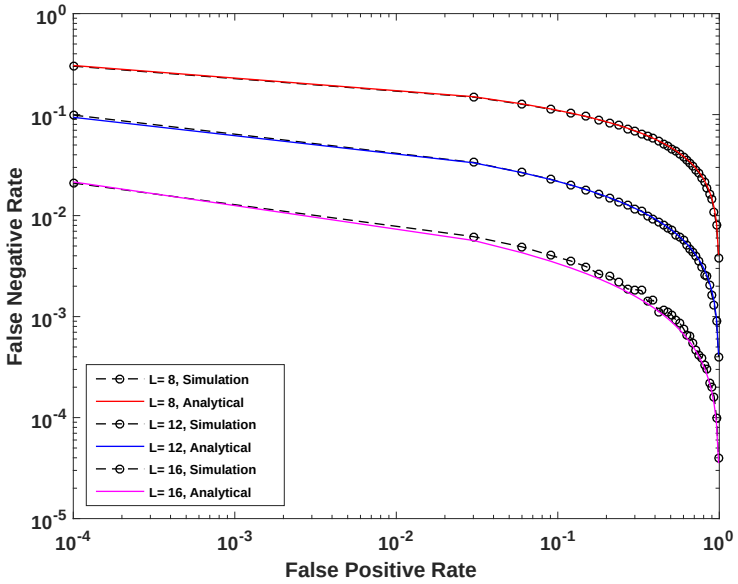

Figure 4.12: CROC curves for INR =-15 dB and L=8, 12, 16 sensing samples, when PU does not change its behavior during the sensing time.

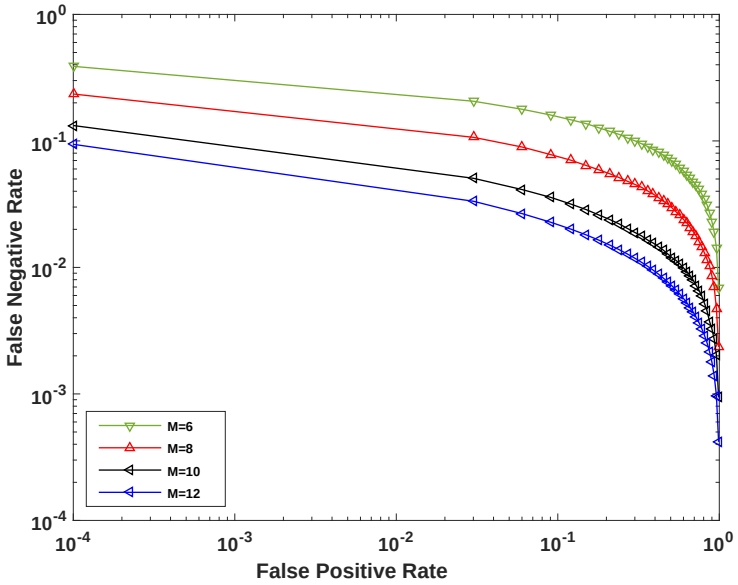

Figure 4.13: CROC curves for INR =-15 dB for reappearing PU with different number of active PU samples M in the sensing interval L+M=12.

having fast detection. Fig. 4.15 compares the EVM detector with energy detection in terms of the number of samples used. It can be seen that EVM outperforms the energy detector even at smaller sample size. In Fig. 4.16 we have compared the

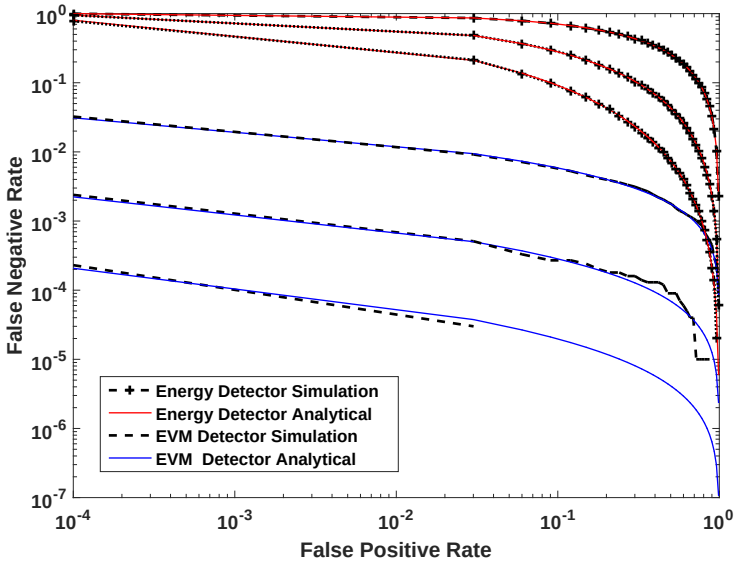

Figure 4.14: Comparison of CROC curves between our proposed EVM detector and conventional energy detector for L=12 at INRs of -5 dB, 0 dB and 2 dB from top to bottom.

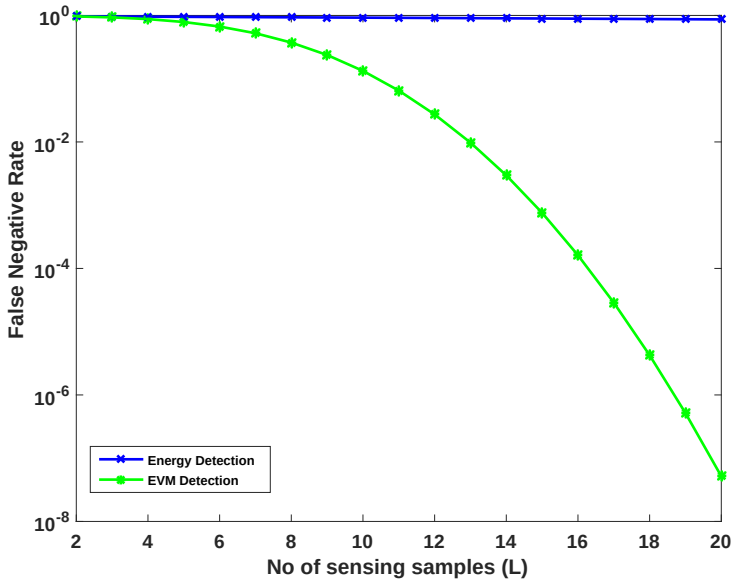

Figure 4.15: Comparison between conventional energy detector and our proposed EVM detector with different number of sensing samples at INR of -5 dB.

secondary throughput versus sensing time for conventional energy detector and EVM detector with parameters (target probability of detection = 0.9, frame duration T=

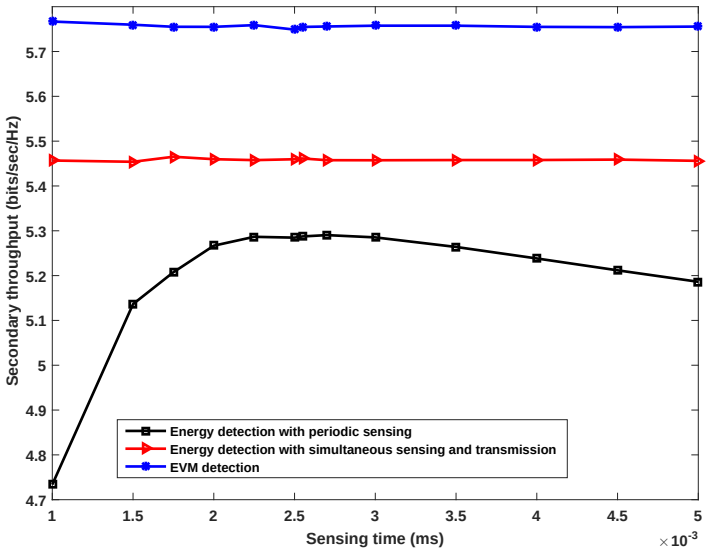

Figure 4.16: Comparison curve of the secondary throughput versus sensing time between conventional energy detector and EVM detector.

100 ms, INR= -15 dB and secondary SNR = 20 dB). We have used the throughput expressions which are derived in (4.41) and (4.44) for periodic sensing and simultaneous sensing and transmission respectively. We plug in our derived probability of false alarm (4.13) and probability of detection (4.31). From the figure, we can see a tradeoff between throughput and sensing time for the periodic sensing approach as noted in [29]. It can be seen that the optimum sensing time for periodic sensing is 2.5 ms and the simultaneous sensing and transmission approach achieves higher throughput in comparison to the periodic sensing approach for all the considered values of sensing duration. Moreover, EVM detection approach achieves higher throughput in comparison to energy detection for periodic sensing and simultaneous sensing and transmission approaches i.e the EVM approach achieves 5.75 bits/s/Hz whereas energy detection with simultaneous sensing and transmission achieves 5.45 bits/s/Hz which gives 0.3 bits/s/Hz increased throughput, which is a considerable gain. Therefore, it can be concluded that the proposed EVM detector performs better than the energy detection approach for both periodic sensing and simultaneous sensing and

transmission.

4.8 Chapter Summary

We have studied the performance of an EVM based detector that monitors the reappearing PUs during ongoing SU transmission. We have followed the widely used IEEE 802.11ac standards for the use of OFDM. The performance of the proposed algorithm has been analysed by deriving probabilities of detection and false alarm for AWGN channels. The proposed algorithm has low computational complexity compared to [4], [8] and [10]. The sliding window method in [4] calculates the energy ratio between two windows, meaning it has a complexity that is approximately twice that of the energy detector. Perfect decoding is required in [8] which is hard to achieve and [10] requires the SU to insert periodic zero-energy intervals which increases the overhead. As our system uses only the inherent pilots of the OFDM systems, our system can significantly enhance the performance of OFDM based CR networks without sacrificing system throughput along with achieving improved detection performance. Exact analyses were presented which determine the probabilities of type I and type II errors both in the case where the PU is present throughout the sensing interval, and in the case where the PU reappears during a sensing interval. A low complexity Laplacian approximation for the type I and type II error probabilities was also presented. Simulation results show the significant advantages of the proposed detection.

Chapter 5

Exact Quickest Spectrum Sensing for EVM Based Change Detection

5.1 Introduction

In chapter 4, we analyzed EVM based detection for a fixed sample size. There, a block of samples was taken, the EVM test statistic was calculated and subsequently a decision made by comparing the value of the test statistic to a predetermined threshold. Although, we have used several small blocks instead of a single long sensing block, there are two major concerns. One is that the decision is unreliable for small block size and considerable detection delay occurs for a large block size. The other is that the observations both before and after a change may appear in the same block, thus the decision may be in error. A sensing decision will be reached only after receiving all the samples as originally planned when defining the threshold. This may introduce significant delays, which may either result in interference for the PUs or reduce the data rate by shortening the transmission window of the SUs [132]. For these reasons, sequential detectors are considered as the best alternative to fixed block length detectors for the application of spectrum sensing [133].

In this chapter we apply the sequential change detection also known as the quickest detection method to the EVM based detector for detecting the reappearing PU during ongoing SU communication with the aim of minimum detection delay. Quickest detection performs a statistical test to detect the change of distribution in observations in order to attain agile and robust spectrum sensing [91]. Our aim is to develop a statistical framework to analyze detection delay, subject to certain false alarm con-

straints, and more importantly to design a scheme that can minimize the detection delay. The non-sequential spectrum monitoring methods mentioned in [27,70,93,134] focus on maximizing probability of detection subject to a certain false alarm rate. When the PU reappears, the SU needs to detect its transmission quickly to vacate the channel and when the PU stops transmission, the SU must be able to detect the absence of the PU quickly. Therefore, besides probability of detection, detection delay is an important performance metric in measuring the efficient utilization of the spectrum. Quickest detection is used to obtain the minimal detection delay subject to given false alarm constraints, and is more efficient for dynamic spectrum access [91], [135].

The red dashed line in Fig. 5.1 is the EVM calculated during the whole sensing interval. We can see PU change its status only once throughout the SU transmission period, i.e., the PU arrives at the 100^{th} block and persists for the remainder of the sensing period. In Fig. 5.2, PU changes its status twice, i.e., it arrives at the 75^{th} block, remains active for 75 samples before disappearing at the 150^{th} block. Recall that, PU status change and its detection with EVM are all happening during SU

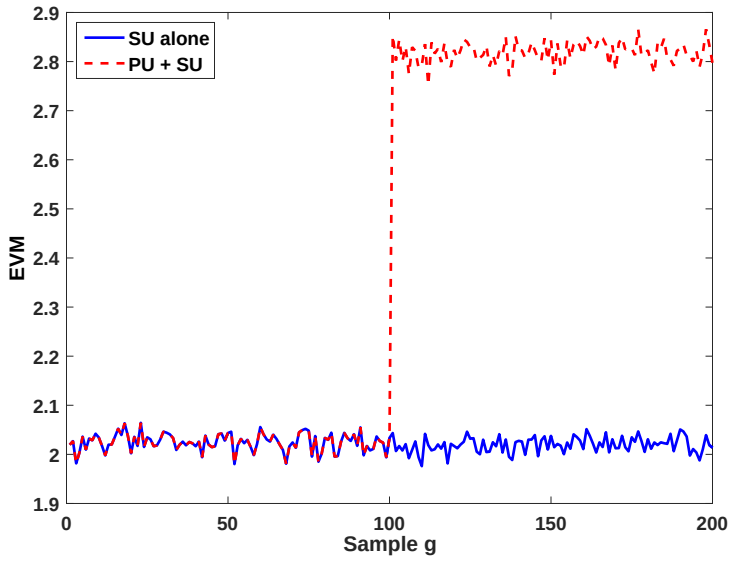

Figure 5.1: EVM response when PU arrives at the 100^{th} time sample (INR=-10 dB).

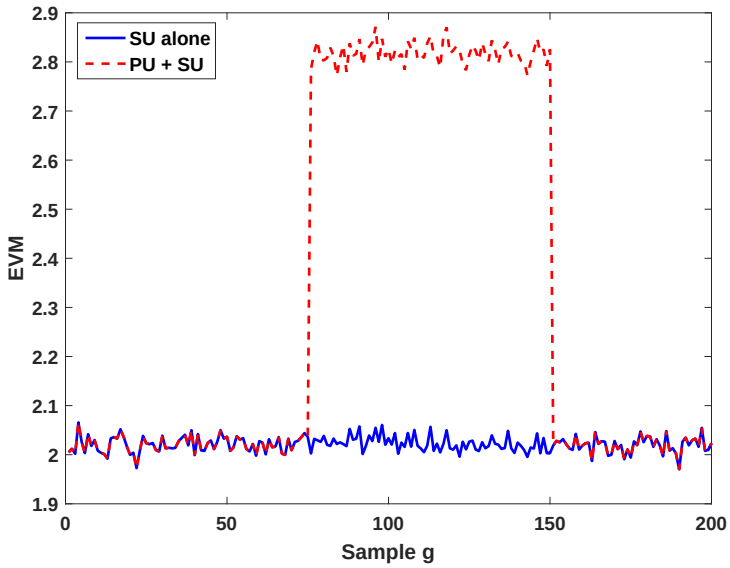

Figure 5.2: EVM response when PU arrives at the 75^{th} time sample (INR=-10 dB) and departs at the 150^{th} time sample.

transmission. When the PU starts using the channel, the SU needs to detect the existence of the PU as quickly as possible in order to vacate the channel without causing any significant interference to the transmission of the PU. In contrast, when the PU stops transmission, the SU must be able to detect its absence as soon as possible to enable the SU to fully utilize the unused spectrum for its transmission. Fig. 5.2 reflects both conditions. Therefore, the entry and exit of the PU has to be determined with minimum detection delay in order to overcome these issues. This is only possible if we cast the hypothesis detection problem within the framework of quickest detection. We now apply quickest detection to know as soon as possible when the PU appears within the sensing interval to ensure that the SUs can vacate the channel in time for the next SU slot.

Full-Duplex (FD) energy detection [29, 31, 32] also can be employed for the application of quickest detection. The idea is to apply SIC to cancel the self interfering signal, and to perform energy detection spectrum sensing on the remaining signal. In [29, 31, 32], the SU signal is typically treated as unknown at the receiver, and the

effectiveness of SIC is represented using a linear "self-interference mitigation coefficient" which is applied to degrade the effectiveness of spectrum sensing. However, they do not account for error propagation from incorrect SU decisions feeding into the SIC process. In this thesis, we assume that the received SU pilot symbols are perfectly removed for calculating the EVM statistic, with remaining synchronization and channel estimation errors treated as AWGN having identical variance for H_0 and H_1.

The rest of the chapter is organized as follows. Section 5.2 describes the system model and gives the PDF's for the H_0 (PU absent) and H_1 (PU present) hypotheses. In Section 5.3, quickest detection is discussed. The application of quickest detection using EVM test statistic is presented in Section 5.4. Performance analysis and results are presented in Section 5.5 and 5.6, respectively. Finally, Section 5.7 concludes the chapter.

5.2 System model

We use the system model as described in chapter 3. The only difference here is the application of the CUSUM algorithm after EVM calculation as shown in Fig. 5.3. We consider that the channel is idle at the beginning and thus the SU can access the channel and start transmitting. An SU needs to monitor the channel periodically, and if the PU reappears, the SU needs to vacate the channel as quickly as possible in order to minimize detection delay. Detection delay impacts the duration that the SU may cause harmful interference to the PU. Since, it is clear from Fig. 5.1 and 5.2 that the PU can arrive and leave at anytime during SU transmission, we model the PU reappearance problem as an EVM based change detection and study the quickest spectrum sensing performance as shown in Fig. 5.4.

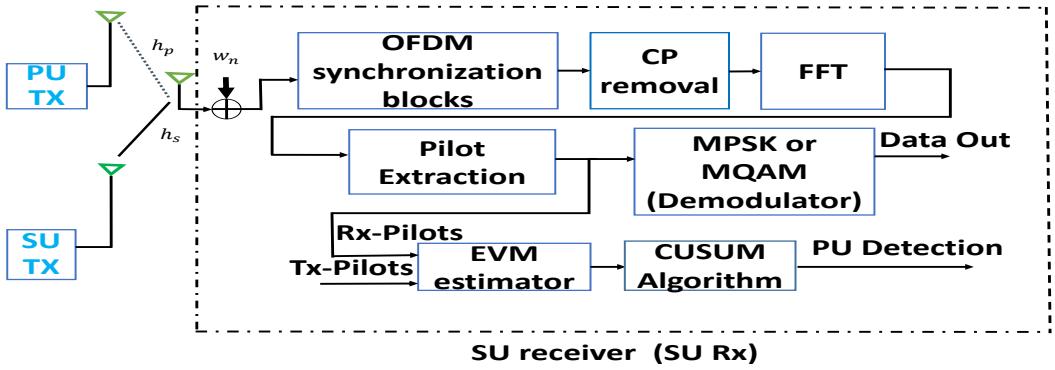

Figure 5.3: Block diagram of EVM based CUSUM detector.

In chapter 4, (4.6), we derived the EVM test statistic per subcarrier as

$$Z_p(k) = \sqrt{\frac{1}{LE_s|H_{ps}(k,l)|^2}\sum_{l=0}^{L}\left|E_p(k,l)\right|^2}, \tag{5.1}$$

where

$$E_p(k,l) = \begin{cases} W_p(k,l), & H_0 \\ H_p(k,l)I_p(k,l) + W_p(k,l), & H_1. \end{cases} \tag{5.2}$$

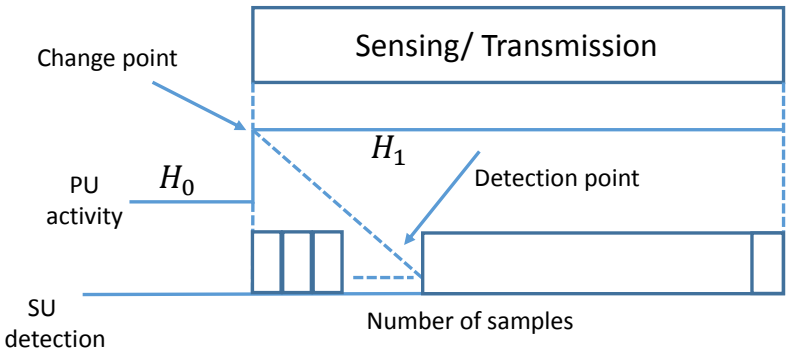

Figure 5.4: EVM based change point detection of PU reappearance.

We found that the PDF of the decision statistic Z in the absence of the PU is given by

$$f_{Z|H_0}(y) = \frac{L^L 2^{1-L} y^{2L-1} e^{\frac{-Ly^2}{2\sigma_w^2}}}{\sigma_w^{2L}\Gamma(L)}, \quad y > 0. \tag{5.3}$$

We now consider two different types of PU as below:

Case I: We assume PU to be an independent Gaussian random signal with zero mean and variance σ_I^2. Accordingly, Z follows a central chi distribution whose PDF can be written as

$$f_{Z|H_1}(y) = \frac{L^L}{2^{L-1}(\sigma_I^2 + \sigma_w^2)^L \Gamma(L)} y^{2L-1} e^{\frac{-Ly^2}{2(\sigma_I^2+\sigma_w^2)}}. \tag{5.4}$$

Case II: We assume the PU signal to be an unknown deterministic signal whose symbol duration is longer than the sensing interval. In this case, Z follows a non-central chi-distribution with non-central parameter $\beta = \sqrt{2L\gamma}$, where $\gamma = \frac{\mu_I^2}{\sigma_w^2}$ is the interference to noise ratio (INR). The PDF under H_1 can thus be expressed as

$$f_{Z|H_1}(y) = \frac{e^{-\left(\frac{\frac{y^2}{\sigma_w^2}+\beta^2}{2}\right)} y^{2L} \beta I_{L-1}\left(\frac{\beta y}{\sigma_w}\right)}{\sigma_w^L (\beta y)^L}, \tag{5.5}$$

5.3 Quickest detection

This section applies the results from Section 5.2 to introduce quickest detection based on the EVM metric. In quickest detection it is assumed that it is known which hypothesis is true and that a change to the other hypothesis will be detected with as little detection delay as possible. Contrary to evaluating the probabilities of detection P_D and false alarm P_F as in block detection, the design criteria for quickest detection are the mean time to detection τ_D and the mean time to false alarm τ_F. A well known

algorithm used in quickest detection is the cumulative sum (CUSUM) algorithm [136]. It evaluates recursively on a sample-by-sample basis, so we set the number of sensing samples L to be 1 [91, 132, 137].

Without loss of generality, we assume in the following that before an unknown change time τ, hypothesis H_0 is true and at time τ transmission of the PU starts, i.e., hypothesis H_1 becomes true. Let U_t be a sequence of random variables with a probability density $f_{\theta 0}(u)$. Before an unknown change time i.e. for $t < \tau$, the parameter θ is equal to θ_0, and after the change time i.e. for $t \geq \tau$, it is equal to θ_1. Samples $u(t)$ are taken in order to detect the change from $H_0 \rightarrow H_1$. The SU observes the samples sequentially and employs the CUSUM algorithm to detect the PU via a change in the EVM distribution. The CUSUM algorithm relies on the log-likelihood ratio of the received sample at time index t : $l_u(t) = \ln\left\{\frac{f_{\theta 1}(u(t))}{f_{\theta 0}(u(t))}\right\}$. The CUSUM algorithm detects the abrupt change at sample

$$T = \inf(t : B_u(t) \geq \psi), \tag{5.6}$$

where ψ is a threshold and $B(t)$ is the CUSUM statistic defined as [91].

$$B_u(t) = \max_{k \leq t} \sum_{i=k+1}^{t} l_u(i). \tag{5.7}$$

Intuitively, T is the first time that the metric $B_u(t)$ passes the threshold ψ. The log likelihood ratio in (5.7) is given by

$$l_u(i) = \ln\left\{\frac{f_{\theta 1}(u(i))}{f_{\theta 0}(u(i))}\right\}. \tag{5.8}$$

A cumulative sum of the log-likelihood ratios of consecutive samples is formed by the CUSUM algorithm. A convenient recursive formulation of the CUSUM statistic, $B_u(t)$, can be given as [89, 136]

$$B_u(t+1) = \{B(t) + l_u(t)\}^+, \tag{5.9}$$

where $x^+ = \max(x, 0)$. Therefore, the CUSUM statistic can be computed recursively for $t \geq 0$ by setting $B(t) = 0$. The $B_u(t+1)$ statistic is compared to a threshold, ψ, after each sample and the algorithm will raise an alarm when $B_u(t+1) \geq \psi$, which decides that a change to H_1 has happened or indicates the existence of the PU. We now study the application of quickest detection using the EVM test statistic.

5.4 Application of quickest detection using the EVM test statistic

To adapt the results from Section 5.3, we use the EVM test statistic from (5.1) and use existing results from quickest detection. Depending on whether H_0 or H_1 is true, $Z(k)$ in (5.1) is distributed according to $f_{Z|H_0}(z)$ or $f_{Z|H_1}(z)$, respectively.

Thus, the log-likelihood ratio can be found for the two different cases above by inserting (5.4) and (5.5) into its definition as

Case I:

$$l(z) = ln\left\{\frac{f_{Z|H_1}(z)}{f_{Z|H_0}(z)}\right\} = ln\left\{\frac{\frac{L^L 2^{1-L} z^{2L-1} e^{-\frac{Lz^2}{2(\sigma_I^2+\sigma_w^2)}}}{(\sigma_I^2+\sigma_w^2)^L \Gamma(L)}}{\frac{L^L 2^{1-L} z^{2L-1} e^{\frac{-Lz^2}{2\sigma_w^2}}}{\sigma_w^{2L}\Gamma(L)}}\right\} \tag{5.10}$$

$$= ln\left\{\frac{L^L 2^{1-L} z^{2L-1} e^{\frac{-Lz^2}{2(\sigma_I^2+\sigma_w^2)}}}{(\sigma_I^2+\sigma_w^2)^L \Gamma(L)} \times \frac{(\sigma_w^2)^L \Gamma(L)}{L^L 2^{1-L} z^{2L-1} e^{-\frac{Lz^2}{2\sigma_w^2}}}\right\}$$

$$= ln\left\{\frac{e^{\frac{-Lz^2}{2(\sigma_I^2+\sigma_w^2)}}}{(\sigma_I^2+\sigma_w^2)} \times \frac{\sigma_w^2}{e^{-\frac{Lz^2}{2\sigma_w^2}}}\right\}$$

$$= ln\left\{e^{\frac{Lz^2\sigma_I^2}{2\sigma_w^2(\sigma_I^2+\sigma_w^2)}}\right\} + L\ ln\left\{\frac{\sigma_w^2}{\sigma_I^2+\sigma_w^2}\right\}$$

$$= \frac{Lz^2\sigma_I^2}{2\sigma_w^2(\sigma_I^2+\sigma_w^2)} + L\ ln\left\{\frac{\sigma_w^2}{\sigma_w^2+\sigma_I^2}\right\}$$

$$= \frac{z^2\sigma_I^2}{2\sigma_w^2(\sigma_I^2+\sigma_w^2)} + ln\left\{\frac{\sigma_w^2}{\sigma_w^2+\sigma_I^2}\right\}. \tag{5.11}$$

Case II:

$$l(z) = ln\left\{\frac{f_{Z|H_1}(z)}{f_{Z|H_0}(z)}\right\} = ln\left\{\frac{\frac{e^{-\left(\frac{\frac{z^2}{\sigma_w^2}+\beta^2}{2}\right)} z^{2L}\beta I_{L-1}\left(\frac{\beta z}{\sigma_w}\right)}{\sigma_w^L(\beta z)^L}}{\frac{L^L 2^{1-L} z^{2L-1} e^{\frac{-Lz^2}{2\sigma_w^2}}}{\sigma_w^{2L}\Gamma(L)}}\right\} \tag{5.12}$$

which contains the PDF of the chi and noncentral chi distribution. Note L=1 and $\Gamma(L) = (L-1)!$ is the Gamma function, where L is an integer. Thus, (5.12) can be re-written as

$$l(z) = ln\left\{e^{\left(\frac{\beta^2}{2}\right)} I_0\left(\frac{\beta z}{\sigma_w}\right)\right\}, \tag{5.13}$$

where I_0 is the zero order modified Bessel function of the first kind.

In order to achieve further simplification, we know that a zero order modified Bessel function of the first kind can be approximately replaced by an exponential function when the term $\left(\frac{\beta z}{\sigma_w}\right)$ is large [138]. Then (5.13) can be rewritten as

$$\begin{aligned} l(z) &= ln\left\{e^{\left(\frac{\beta^2}{2}\right)} e^{\left(\frac{\beta z}{\sigma_w}\right)}\right\} \\ &= ln\left\{e^{\left(\frac{\beta^2}{2}+\frac{\beta z}{\sigma_w}\right)}\right\} \\ &= \frac{\beta(\beta\sigma_w + 2z)}{2\sigma_w} \end{aligned} \tag{5.14}$$

Using the log-likelihood ratios in (5.11) or (5.13), we can write the CUSUM algorithm for our model as:

$$g(z+1) = [g(z) + l(z)]^+. \tag{5.15}$$

Hence, we can compute $g(z)$ recursively, by setting $g(0) = 0$. In summary, the algorithm works as follows: the SU computes $l(z)$ using (5.11) or (5.13) after each

sample, computes the statistic $g(m)$ using (5.15), and compares this statistic with a threshold ψ. If $g(z)$ is larger than ψ, the algorithm declares that the PU is present.

5.5 Performance analysis

Let T denote the sample number at which the change is detected and τ be the sample number when the change actually occurs. If $T > \tau$, then the detection delay is $T - \tau$. On the other hand, the event $T < \tau$ is a false alarm event and $\bar{T}_0 = \mathbb{E}_{f0}[T]$ is the mean time to false alarm which is measured when there is no change in the EVM distribution. The false alarm rate is then defined as $P_{FA}(T) = \frac{1}{\mathbb{E}_{f0}[T]}$. The CUSUM algorithm is asymptotically minimax optimal with respect to Lorden's measure of the worst-case detection delay. Based on Lorden's formulation, the worst-case detection delay is denoted by [89, 91, 139].

$$\overline{T_d} = \sup_{\tau \geq 1} \text{ess sup } \mathbb{E}_{f_1}[T - \tau | T \geq \tau], \tag{5.16}$$

where $\mathbb{E}_{f_1}$ denotes the expectation operator when the change occurs at sample number τ. Thus, the quickest detection problem for CR is to obtain a strategy that can minimize $\overline{T_d}$, while fulfilling the given false alarm constraint. The threshold ψ can be set based on the lower bound on $\bar{T}_0$, where the bound can be expressed as [89, 91]

$$\bar{T}_0 \geq e^{\psi}. \tag{5.17}$$

Alternatively, the threshold values can be set in an arbitrary way to give a desired range of detection delay or false alarm rate.

5.6 Results

In this section we present some simulation results to evaluate the quickest sensing performance for EVM based change detection in the Gaussian channel. Fig. 5.5 shows a typical realization of the CUSUM EVM and CUSUM ED statistics, when

the PU starts transmission at τ=100. We have set SU SNR = 6 dB. As expected, the CUSUM test statistic tends to reset to a value of zero prior to the PU transmission and grows continuously after the change time τ. We have simulated for both cases of PU as considered in Section 5.2. The CUSUM algorithm is sensitive to uncertainty in parameters [91]. Therefore, the cumulative sum for an unknown deterministic signal does not increase much which is the price we have to pay for the signal not being known. However, for a known Gaussian random signal the cumulative sum of the CUSUM increases more rapidly after m=100 than the CUSUM ED, thus a large difference is observed before and after the PU appearing. Thus, it is very easy to detect the change of spectrum activities by using an appropriate threshold with CUSUM EVM. This is because the CUSUM algorithm entirely relies on the instantaneous log-likelihood ratio $l(m)$ defined by (5.11) and (5.13) which depends on the PDF of the signal samples, and thus on its different parameters. Figs. 5.6 and 5.7 show the characteristics of the proposed quickest EVM by varying P_{FA} for the average detection delay in comparison to that of the quickest ED in [135]. Simulations use 5000 trials, where each trial has 200 samples. PU begins transmission at τ= 100. We have set the threshold values to ψ=3, 3.5, 4, 4.5, 5, 6, 6.5, 7 to give a reasonable range of average detection delay or P_{FA} values as mentioned in [135]. We measure the average detection delay and P_{FA} based on the pre-determined threshold values. It is clear from Fig. 5.6 that for both quickest EVM and quickest ED, the stricter P_{FA} is, the greater detection delay we have. We can see that if we constrain ourselves to a small rate of false alarm for assuring the efficiency of opportunistic accessing, the proposed EVM based quickest sensing algorithms perform better than the energy detection for all instances of considered INR. This reinforces the results of chapter 4 which show that EVM spectrum sensing performs better than energy detection spectrum sensing for a fixed number of samples.

Since, the modified Bessel function is computationally complex we have provided a low complexity approximate solution in (5.14). Fig. 5.8 shows the simulated results. It provides the asymptotic results of the CUSUM algorithm. Fig. 5.8 shows

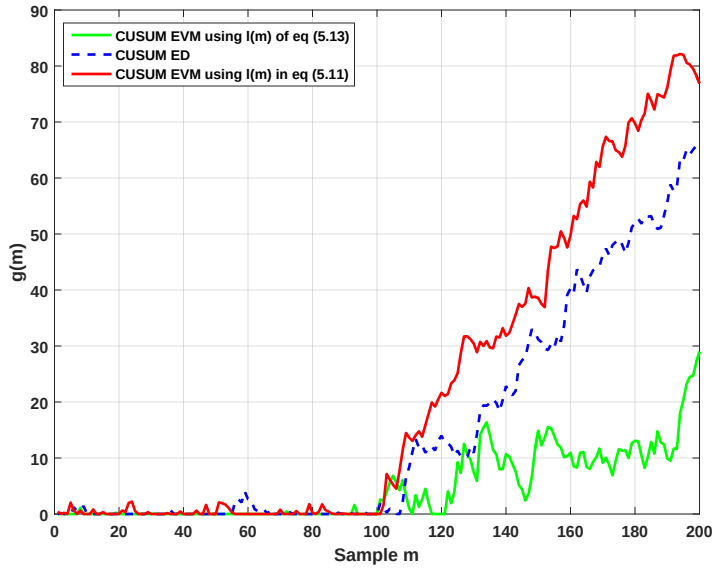

Figure 5.5: CUSUM metric for typical realization of the CUSUM EVM and CUSUM energy detection (ED) method statistic, when $\tau = 100$ and INR $= 5$ dB.

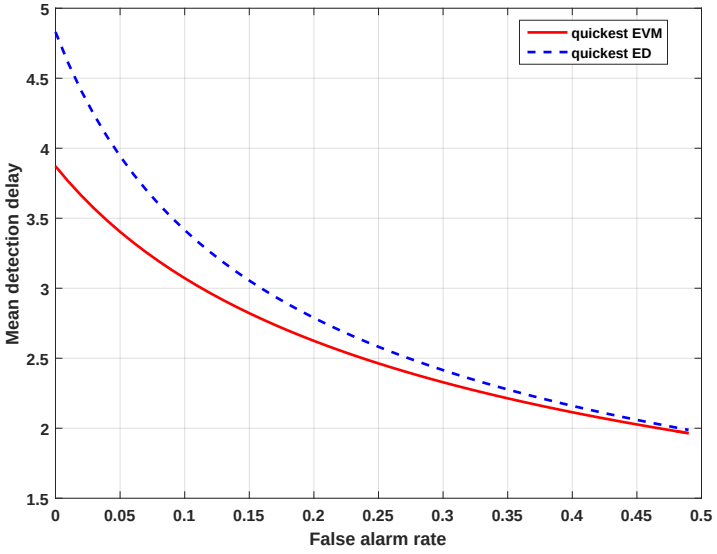

Figure 5.6: Comparison between the performance of the quickest EVM and quickest ED for INR= 5 dB.

that the approximation over-estimates CUSUM, particularly at lower values of INR. However, this approximation is useful for realizing the performance of the proposed quickest EVM detection over practical wireless fading channels like Nakagami-m fading that contains $I_0(z)$ term in the PDF expression [140].

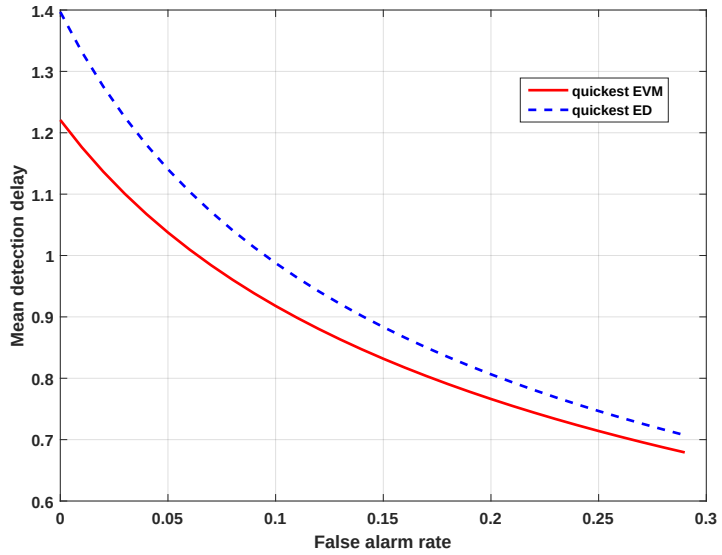

Figure 5.7: Comparison between the performance of the quickest EVM and quickest ED for INR= 10 dB.

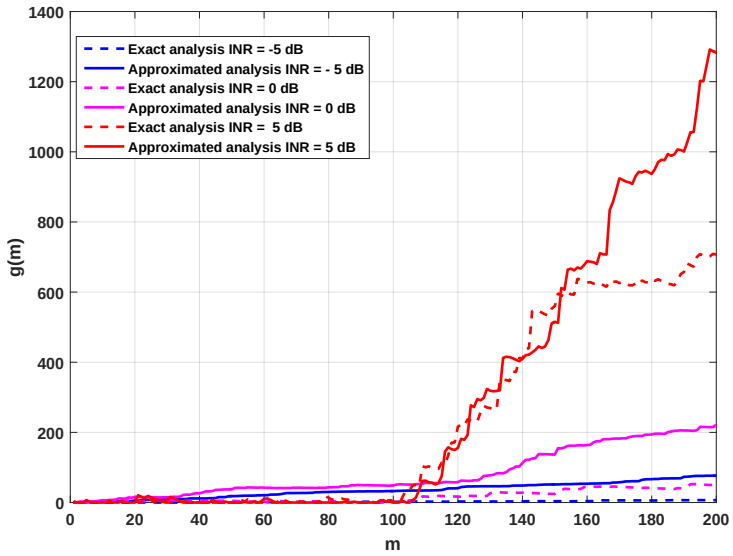

Figure 5.8: A typical realization of the exact CUSUM EVM and approximated CUSUM EVM when $\tau = 100$ and INR = -5, 0 and 5 dB.

5.7 Chapter Summary

We have studied the effectiveness of exact quickest EVM based spectrum sensing. Detection theory is applied to EVM spectrum sensing to achieve agile and robust performance. The proposed system has been designed to detect the reappearing PU during ongoing SU transmission so that the SU can stop interfering as quickly as possible. Simulation results show that quickest EVM detection outperforms the quickest ED scheme. These results reinforce the results of chapter 4 which show that EVM spectrum sensing performs better than energy detection based spectrum sensing.

Chapter 6

Conclusions and future works

In this chapter we summarize the novel contributions of this thesis and highlight several possible directions for future work.

6.1 Conclusions

The current fixed spectrum allocation policies and the increasing demand for wireless services and applications have led to the problem of spectrum scarcity. In this regard, CR has emerged as a potential solution to efficiently utilize the unused spectrum. The thesis has primarily focused on the interweave paradigm among the three CR paradigms considered in the literature. Under this paradigm, the SUs are allowed to opportunistically utilize a frequency band when it is not being used. This is accompanied by the process of spectrum sensing. Spectrum sensing can be categorized into two types [59] : out-of-band sensing and in-band sensing. Out-of-band sensing searches for an idle channel by sensing multiple channels sequentially until an available channel is found. Once the channel is utilized, in-band sensing must promptly detect the return of PUs so that SUs can vacate the channel immediately upon detection of returning PUs. It is desirable to perform in-band sensing as frequently as possible for fast detection of the returning PUs. However, such sensing incurs significant overhead and requires the SU to stop its transmission periodically. Therefore it is desirable to search for a method by which SUs can monitor the frequency band without interrupting their communications.

In this thesis, we propose an in-band sensing scheme suitable for an OFDM based CR network that permits SUs to perform spectrum monitoring during transmission. This

monitoring technique supplements the traditional spectrum sensing and provides enhanced communications efficiency. We have considered the use of the EVM metric for monitoring the reappearing PU during the reception of packets. EVM is measured as a difference between the received and known transmitted pilots. Throughout the thesis, we have followed the IEEE 802.11 ac pilot structure by way of practical example although the analysis presented in the thesis is general and may apply to any pilot tone pattern. EVM has several advantages which are extremely useful for developing practical CR. Firstly, it facilitates simultaneous sensing and transmission by the SU. Secondly, it removes the need for the sophisticated SIC method as required by FD spectrum sensing techniques since the SU transmitted signal gets canceled out during EVM calculation. Thirdly, it utilizes fewer symbols and provides results well before demodulation and decoding and gives us real time results.

The main focus of the thesis was to develop an EVM based spectrum monitoring technique for OFDM based CR networks. The primary objectives are to increase the detection performance and enhance throughput of the CR enabled SUs. The objectives have been achieved successfully. As common in the research area of spectrum monitoring, theoretical analytical performance of the proposed solution is evaluated.

The main contributions of this thesis are

- In Chapter 3, we proposed an EVM based PU monitoring technique. We utilized the inherent pilot tones embedded in OFDM to measure the EVM. The EVM is calculated as a difference between the received and transmitted pilot tones. The results show that a step change in the EVM curve is sufficient to clearly distinguish between the two hypotheses H_0 and H_1. In the absence of the PU in the band, the calculated EVM involves only noise and receiver impairments such as estimation errors. Therefore, the EVM remains static as the impairment variance does not change significantly over time. However, once the PU appears, the EVM additionally includes the PU interference, which results in a step change in EVM when the PU is detected.

- In Chapter 4, we studied the performance of the EVM detector in an AWGN channel. We derived an analytical form of the PDF of the EVM based detector based on the exact representation of chi distributions. We analyzed the performance by deriving the type I and type II error probabilities. Furthermore, from the fundamental theorem of central and non-central chi distributions, we derived a novel analytic expression for type I and type II error probabilities accounting for the specific scenario of detecting a reappearing PU during secondary transmission. In addition, we provided a simple analytic expression for type I and type II error probabilities by making use of Laplacian approximation for a chi random variable. This approximation facilitates spectrum sensing even with a small number of samples unlike the Gaussian approximation which requires a large number of sensing samples. We also analysed the throughput performance of the EVM detector.

  The CROC performance analysis showed that our method outperformed the energy detection method. The throughput performance of our system was enhanced in comparison to energy detection.

- We studied the effectiveness of exact quickest EVM based spectrum sensing. The theory of detection was applied to spectrum sensing to achieve agile and robust performance. The proposed system was designed to detect the reappearing PU during ongoing SU transmission so that the SU can avoid the interference as quickly as possible. Simulation results showed that quickest EVM detection outperforms the quickest energy detection scheme. These results reinforced the results of Chapter 4 which showed that EVM based spectrum sensing performs better than energy detection based spectrum sensing.

To conclude, this thesis has shown the benefits of EVM based detection solutions for OFDM based CR networks. Two types of detection methods viz. block based and quickest detection were described and simulated. The results from both methods showed significant advantages over energy detection methods. Our results showed

that the EVM based PU monitoring approach is potentially more suitable for CR technology than the energy detection approach.

6.2 Future works

In this section we indicate some possible future research directions which should be considered to further enhance the performance of the systems we have developed in this thesis.

- In our thesis, our EVM calculation assumes that the channel is both known and static. In practice, neither is true. Analyzing the impact of an unknown and estimated channel on our detection performance would be useful and interesting.

- We have used EVM to detect the reappearance of the PU by utilizing the inherent pilot tones of the OFDM system. The system has been investigated without any RF impairments. However, several RF impairments like IQ mismatch, phase noise, PA nonlinearity, carrier frequency offset (CFO) and sampling frequency offset (SFO) degrade the performance of EVM. This will affect the detection performance. It would be interesting to study the combined effect of these RF impairments on EVM and analyse the detection performance accordingly.

- The system model in this thesis has been considered in the framework of single input single output (SISO) systems. However, it would be interesting to analyse our system in the context of multiple input multiple output (MIMO). Furthermore, we have assumed an AWGN channel throughout the thesis, however this can be extended to other practical fading channels such as Rayleigh, Rician , Nakagami, $\eta - \mu$ and $k - \mu$ channels.

- In Chapter 4, we have done a preliminary analysis of throughput performance using an EVM based block detection approach. It could be interesting to conduct a throughput analysis using EVM based quickest spectrum sensing and compare the achievable throughput and efficiency of these two approaches.

- Another possible extension of our work could be to rate adaptation. The traditional rate adaptation algorithms in CR try to cope with fading and PU interference by varying the transmission rate in response to either packet losses or SNR variations. However, these are not done at a per symbol level that explains the bursty nature of the PU, which can arrive at anytime within the SU frame transmission. The same PHY rate is used over an entire duration of frame transmission which causes significant performance degradation when the channel quality changes within a frame transmission. Such channel changes can cause consecutive transmission errors leading to severe inefficiencies in symbol retransmissions. To improve performance, the SU transmitter should adaptively change its PHY rate at the symbol level. As EVM detection allows the SU receiver to detect PU emergence mid packet, it can be considered as a convenient symbol level performance metric. We can use the EVM as the CSI feedback from the receiver, for the transmitter to perform power and rate selection. Thus, we can achieve a reliable frame transmission using an EVM based symbol-level rate adaptation according to the PU traffic. In doing so, we can expect a significant gain in throughput performance.

Bibliography

[1] B. Kumar, S. Kumar Dhurandher, and I. Woungang, "A survey of overlay and underlay paradigms in cognitive radio networks," *International Journal of Communication Systems*, vol. 31, no. 2, p. e3443, 2018.

[2] K. Shuaib *et al.*, "Cognitive radio for smart grid with security considerations," *Computers*, vol. 5, no. 2, p. 7, Apr. 2016.

[3] M. Elo, "Orthogonal frequency division multiplexing," *Keithley Instruments, Inc*, 2007.

[4] Ericsson Mobility Report: On the pulse of the Networked Society. [Online]. Available: https://www.ericsson.com/assets/local/mobility-report/documents/2016/ericsson-mobility-report-november-2016.pdf

[5] J. G. Andrews, S. Buzzi, W. Choi, S. V. Hanly, A. Lozano, A. C. Soong, and J. C. Zhang, "What will 5g be?" *IEEE Journal on Selected Areas in Communications*, vol. 32, no. 6, pp. 1065–1082, 2014.

[6] B. Wang and K. R. Liu, "Advances in cognitive radio networks: A survey," *IEEE Journal of Selected Topics in Signal Processing*, vol. 5, no. 1, pp. 5–23, 2011.

[7] C.-S. Sum *et al.*, "Cognitive communication in TV white spaces: An overview of regulations, standards, and technology," *IEEE Communications Magazine*, vol. 51, no. 7, pp. 138–145, Jul. 2013.

[8] OFCOM, "Regulatory requirements for white space device in the UHF TV band," Tech. Rep., July. 2012.

[9] I. F. Akyildiz, W.-Y. Lee, M. C. Vuran, and S. Mohanty, "Next generation/dynamic spectrum access/cognitive radio wireless networks: a survey," *Computer Networks*, vol. 50, no. 13, pp. 2127–2159, 2006.

[10] K. Patil, R. Prasad, and K. Skouby, "A survey of worldwide spectrum occupancy measurement campaigns for cognitive radio," in *International Conference on Devices and Communications*, Feb. 2011, pp. 1–5.

[11] FCC, "Spectrum policy task force report," ET Docket 02-155, Nov. 02 2002.

[12] S.-H. Hwang and M.-J. Rim, "Adaptive operation scheme for quiet period in IEEE 802.22 system," in *International Conference on ICT Convergence*, 2011, pp. 482–484.

[13] A. Goldsmith, S. A. Jafar, I. Marić, and S. Srinivasa, "Breaking spectrum gridlock with cognitive radios: An information theoretic perspective," in *Proceedings of the IEEE*, vol. 97, no. 5, 2009, pp. 894–914.

[14] J. M. Iii, "An integrated agent architecture for software defined radio," *PhD dissertation, KTH Royal Institute of Technology*, 2000.

[15] K. Chang and B. Senadji, "Spectrum sensing optimisation for dynamic primary user signal," *IEEE Transactions on Communications*, vol. 60, no. 12, pp. 3632–3640, 2012.

[16] Y.-C. Liang, Y. Zeng, E. C. Peh, and A. T. Hoang, "Sensing-throughput tradeoff for cognitive radio networks," *IEEE Transactions on Wireless Communications*, vol. 7, no. 4, pp. 1326–1337, 2008.

[17] Y. Pei, A. T. Hoang, and Y.-C. Liang, "Sensing-throughput tradeoff in cognitive radio networks: How frequently should spectrum sensing be carried out?" in *IEEE International Symposium on Personal, Indoor and Mobile Communications*, Sept. 2007, pp. 1–5.

[18] S. Stotas and A. Nallanathan, "Overcoming the sensing-throughput tradeoff in cognitive radio networks," in *IEEE International Conference on Communication Systems*, 2010, pp. 1–5.

[19] S. K. Sharma, S. Chatzinotas, and B. Ottersten, "A hybrid cognitive transceiver architecture: Sensing-throughput tradeoff," in *IEEE International Conference on Cognitive Radio Oriented Wireless Networks and Communications*, Jun. 2014, pp. 143–149.

[20] S.-Y. Liu and J.-W. Chong, "A study of joint tracking algorithms of carrier frequency offset and sampling clock offset for OFDM-based WLANS," in *IEEE International Conference on Circuits and Systems and West Sino Expositions*, vol. 1, 2002, pp. 109–113.

[21] W. S. Jeon, D. G. Jeong, J. A. Han, G. Ko, and M. S. Song, "An efficient quiet period management scheme for cognitive radio systems," *IEEE Transactions on Wireless Communications*, vol. 7, no. 2, 2008.

[22] A. Ali and W. Hamouda, "Spectrum monitoring using energy ratio algorithm for OFDM-based cognitive radio networks," *IEEE Transactions on Wireless Communications*, vol. 14, no. 4, pp. 2257–2268, 2015.

[23] W. Lee and D.-H. Cho, "Concurrent spectrum sensing and data transmission scheme in a CR system," in *IEEE Wireless Communications and Networking Conference*, 2012, pp. 1326–1330.

[24] S. Stotas and A. Nallanathan, "On the throughput and spectrum sensing enhancement of opportunistic spectrum access cognitive radio networks," *IEEE Transactions on Wireless Communications*, vol. 11, no. 1, pp. 97–107, 2012.

[25] J. C. Clement, D. Emmanuel, and J. J. Winston, "Improving sensing and throughput of the cognitive radio network," *Circuits, Systems, and Signal Processing*, vol. 34, no. 1, pp. 249–267, 2015.

[26] J. Ko, H. Ko, and C. Kim, "Fast primary user detection during ongoing opportunistic transmission in OFDM-based cognitive radio," *Wireless Personal Communications*, vol. 70, no. 4, pp. 1463–1471, 2013.

[27] S. W. Boyd, J. M. Frye, M. B. Pursley, and T. C. Royster IV, "Spectrum monitoring during reception in dynamic spectrum access cognitive radio networks," *IEEE Transactions on Communications*, vol. 60, no. 2, pp. 547–558, 2012.

[28] W. Afifi and M. Krunz, "Adaptive transmission-reception-sensing strategy for cognitive radios with full-duplex capabilities," in *IEEE International Symposium on Dynamic Spectrum Access Networks (DYSPAN)*, Apr. 2014, pp. 149–160.

[29] A. Nasser *et al.*, "Spectrum sensing for half and full-duplex cognitive radio," in *Spectrum Access and Management for Cognitive Radio Networks*. Springer, 2017, pp. 15–50.

[30] W. Cheng, X. Zhang, and H. Zhang, "Full duplex spectrum sensing in non-time-slotted cognitive radio networks," in *IEEE Military Communications Conference*, 2011, pp. 1029–1034.

[31] T. Riihonen and R. Wichman, "Energy detection in full-duplex cognitive radios under residual self-interference," in *IEEE International Conference on Cognitive Radio Oriented Wireless Networks and Communications*, 2014, pp. 57–60.

[32] X. Yan, I. Ahmad, M. Gao, J. Yang, Y. Zhang, Z. Feng, and Y. Zhang, "Improved energy detector for full duplex sensing," in *IEEE Vehicular Technology Conference*, 2014, pp. 1–5.

[33] M. Morant, A. Macho, and R. Llorente, "On the suitability of multicore fiber for LTE–advanced MIMO optical fronthaul systems," *Journal of Lightwave Technology*, vol. 34, no. 2, pp. 676–682, 2016.

[34] K. Saito, A. Benjebbour, A. Harada, Y. Kishiyama, and T. Nakamura, "Link-level performance of downlink NOMA with SIC receiver considering error vector magnitude," in *IEEE Vehicular Technology Conference*, 2015, pp. 1–5.

[35] T. L. Jensen and T. Larsen, "Robust computation of error vector magnitude for wireless standards," *IEEE Transactions on Communications*, vol. 61, no. 2, pp. 648–657, 2013.

[36] S. Srinivasa and S. A. Jafar, "Cognitive radios for dynamic spectrum access-the throughput potential of cognitive radio: A theoretical perspective," *IEEE Communications Magazine*, vol. 45, no. 5, pp. 73–79, 2007.

[37] J. Hu, L.-L. Yang, and L. Hanzo, "Optimal queue scheduling for hybrid cognitive radio maintaining maximum average service rate under delay constraints," in *IEEE Global Communications Conference (GLOBECOM)*, 2012, pp. 1398–1403.

[38] K. S. Manosha, N. Rajatheva, and M. Latva-aho, "Overlay/underlay spectrum sharing for multi-operator environment in cognitive radio networks," in *IEEE Vehicular Technology Conference*, 2011, pp. 1–5.

[39] J. Si, Z. Li, J. Chen, and H. Huang, "On the performance of cognitive relay networks with cooperative spectrum sensing," in *IEEE International Conference on Communications*, 2012, pp. 1709–1714.

[40] P. A. Morreale and K. Terplan, *CRC handbook of modern telecommunications*. CRC press, 2009.

[41] E. Biglieri, *Principles of cognitive radio*. Cambridge University Press, 2013.

[42] A. M. Wyglinski, M. Nekovee, and T. Hou, *Cognitive radio communications and networks: principles and practice*. Academic Press, 2009.

[43] T. Alpcan, H. Boche, M. L. Honig, and H. V. Poor, *Mechanisms and games for dynamic spectrum allocation*. Cambridge University Press, 2013.

[44] X. Chu, D. López-Pérez, Y. Yang, and F. Gunnarsson, *Heterogeneous Cellular Networks: Theory, Simulation and Deployment*. Cambridge University Press, 2013.

[45] M. H. Costa, "Writing on dirty paper (corresp.)," *IEEE Transactions on Information Theory*, vol. 29, no. 3, pp. 439–441, 1983.

[46] L. Berlemann and S. Mangold, *Front Matter*. Wiley Online Library, 2009.

[47] U. Erez and S. ten Brink, "A close-to-capacity dirty paper coding scheme," *IEEE Transactions on Information Theory*, vol. 51, no. 10, pp. 3417–3432, 2005.

[48] K. Sithamparanathan and A. Giorgetti, *Cognitive Radio Techniques: Spectrum Sensing, Interference Mitigation, and Localization*. Artech house, 2012.

[49] S. Huang, X. Liu, and Z. Ding, "Optimal transmission strategies for dynamic spectrum access in cognitive radio networks," *IEEE Transactions on Mobile Computing*, vol. 8, no. 12, pp. 1636–1648, 2009.

[50] Y. Xing, R. Chandramouli, S. Mangold *et al.*, "Dynamic spectrum access in open spectrum wireless networks," *IEEE Journal on Selected Areas in Communications*, vol. 24, no. 3, pp. 626–637, 2006.

[51] P. Thakur, A. Kumar, S. Pandit, G. Singh, and S. Satasia, "Frame structures for hybrid spectrum accessing strategy in cognitive radio communication system," in *IEEE International Conference on Contemporary Computing*, 2016, pp. 1–6.

[52] X. Kang, Y.-C. Liang, H. K. Garg, and L. Zhang, "Sensing-based spectrum sharing in cognitive radio networks," *IEEE Transactions on Vehicular Technology*, vol. 58, no. 8, pp. 4649–4654, 2009.

[53] F. Zeng and X. Liu, "Performance analysis of adaptive sensing in cognitive radio networks with hybrid interweave-underlay," in *IEEE International Conference on Information Science and Control Engineering*, 2017, pp. 1576–1581.

[54] D. Wang, Z. Li, N. Zhang, P. Qi, and X. S. Shen, "High order cumulants based spectrum sensing and power recognition in hybrid interweave-underlay

spectrum access," in *IEEE International Conference on Communications*, 2017, pp. 1–6.

[55] T. M. C. Chu, H. Phan, and H.-J. Zepernick, "Hybrid interweave-underlay spectrum access for cognitive cooperative radio networks," *IEEE Transactions on Communications*, vol. 62, no. 7, pp. 2183–2197, 2014.

[56] S. Kusaladharma and C. Tellambura, "Impact of beacon misdetection on aggregate interference for hybrid underlay-interweave networks," *IEEE Communications Letters*, vol. 17, no. 11, pp. 2052–2055, 2013.

[57] M. Jazaie and A. R. Sharafat, "Downlink capacity and optimal power allocation in hybrid underlay–interweave secondary networks," *IEEE Transactions on Wireless Communications*, vol. 14, no. 5, pp. 2562–2570, 2015.

[58] Y. Xiao and F. Hu, *Cognitive radio networks*. CRC press, 2008.

[59] I. F. Akyildiz, W.-Y. Lee, and K. R. Chowdhury, "Crahns: Cognitive radio ad hoc networks," *AD hoc networks*, vol. 7, no. 5, pp. 810–836, 2009.

[60] T. Yucek and H. Arslan, "A survey of spectrum sensing algorithms for cognitive radio applications," *IEEE communications Surveys and Tutorials*, vol. 11, no. 1, pp. 116–130, 2009.

[61] Y.-C. Liang, K.-C. Chen, G. Y. Li, and P. Mahonen, "Cognitive radio networking and communications: An overview," *IEEE Transactions on Vehicular Technology*, vol. 60, no. 7, pp. 3386–3407, 2011.

[62] N. Muchandi and R. Khanai, "Cognitive radio spectrum sensing: A survey," in *IEEE International Conference on Electrical, Electronics, and Optimization Techniques*, 2016, pp. 3233–3237.

[63] M. Z. Alom, T. K. Godder, and M. N. Morshed, "A survey of spectrum sensing techniques in cognitive radio network," in *IEEE International Conference on Advances in Electrical Engineering*, 2015, pp. 161–164.

[64] A. Ali and W. Hamouda, "Advances on spectrum sensing for cognitive radio networks: Theory and applications," *IEEE Communications Surveys and Tutorials*, vol. 19, no. 2, pp. 1277–1304, 2016.

[65] M. Subhedar and G. Birajdar, "Spectrum sensing techniques in cognitive radio networks: A survey," *International Journal of Next-Generation Networks*, vol. 3, no. 2, pp. 37–51, 2011.

[66] V. Ramani and S. K. Sharma, "Cognitive radios: A survey on spectrum sensing, security and spectrum handoff," *China Communications*, vol. 14, no. 11, pp. 185–208, Nov 2017.

[67] F. F. Digham, M.-S. Alouini, and M. K. Simon, "On the energy detection of unknown signals over fading channels," in *IEEE International Conference on Communications*, vol. 5, 2003, pp. 3575–3579.

[68] S. P. Herath, N. Rajatheva, and C. Tellambura, "Energy detection of unknown signals in fading and diversity reception," *IEEE Transactions on Communications*, vol. 59, no. 9, pp. 2443–2453, 2011.

[69] D. Cabric, A. Tkachenko, and R. W. Brodersen, "Spectrum sensing measurements of pilot, energy, and collaborative detection," in *IEEE Military Communications Conference*, 2006, pp. 1–7.

[70] F. F. Digham, M.-S. Alouini, and M. K. Simon, "On the energy detection of unknown signals over fading channels," *IEEE Transactions on Communications*, vol. 55, no. 1, pp. 21–24, 2007.

[71] V. K. Bhargava, "Advances in cognitive radio networks," in *IEEE International Conference on Advanced Technologies for Communications*, 2008, pp. xxi–xxi.

[72] H. Arslan, *Cognitive radio, software defined radio, and adaptive wireless systems*. Springer, 2007, vol. 10.

[73] E. Hossain, D. Niyato, and Z. Han, *Dynamic spectrum access and management in cognitive radio networks*. Cambridge university press, 2009.

[74] A. Papoulis and S. U. Pillai, *Probability, random variables, and stochastic processes*. Tata McGraw-Hill Education, 2002.

[75] V. Cevher, R. Chellappa, and J. H. McClellan, "Gaussian approximations for energy-based detection and localization in sensor networks," in *IEEE Workshop on Statistical Signal Processing*, 2007, pp. 655–659.

[76] G. Taricco, "On the accuracy of the gaussian approximation with linear cooperative spectrum sensing over rician fading channels," *IEEE Signal Processing Letters*, vol. 17, no. 7, pp. 651–654, 2010.

[77] H. Tang, "Some physical layer issues of wide-band cognitive radio systems," in *IEEE International Symposium on New frontiers in Dynamic Spectrum Access Networks*, 2005, pp. 151–159.

[78] S. M. Kay, "Fundamentals of statistical signal processing, vol. ii: Detection theory," *Signal Processing. Upper Saddle River, NJ: Prentice Hall*, 1998.

[79] Y. Zeng, Y.-C. Liang, A. T. Hoang, and R. Zhang, "A review on spectrum sensing for cognitive radio: challenges and solutions," *EURASIP Journal on Advances in Signal Processing*, vol. 2010, no. 1, p. 381465, 2010.

[80] L. Doyle, *Essentials of cognitive radio*. Cambridge University Press, 2009.

[81] W. A. Gardner, A. Napolitano, and L. Paura, "Cyclostationarity: Half a century of research," *Signal processing*, vol. 86, no. 4, pp. 639–697, 2006.

[82] S. Haykin, D. J. Thomson, and J. H. Reed, "Spectrum sensing for cognitive radio," *Proceedings of the IEEE*, vol. 97, no. 5, pp. 849–877, 2009.

[83] F. R. Yu and H. Tang, *Cognitive radio mobile ad hoc networks*. Springer, 2011, vol. 507.

[84] S. J. Shellhammer *et al.*, "Spectrum sensing in IEEE 802.22," *IAPR Wksp. Cognitive Info. Processing*, pp. 9–10, 2008.

[85] Y. Zeng and Y.-C. Liang, "Eigenvalue-based spectrum sensing algorithms for cognitive radio," *IEEE Transactions on Communications*, vol. 57, no. 6, 2009.

[86] ——, "Spectrum-sensing algorithms for cognitive radio based on statistical covariances," *IEEE Transactions on Vehicular Technology*, vol. 58, no. 4, pp. 1804–1815, 2009.

[87] A. Kortun, T. Ratnarajah, M. Sellathurai, C. Zhong, and C. B. Papadias, "On the performance of eigenvalue-based cooperative spectrum sensing for cognitive radio," *IEEE Journal of Selected Topics in Signal Processing*, vol. 5, no. 1, pp. 49–55, 2011.

[88] S. Kim, W. Choi, Y. Choi, J. Lee, and Y. Han, "Interference reduction of cellular relay networks in multiple-cell environment by spectrum agility," in *IEEE International Symposium on Personal, Indoor and Mobile Radio Communications*, 2008, pp. 1–5.

[89] M. Basseville, I. V. Nikiforov *et al.*, *Detection of abrupt changes: theory and application*. Prentice Hall Englewood Cliffs, 1993, vol. 104.

[90] H. V. Poor and O. Hadjiliadis, *Quickest detection*. Cambridge University Press Cambridge, 2009, vol. 40.

[91] L. Lai, Y. Fan, and H. V. Poor, "Quickest detection in cognitive radio: A sequential change detection framework," in *IEEE Global Telecommunications Conference (GLOBECOM)*, 2008, pp. 1–5.

[92] H. Li, C. Li, and H. Dai, "Quickest spectrum sensing in cognitive radio," in *IEEE Annual Conference on Information Sciences and Systems*, 2008, pp. 203–208.

[93] N. Nepal, P. A. Martin, and D. P. Taylor, "EVM based primary user monitoring in cognitive radio systems," in *Vehicular Technology Conference*, 2016, pp. 1–5.

[94] B. Dusza, K. Daniel, and C. Wietfeld, "Error vector magnitude measurement accuracy and impact on spectrum flatness behavior for OFDM-based WiMAX and LTE systems," in *International Conference on Wireless Communications, Networking and Mobile Computing*, 2009, pp. 1–4.

[95] R. A. Shafik, M. S. Rahman, and A. R. Islam, "On the extended relationships among EVM, BER and SNR as performance metrics," in *International Conference on Electrical and Computer Engineering*, 2006, pp. 408–411.

[96] M. R. Kuppusamy, S. M. Bokhari, and B. M. Anjaneyalu, "Error vector magnitude (EVM)-based constellation combiner for cooperative relay network," *IEEE Communications Letters*, vol. 20, no. 2, pp. 304–307, Feb. 2016.

[97] H. A. Mahmoud, T. Yucek, and H. Arslan, "OFDM for cognitive radio: merits and challenges," *IEEE Wireless Communications*, vol. 16, no. 2, 2009.

[98] T. Hwang, C. Yang, G. Wu, S. Li, and G. Y. Li, "OFDM and its wireless applications: A survey," *IEEE Transactions on Vehicular Technology*, vol. 58, no. 4, pp. 1673–1694, 2009.

[99] M. Speth, S. Fechtel, G. Fock, and H. Meyr, "Optimum receiver design for ofdm-based broadband transmission. ii. a case study," *IEEE Transactions on communications*, vol. 49, no. 4, pp. 571–578, 2001.

[100] X. Li, D. Peng, and G. Wang, "A novel measurement of error vector magnitude for td-lte termination," in *IEEE International Congress on Image and Signal Processing*, 2012, pp. 1745–1749.

[101] S. Parthasarathy, S. Kumar, R. K. Ganti, S. Kalyani, and K. Giridhar, "Error vector magnitude analysis in generalized fading with co-channel interference," *IEEE Transactions on Communications*, vol. PP, no. 99, pp. 1–1, 2017.

[102] V. A. Thomas, S. Kumar, S. Kalyani, M. El-Hajjar, K. Giridhar, and L. Hanzo, "Error vector magnitude analysis of fading SIMO channels relying on MRC reception," *IEEE Transactions on Communications*, vol. 64, no. 4, pp. 1786–1797, Apr. 2016.

[103] C.-I. Badoi, N. Prasad, V. Croitoru, and R. Prasad, "5G based on cognitive radio," *Wireless Personal Communications*, vol. 57, no. 3, pp. 441–464, 2011.

[104] N. Khambekar, L. Dong, and V. Chaudhary, "Utilizing ofdm guard interval for spectrum sensing," in *IEEE Conference on Wireless Communications and Networking*, 2007, pp. 38–42.

[105] M. Lin, Q. Zhang, and Q. Xu, "EVM simulation and its comparison with BER for different types of modulation," in *IEEE Region 10 International Conference (TENCON)*, 2007, pp. 1–4.

[106] R. A. Shafik, M. S. Rahman, A. Islam, and N. S. Ashraf, "On the error vector magnitude as a performance metric and comparative analysis," in *IEEE International Conference on Emerging Technologies*, 2006, pp. 27–31.

[107] M. D. McKinley, K. A. Remley, M. Myslinski, J. S. Kenney, D. Schreurs, and B. Nauwelaers, "Evm calculation for broadband modulated signals," in *Automatic RF Techniques Group (ARFTG) Measurement Conference*, 2004, pp. 45–52.

[108] J.-J. Van De Beek, O. Edfors, M. Sandell, S. K. Wilson, and P. O. Borjesson, "On channel estimation in OFDM systems," in *IEEE Conference on Vehicular Technology*, vol. 2, 1995, pp. 815–819.

[109] Y. Zhao and A. Huang, "A novel channel estimation method for OFDM mobile communication systems based on pilot signals and transform-domain processing," in *IEEE Conference on Vehicular Technology*, vol. 3, 1997, pp. 2089–2093.

[110] Y. Shen and E. Martinez, "Channel estimation in OFDM systems," *Application note, Freescale semiconductor*, 2006.

[111] B. Song, W. Zhang, and L. Gui, "Comb type pilot aided channel estimation in space time block coded OFDM systems," in *IEEE International Conference on Wireless Communications, Networking and Mobile Computing*, vol. 1, 2005, pp. 202–206.

[112] M.-H. Hsieh and C.-H. Wei, "Channel estimation for OFDM systems based on comb-type pilot arrangement in frequency selective fading channels," *IEEE Transactions on Consumer Electronics*, vol. 44, no. 1, pp. 217–225, 1998.

[113] R. Liu, Y. Li, H. Chen, and Z. Wang, "EVM estimation by analyzing transmitter imperfections mathematically and graphically," *Analog Integrated Circuits and Signal Processing*, vol. 48, no. 3, pp. 257–262, 2006.

[114] S. Parthasarathy, S. Kumar, R. K. Ganti, S. Kalyani, and K. Giridhar, "Error vector magnitude analysis in generalized fading with co-channel interference," *IEEE Transactions on Communications*, vol. 66, no. 1, pp. 345–354, 2018.

[115] U. Mir, L. Merghem-Boulahia, M. Esseghir, and D. Gaïti, "A Markov Process for Dynamic Spectrum Access," in *IEEE International Conference on New Technologies, Mobility and Security (NTMS)*, 2011, pp. 1–5.

[116] L. Csurgai-Horváth and J. Bito, "Primary and secondary user activity models for cognitive wireless network," in *IEEE International Conference on Telecommunications (ConTEL)*, 2011, pp. 301–306.

[117] S. Bayhan and F. Alagöz, *A Markovian approach for best-fit channel selection in cognitive radio networks*. Elsevier, 2014, vol. 12.

[118] A. W. Min and K. G. Shin, "Exploiting multi-channel diversity in spectrum-agile networks," in *IEEE Conference on Computer Communications (INFOCOM)*, 2008.

[119] Y. Li, Y.-n. Dong, H. Zhang, H.-t. Zhao, H.-x. Shi, and X.-x. Zhao, "Spectrum usage prediction based on high-order markov model for cognitive radio

networks," in *IEEE International Conference on Computer and Information Technology (CIT)*, 2010, pp. 2784–2788.

[120] J. C. Bellamy, *Digital Telephony (Wiley Series in Telecommunications and Signal Processing)*. Wiley-Interscience, 2000.

[121] S. Geirhofer, L. Tong, and B. M. Sadler, "Cognitive radios for dynamic spectrum access-dynamic spectrum access in the time domain: Modeling and exploiting white space," *IEEE Communications Magazine*, vol. 45, no. 5, pp. 66–72, 2007.

[122] M. Duarte, A. Sabharwal, V. Aggarwal, R. Jana, K. Ramakrishnan, C. W. Rice, and N. Shankaranarayanan, "Design and characterization of a full-duplex multiantenna system for WiFi networks," *IEEE Transactions on Vehicular Technology*, vol. 63, no. 3, pp. 1160–1177, Mar. 2014.

[123] D. Bharadia, E. McMilin, and S. Katti, "Full duplex radios," *in ACM SIGCOMM Computer Communication Review*, vol. 43, no. 4, pp. 375–386, 2013.

[124] S. Atapattu, C. Tellambura, and H. Jiang, "Energy detection of primary signals over η-μ fading channels," in *IEEE International Conference on Industrial and Information Systems (ICIIS)*, 2009, pp. 118–122.

[125] Y. Chen, "Improved energy detector for random signals in gaussian noise," *IEEE Transactions on Wireless Communications*, vol. 9, no. 2, 2010.

[126] S. Atapattu, C. Tellambura, and H. Jiang, "Performance of an energy detector over channels with both multipath fading and shadowing," *IEEE Transactions on Wireless communications*, vol. 9, no. 12, pp. 3662–3670, 2010.

[127] J. E. Salt and H. H. Nguyen, "Performance prediction for energy detection of unknown signals," *IEEE Transactions on Vehicular Technology*, vol. 57, no. 6, pp. 3900–3904, 2008.

[128] I. S. Gradshteyn and I. M. Ryzhik, *Table of integrals, series, and products*. Academic press, 2014.

[129] D. A. Shnidman, "The calculation of the probability of detection and the generalized Marcum Q-function," *IEEE Transactions on Information Theory*, vol. 35, no. 2, pp. 389–400, Mar. 1989.

[130] B. Aazhang, J. Lilleberg, and G. Middleton, "Spectrum sharing in a cellular system," in *Proceedings of the 8th IEEE International Symposium on Spread Spectrum Techniques and Applications*, 2004, pp. 355–359.

[131] N. L. Johnson, S. Kotz, and N. Balakrishnan, *Continuous Univariate Distributions*, vol. 2, 2nd ed. New York., John Wiley and Sons, 1995.

[132] M. Arts, A. Bollig, and R. Mathar, "Exact quickest spectrum sensing algorithms for eigenvalue-based change detection," in *IEEE International Conference on Ubiquitous and Future Networks (ICUFN)*, 2016, pp. 235–240.

[133] A. Wald, *Sequential analysis*. Courier Corporation, 1973.

[134] C. Cordeiro, M. Ghosh, D. Cavalcanti, and K. Challapali, "Spectrum sensing for dynamic spectrum access of TV bands," in *IEEE International Conference on Cognitive Radio Oriented Wireless Networks and Communications)*, May. 2008, pp. 225–233.

[135] E. Hanafi, P. A. Martin, P. J. Smith, and A. J. Coulson, "Performance of quickest spectrum sensing over various fading channels," in *IEEE Communications Theory Workshop (AusCTW)*, 2013, pp. 69–74.

[136] E. S. Page, "Continuous inspection schemes," *Biometrika*, vol. 41, no. 1/2, pp. 100–115, 1954.

[137] H. Li, "Cyclostationary feature based quickest spectrum sensing in cognitive radio systems," in *Vehicular Technology Conference Fall (VTC 2010-Fall), 2010 IEEE 72nd*. IEEE, 2010, pp. 1–5.

[138] A. Erdelyi, W. Magnus, and F. Oberhettinger, "M. abramowitz and ia stegun, handbook of mathematical functions," 1972.

[139] G. Lorden, "Procedures for reacting to a change in distribution," *The Annals of Mathematical Statistics*, pp. 1897–1908, 1971.

[140] A. AlSaammare, M. Shaqfeh, and H. Alnuweiri, "A simple and efficient approximation to the modified bessel functions and its applications to rician fading," in *IEEE GCC Conference and Exhibition*, 2013, pp. 351–354.